

Conformational transmission in phospholipids and the relation with the protein-mediated bilayer transport

Citation for published version (APA):

Meulendijks, G. H. W. M. (1988). *Conformational transmission in phospholipids and the relation with the protein-mediated bilayer transport*. [Phd Thesis 1 (Research TU/e / Graduation TU/e), Chemical Engineering and Chemistry]. Technische Universiteit Eindhoven. <https://doi.org/10.6100/IR282492>

DOI:

[10.6100/IR282492](https://doi.org/10.6100/IR282492)

Document status and date:

Published: 01/01/1988

Document Version:

Publisher's PDF, also known as Version of Record (includes final page, issue and volume numbers)

Please check the document version of this publication:

- A submitted manuscript is the version of the article upon submission and before peer-review. There can be important differences between the submitted version and the official published version of record. People interested in the research are advised to contact the author for the final version of the publication, or visit the DOI to the publisher's website.
- The final author version and the galley proof are versions of the publication after peer review.
- The final published version features the final layout of the paper including the volume, issue and page numbers.

[Link to publication](#)

General rights

Copyright and moral rights for the publications made accessible in the public portal are retained by the authors and/or other copyright owners and it is a condition of accessing publications that users recognise and abide by the legal requirements associated with these rights.

- Users may download and print one copy of any publication from the public portal for the purpose of private study or research.
- You may not further distribute the material or use it for any profit-making activity or commercial gain
- You may freely distribute the URL identifying the publication in the public portal.

If the publication is distributed under the terms of Article 25fa of the Dutch Copyright Act, indicated by the "Taverne" license above, please follow below link for the End User Agreement:

www.tue.nl/taverne

Take down policy

If you believe that this document breaches copyright please contact us at:

openaccess@tue.nl

providing details and we will investigate your claim.

**CONFORMATIONAL TRANSMISSION IN PHOSPHOLIPIDS
AND THE RELATION WITH
THE PROTEIN-MEDIATED BILAYER TRANSPORT**

PROEFSCHRIFT

**TER VERKRIJGING VAN DE GRAAD VAN DOCTOR AAN
DE TECHNISCHE UNIVERSITEIT EINDHOVEN, OP GEZAG
VAN DE RECTOR MAGNIFICUS, PROF. DR. F.N. HOOGHE,
VOOR EEN COMMISSIE AANGEWEEZEN DOOR HET COLLEGE
VAN DEKANEN IN HET OPENBAAR TE VERDEDIGEN OP
DINSDAG 22 MAART 1988 TE 16.00 UUR**

DOOR

GIJSBERTUS HENRICUS WILHELMUS MARIA MEULENDIJKS

GEBOREN TE HELMOND

DIT PROEFSCHRIFT IS GOEDGEKEURD

DOOR DE PROMOTOREN:

PROF. DR. H.M. BUCK

EN

PROF. DR. R.J.M. NOLTE

CO-PROMOTOR:

DR. IR. J.W. DE HAAN

aan Joyce

aan mijn ouders

Contents

Abbreviations	7
Chapter 1	
General introduction	8
1.1 The aggregation of phospholipids	8
1.2 Biological membranes	9
1.3 Conformational transmission in phospholipids	11
1.4 Scope of this thesis	13
References	14
Chapter 2	
Conformational transmission in the glyceryl backbone of phospholipid model compounds, induced by a P(IV) into trigonal bipyramidal P(V) transition	17
2.1 Introduction	19
2.2 Results and discussion	20
2.2.1 Assignment of the proton resonances	20
2.2.2 Conformational analysis	22
2.3 Experimental section	31
2.3.1 Spectroscopy	31
2.3.2 Materials	32
2.3.3 Synthesis	32
References and notes	38
Chapter 3	
Conformational transmission in anionic phospholipids. The influence of headgroup charge on the conformational distribution in the glyceryl backbone	41
3.1 Introduction	42
3.2 Results and discussion	43
3.2.1 MNDO calculations	43
3.2.2 Conformational analysis	44
3.3 Experimental section	47
3.3.1 Methods	47
3.3.2 Materials and synthesis	47
References and notes	48

Chapter 4	
Conformational transmission in condensed lipid model compounds with four coordinated phosphorus and five coordinated silicon headgroups	49
4.1 Introduction	51
4.2 Results	53
4.2.1 Conformational transmission in solution	53
4.2.2 Conformational transmission in the solid state	55
4.3 Discussion	59
4.4 Concluding remarks	63
4.5 Experimental section	63
4.5.1 NMR spectroscopy	63
4.5.2 Synthesis	64
References and notes	67
Chapter 5	
A ^{13}C CP-MAS NMR study on the chain packing in anhydrous and hydrated DL- and L-dipalmitoyl-phosphatidylcholine	70
5.1 Introduction	71
5.2 Results	72
5.2.1 Anhydrous DL- and L-DPPC	72
5.2.2 Addition of water to anhydrous DL-DPPC	75
5.2.3 Addition of water to anhydrous L-DPPC	76
5.3 Discussion	77
5.4 Concluding remarks	81
5.5 Experimental section	82
5.5.1 Materials	82
5.5.2 NMR spectroscopy and DSC analysis	82
References	83

Chapter 6	
The different influences of ether and ester phospholipids on the conformation and transport properties of gramicidin A.	85
A molecular modelling and experimental study	
6.1 Introduction	86
6.2 Procedures for calculational studies	89
6.2.1 Starting conformations	89
6.2.2 Methods	90
6.3 Results	93
6.3.1 Molecular modelling	93
6.3.2 Ion efflux measurements	98
6.4 Discussion	100
6.5 Concluding remarks	104
6.6 Experimental section	104
6.6.1 Materials	104
6.6.2 Methods	104
6.6.3 Ion efflux measurements	105
6.6.4 Determination of the number of gramicidin channels per vesicle	106
References	107
Chapter 7	
Gramicidin-mediated ion transport in dependence on the phospholipid composition	110
7.1 Introduction	111
7.2 Results and discussion	113
7.3 Concluding remarks	117
7.4 Experimental section	118
References	119
Summary	120
Samenvatting	123
Curriculum vitae	126
Dankwoord	127

Abbreviations

Ala	Alanine
CP-MAS	Cross polarisation with magic angle spinning
DHPC	Dihexadecylphosphatidylcholine
DMPC	Dimyristoylphosphatidylcholine
DOPC	Dioleoylphosphatidylcholine
DPiBP	(Dipalmitoylglyceryl)isobutylphosphate
DPG	Dipalmitoylglycerol
DPPC	Dipalmitoylphosphatidylcholine
PPS	Dipalmitoylphosphatidylserine
DSC	Differential Scanning Calorimetry
EYPC	Egg-Yolk Phosphatidylcholine
GA	Gramicidin A
Gly	Glycine
GM ⁻	Gramicidin M ⁻
k _i	Scaled first order rate constant
Leu	Leucine
LUV	Large unilamellar vesicle
NMR	Nuclear Magnetic Resonance
Phe	Phenylalanine
PS	Phosphatidylserine
sn	Stereospecific numbering
TBP	Trigonal Bipyramidal
T _f	Phase transition temperature
TMS	Tetramethyl silane
Trp	Tryptophane
Val	Valine

CHAPTER 1

General introduction

1.1 The aggregation of phospholipids

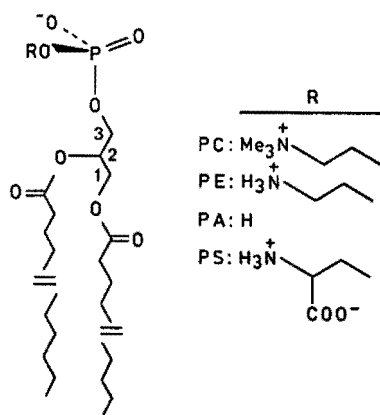


Fig. 1. Some phospholipids. Common names for the hydrocarbon chains used in this thesis: saturated: palmitoyl (P), $C_{15}H_{31}COO$; hexadecyl, $C_{16}H_{33}O$ (H); and unsaturated: oleoyl (O), $C_{17}H_{33}COO$ with a cis double bond.

Phospholipids form the most common class of lipids that are encountered in a biological membrane. They are made up of a polar headgroup and one or two apolar chains, which are esterified to glycerol. The headgroup can be zwitterionic as in phosphatidylcholines (PC) and phosphatidylethanolamines (PE), or charged as in phosphatidylserine (PS) and phosphatidic acid (PA) (Fig. 1). Because of this property phospholipids form various kinds of aggregates, dependent on the polarity of the solvent and the number of chains (Fig. 2) [1]. In water the lipids face with their

headgroups the aqueous exterior whilst the hydrophobic region is sequestered from water, forming a continuous hydrophobic phase. It has been suggested that the geometry of the aggregate is related to the shape of the molecule, in particular to the ratio of the cross-sectional areas occupied by the headgroup and the hydrocarbon chains [2]. According to this concept phospholipids with two hydrocarbon chains form a bilayer, whereas lysophospholipids, lacking one chain, will aggregate in a micellar form in an aqueous medium. In apolar solvents these lipids adopt an inverted micellar structure. The biologically important structure of the bilayer can occur as two-dimensional sheets or can be curved, thereby enclosing a spherical volume (vesicles).

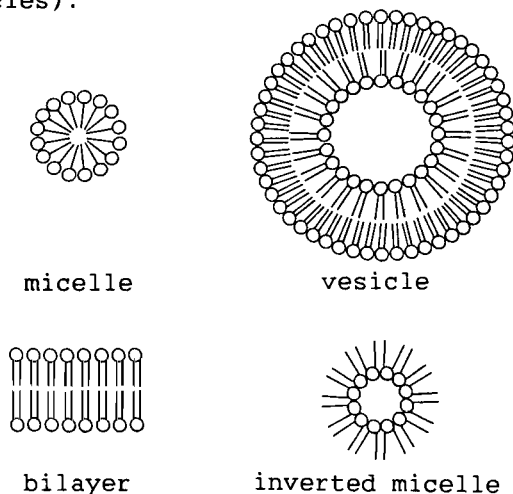


Fig. 2. Aggregational states of phospholipids.

1.2 Biological membranes

The bilayer form was originally proposed as an arrangement for biological membranes by Gorter and Grendel in 1925 [3]. Two general features of the bilayer are important for the functioning of a biological membrane. First the hydrocarbon core makes the bilayer essentially imperme-

able to polar biological molecules and ions. Secondly a bilayer formed of naturally occurring phospholipids is highly deformable under physiological conditions without losing its coherence.

Permeability of the bilayer can only be brought about by a local deformation of the geometry [4-7] or by specific transport proteins. Ion transport is a very important process in living organisms and is an intermediate step in signal transmission in nerves [8-11] and the relaxation of muscles. Two types of protein mediated transport are known [12], i.e. via a carrier protein [13,14] or via a channel forming protein [13,15]. The carrier protein binds specific ions at one side of a membrane, and diffuses to the other side where the ion is released. Channel forming peptides or proteins like gramicidin, span the membrane in such a manner that the hydrophobic residues penetrate in the apolar core and the amide groups are lined up in a helix structure through which ions can migrate. A similar transport mechanism occurs when the polar residues of various subunits of a large protein cluster to form a channel.

The idea that proteins are associated with membranes was already proposed in 1935 [16], and resulted in the fluid-mosaic model of a continuous phospholipid bilayer with proteins free to move within the bilayer [17]. In subsequent studies it has been demonstrated that this model is an oversimplification. For certain proteins (for example bacteriorhodopsin [18,19]) it is established that they are almost anchored in the bilayer. Furthermore, in the fluid mosaic model, lipids have been assigned essentially a structural role in forming a matrix for proteins or a barrier. However, the characterization of the lipid composition of plasma membranes and various subcellar membranes has revealed a rich diversity of lipid compounds, not only within one organism but also from species to species for the same cell type. Such a variation seems to be hardly meaningful if the lipids are only structural elements in cell membranes. Therefore a progressively larger

number of studies addresses the functional role of lipids in the modulation of for instance protein activity. The phospholipid headgroup is faced towards the aqueous medium, and is therefore easily accessible to signal molecules. It has indeed been shown that some anaesthetics [20] and certain divalent ions [21-23] have a pronounced effect on the conformation of the phospholipid headgroup. Such conformational changes result in a mismatch between the cross-sectional area of the headgroup and that of the hydrocarbon chains. As a consequence, the delicate balance of Van der Waals and electrostatic forces between lipid acyl chains and headgroups respectively, is disturbed. A new optimum is reached when the hydrocarbon chains of the lipid reorientate with respect to the plane of the bilayer (chain-tilt), thus changing the effective cross-sectional area. Alternatively, the regions void of Van der Waals contacts, may also be filled up by an increase in the number of intramolecular gauche transformations in the hydrocarbon chain [24]. Such rearrangements can occur very locally in the membrane, resulting in areas with a different fluidity with respect to the bulk of the lipids (domains) [25-29]. It is obvious that the fluidity can affect the conformation and/or diffusion rate of membrane proteins [30,31].

1.3 Conformational transmission in phospholipids

Very recently, an intriguing hypothesis was reported in which one possible origin of domains in membranes was related to a transient coordinational increase round phosphorus from the naturally occurring four (P(IV)) to a five coordinated state with a trigonal bipyramidal (P(V)-TBP) geometry (Fig. 3) [32,33]. Such a transition was visualized as the result of a nucleophilic attack of for instance a water molecule on four coordinated phosphorus, induced by external factors as cation concentration and potential field. Calculations showed an increased electron

density on the axially located oxygens in a P(V)-TBP structure compared with the corresponding oxygens in the P(IV) counterpart [34]. As a result, the concomitantly enhanced repulsion between O(3) and O(2) in the P-O(3)-C(3)-C(2)-O(2) fragment of the glyceryl backbone will cause a shift in the rotameric state around C(2)-C(3) towards a larger fraction of the O(2)-O(3) trans orientation. It was argued that this change leads to a different packing of the lipid chains. The concept of the propagation of a conformational change in the phosphate headgroup towards the hydrocarbon chains is called conformational transmission. Initially, this model, based on the enhancement of the electrostatic repulsion between vicinally orientated oxygens, was demonstrated for simple DNA model compounds [35,36]. Indications about the role of conformational transmission in phospholipids in regulating protein activity, came from a kinetic study in which the protein mediated sodium transport through vesicle walls was measured in dependence on the lipid composition. The results suggested a relation between the efflux rate and the ease of formation of a P(V)-TBP headgroup geometry. For vesicles containing phosphatidylserine the observed acceleration was attributed to the intramolecular partici-

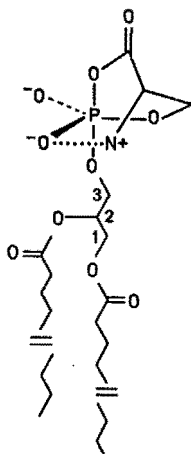


Fig. 3. The intramolecular formation of a P(V)-TBP intermediate of phosphatidylserine.

pation of the carboxylate oxygen of the serine moiety, serving as a fifth ligand in the formation of the TBP geometry. Moreover, the serine fragment was assumed to form a pseudo-equatorial six membered ring, thereby stabilizing the P(V)-TBP (Fig. 3).

1.4 Scope of this thesis

Protein-lipid interactions have been the subject of numerous studies. However, in most investigations the topic is approached from the protein side and hence, it is studied how proteins affect the lipid structure [37]. The subject of this thesis is a further investigation of the conformational transmission in phospholipids as a possible mechanism to modulate the activity of proteins.

Therefore, phospholipid model compounds have been synthesized with phosphorus in a four and five-TBP coordinated state. With high resolution ^1H and ^{13}C NMR the conformational distribution in the glyceryl backbone of the monomeric lipid model compounds was analyzed (chapter 2). The results give experimental support for the hypothesis of Merkelbach and Buck [32,33].

In chapter 3 the concept of conformational transmission is studied in monomeric phospholipids with increasing headgroup charge. MNDO calculations were performed to estimate the effect of the charge enhancement in the headgroup on the electron density of the glyceryl oxygen esterified with the phosphate moiety. On going from the uncharged to the dianionic phospholipid, similar conformational shifts were observed as occur in the transition from P(IV) into P(V)-TBP.

In chapter 4 the effects of conformational transmission on the chain packing in ordered model lipids are observed with ^{13}C CP-MAS NMR. The P(V)-TBP model compound used in chapter 2 could not be solidified. Therefore a novel type of artificial lipid was synthesized with a five

coordinated silicon in the headgroup. This silatrane lipid proved very suitable for studying the effects on the chain packing of an enhanced electron density on the glyceryl oxygen.

In chapter 5 conformational transmission is effectuated by hydration of anhydrous bilayers of the naturally occurring phospholipid dipalmitoylphosphatidylcholine (DPPC). Hydration also results in a change of the headgroup conformation. With ^{13}C CP-MAS changes are monitored in the packing of the acyl chains on going from the anhydrous to the hydrated form of the lipids. To investigate whether chirality of the phospholipids affects the packing mode of the lipids, the hydration study was performed on optically pure and racemic bilayers.

In chapter 6 a molecular modelling and experimental study is described on the conformational effects that phospholipids can have on the transport peptide gramicidin A. Two lipids which differ only in the type of linkage of the hydrocarbon chains to the backbone (i.e. via an ester or ether group), are compared in their ability to modify the conformation of the ionophore gramicidin. The theoretical results are experimentally supplemented by gramicidin-mediated sodium efflux measurements through vesicle walls that are made up of ether and ester phospholipids, respectively.

Finally, in chapter 7, this kinetic study is extended to vesicles containing phosphatidylserine and some of its derivatives to test the validity of the conformational transmission concept. Moreover, other vesicles composed of different phospholipids were prepared to investigate to what extent phospholipids can modulate the gramicidin-mediated ion transport.

References

1. J.H. Fendler, Acc. Chem. Res. 13 (1980) 7.

2. P.R. Cullis and B. de Kruyff, *Biochim. Biophys. Acta* 559 (1979) 399.
3. E. Gorter and F. Grendel, *J. Exp. Med.* 41 (1925) 439.
4. B. de Kruyff, A.J. Verkley, C.J.A. van Echteld, W.J. Gerritsen, C. Mombers, P.C. Noordam and J. de Gier, *Biochim. Biophys. Acta* 555 (1979) 200.
5. J.M. Boggs, *Can. J. Biochem.* 58 (1980) 755.
6. P.C. Noordam, C.J.A. van Echteld, B. de Kruyff, A.J. Verkley and J. de Gier, *Chem. Phys. Lipids* 27 (1980) 222.
7. B. de Kruyff and P.R. Cullis, *Biochim. Biophys. Acta* 601 (1980) 235.
8. B. Hille, *Prog. Biophys. Mol. Biol.* 21 (1970) 1.
9. E. Wanke, E. Carbone and P.L. Testa, *Nature* 287 (1980) 62.
10. G. Strichartz and I. Cohen, *Biophys. J.* 23 (1978) 153.
11. C. Miller and R.L. Rosenberg, *Biochemistry* 18 (1979) 1138.
12. Y.A. Ovchinnikov, *Eur. J. Biochem.* 94 (1979) 321.
13. D.W. Urry, *Top. Curr. Chemistry* 128 (1985) 175.
14. J. Bolard, *Biochim. Biophys. Acta* 864 (1986) 257.
15. S.J. Singer, *Annu. Rev. Biochem.* 43 (1974) 805.
16. J.F. Danielli and E.N. Harvey, *J. Cell. and Comp. Physiol.* 5 (1935) 483.
17. S.J. Singer and G.L. Nicolson, *Science* 175 (1972) 720.
18. M. Poo and R.A. Cone, *Nature* 247 (1974) 438.
19. R.A. Cone, *Nature New Biol.* 36 (1972) 39.
20. Y. Boulanger, S. Schreier and I.C.P. Smith, *Biochemistry* 20 (1981) 6824.
21. U. Strehlow and F. Jähnig, *Biochim. Biophys. Acta* 641 (1981) 301.
22. S.A. McLaughlin, *Curr. Top. Membr. Transp.* 9 (1977) 71.
23. K. Shirane, S. Kuriyama and T. Tokimoto, *Biochim. Biophys. Acta* 769 (1984) 596.
24. E. Bicknell-Brown, K.G. Brown and D. Borchman, *Biochim. Biophys. Acta* 862 (1986) 134.
25. A. Blume, R.J. Wittebort, S.K. Das Gupta and R.G.

- Griffin, *Biochemistry* 21 (1982) 6243.
26. M.F. Brown, G.P. Miljanich and E.A. Dratz, *Biochemistry* 16 (1977) 2640.
 27. S.P. Verma and D.F.H. Wallach, *Biochim. Biophys. Acta* 436 (1976) 307.
 28. T.W. Tillack, M. Wong, M. Alietta and T.E. Thompson, *Biochim. Biophys. Acta* 691 (1982) 261.
 29. S. Massari and R. Colonna, *Biochim. Biophys. Acta* 863 (1986) 264.
 30. J.H. Davis, *Biochim. Biophys. Acta* 737 (1983) 117.
 31. J. Seelig and P.M. McDonald, *Acc. Chem. Res.* 20 (1987) 221.
 32. I.I. Merkelbach, Ph.D. Thesis, Eindhoven University of Technology, 1985.
 33. I.I. Merkelbach and H.M. Buck, *Recl. Trav. Chim. Pays-Bas* 102 (1983) 283.
 34. J.J.C. van Lier, L.H. Koole and H.M. Buck, *Recl. Trav. Chim. Pays-Bas* 102 (1983) 148.
 35. L.H. Koole, E.J. Lanters and H.M. Buck, *J. Am. Chem. Soc.* 106 (1984) 5451.
 36. H.M. Buck, L.H. Koole and M.H.P. van Genderen, *Phosphorus and Sulfur* 30 (1987) 545.
 37. J.A. Killian and B. de Kruyff, *Chem. Phys. Lipids* 40 (1986) 259.

CHAPTER 2*

Conformational transmission in the glyceryl backbone of phospholipid model compounds, induced by a P(IV) into trigonal bipyramidal P(V) transition

Abstract

Triesterified phospholipid model compounds have been synthesized and extensively studied with 300 MHz ^1H NMR in the monomer phase in order to get additional support for the effect of conformational transmission induced by a P(IV) into a trigonal bipyramidal (TBP) P(V) transition. To elucidate any conformational preferences around the C(2)-C(3) bond, the stereospecifically deuterated precursor 1,2-dihexanoyl-(3R)-sn-[3- ^2H]glycerol was synthesized. The results reveal that a coordinational change of phosphorus from four to five is transmitted in a significant increase in population of the conformer in which the vicinally substituted oxygens O(2) and O(3) are trans located. The impact of this transmission seems not to be restricted to conformational changes in the adjacent C(2)-C(3) bond, but is also present in specific rotations around the C(1)-C(2) bond, thereby shifting the C(1)-C(2) conformational equilibrium towards a decreased contribution of the trans arrangement of the acyl chains. As a consequence the interchain distance will be reduced and thus Van der Waals interactions will be maximized. The results are interpreted in terms of increased electron density on O(3) when axially located in a P(V)-TBP, thereby introducing enhanced electrostatic repulsions within the oxygen pairs

* G.H.W.M. Meulendijks, W. van Es, J.W. de Haan and H.M. Buck, Eur. J. Biochem. 157 (1986) 421.

O(3),O(2) and O(3),O(1). Relaxation of this energetically unfavourable geometry leads to the observed conformational shifts. Absence of conformational transmission that was found in P(V)-TBP compounds with the 2-ester group substituted by an alkyl moiety can be considered as additional support for the introduced concept. In the alkyl part of the model phospholipids, however, no conformational changes were observed by means of ^{13}C NMR. Extrapolating this outcome to more condensed phases, a proposition could be made about the mechanism by which conformational changes in the headgroup and/or glyceryl backbone will be compensated.

2.1 Introduction

Phospholipids have been the subject of numerous conformational studies in order to get some insight in their behaviour in biomembranes [1,2]. In this chapter some experimental results are presented on the conformational transmission from the phospholipid headgroup towards the hydrocarbon chains upon a coordinational change of phosphorus from four to five. The role of P(V) trigonal bipyramidal (TBP) intermediates in phospholipid membranes as a trigger for ion transport has been discussed by Merkelbach and Buck [3,4]. These intermediates, visualized as the result of an attack of, for instance, water on a P(IV) geometry, are stabilized by a pseudo six membered ring in an equatorial arrangement, originating from the choline moiety by charge attraction.

Earlier theoretical and experimental investigations conducted in this laboratory on 5-phosphorylated tetrahydrofurfuryls [5,6], which possess essentially the same P-O-C-C-O sequence as encountered in phospholipids, already showed that P(V)-TBP geometries effectuate specific rotations in the adjacent C-C bond if the tetrahydrofurfuryl group occupies an axial position in the TBP. Virtually no conformational transmission effects were found for an equatorial location. Despite the process of phosphorus pseudorotation which involves a fast intramolecular ligand exchange between the axial and equatorial sites, a significantly greater population in comparison with the P(IV) counterpart was found for the conformer in which the vicinally substituted O(1) and O(5) are trans located. The specific rotations are attributed to the enhanced repulsion between O(1) and O(5) as a consequence of the extra electron density on O(5) when axially located in the TBP.

In order to gather experimental evidence for the conformational transmission in phospholipids, a set of trisubstituted P(IV) and P(V)-TBP phospholipid model compounds was synthesized and the rotameric distributions in the

glyceryl backbone were studied with 300 MHz ^1H NMR (Fig. 1). For the conformational analysis a correct assignment of the H(1R), H(1S), H(3R) and H(3S) protons is a prerequisite. For that purpose the stereospecifically deuterated 1,2-dihexanoyl-(3R)-sn-[3- ^2H]glycerol was synthesized from which the P(IV) and P(V)-TBP compounds were derived (for explication of the sn convention see [7]). The results of the conformational analysis around C(2)-C(3) and C(1)-C(2) show that a transition form P(IV) into P(V)-TBP is indeed transmitted into specific rotations in the glyceryl backbone. Furthermore it was examined whether these conformational changes were carried over in specific shifts in the conformational equilibria of the hydrocarbon chains. Such changes can easily be probed with ^{13}C chemical shifts [8]. Contrary to the expectation, the results indicate that no detectable changes occur in the acyl conformational equilibria upon an increase in coordination round phosphorus from four to five. Although the results from the conformational analysis are only valid for the monomeric phase, a prediction is made about the mechanism by which conformational changes in the headgroup and/or glyceryl backbone will be compensated.

2.2 Results and discussion

2.2.1 Assignment of the proton resonances

The proton resonances of H(3R) and H(3S) can be assigned unequivocally when a hydrogen is replaced stereospecifically by deuterium. This exchange was enzymatically achieved, making use of the known stereochemistry introduced by alcohol dehydrogenase, which catalyzes the oxidation of primary alcohols by abstracting the pro R hydrogen. A diaphorase enzyme (with the coenzyme FAD) accomplishes the exchange between the hydrogen of coenzyme NADH and the deuterium of the solvent D_2O [9,10]. Using this

approach, 1,2-isopropylidene-sn-glycerol, obtained from D-mannitol, was converted into the 3R deuterated analogue and via known procedures the (deuterated) structures 1a-d₁ and 1b-d₁ shown in Fig. 1 were synthesized. An expansion of the H(3) NMR pattern of the deuterated P(IV) compound 1a-d₁ reveals that the downfield proton is exchanged by deuterium (Fig. 2), thus this hydrogen can be assigned as pro R [11]. In the P(V)-TBP compound 1b-d₁ the chemical shift difference between H(3R) and H(3S) is almost identical with the isotope effect (0.02 ppm) which causes an upfield shift of the remaining hydrogen [12]. For deuterated 1b a signal was observed 0.02 ppm upfield with respect to the upfield proton in the non-deuterated analogue, thus this resonance comes from the pro S proton. For 1a and 1b it is now firmly established that $\delta(\text{H}(3\text{R})) > \delta(\text{H}(3\text{S}))$ and this assignment will be used for the compounds 1 - 5 as well. For the H(1R) and H(1S) protons the same assignment was applied as was determined for dihexanoylphosphatidylcholine ($\delta(\text{H}(1\text{S})) > \delta(\text{H}(1\text{R}))$) and which accounts for the well-known parallel orientation of the hydrocarbon chains [2].

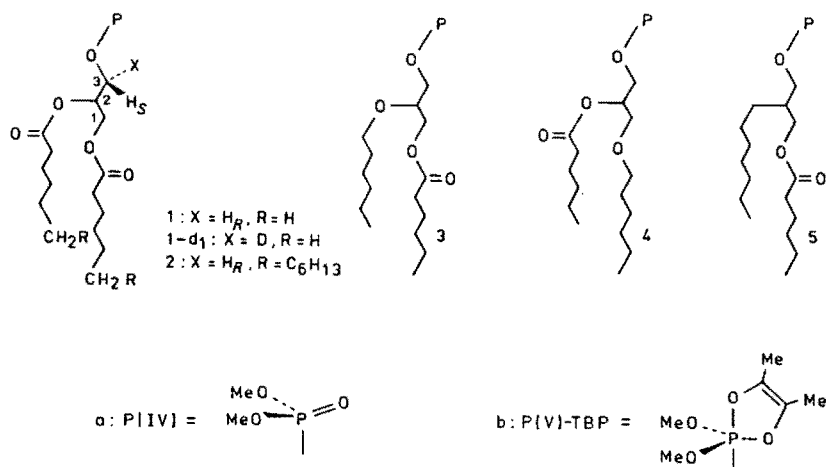


Fig. 1. Structures of the phospholipid model compounds.

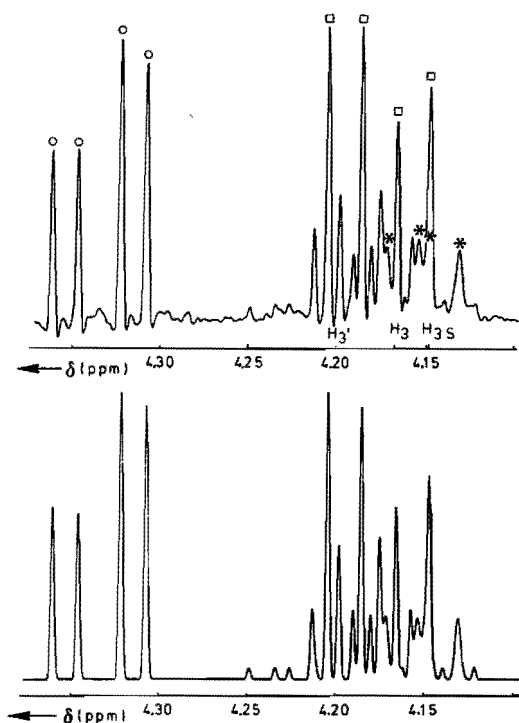


Fig. 2. Experimental (upper trace) and computer simulated (lower trace) 300 MHz ^1H NMR spectrum of $1a\text{-}d_1$ in chloroform- d_1 . The asterisks point out the H(3S) pattern. The other signals belong to H(1R) (\square), H(1S) (Δ) and H(3)/H(3') of the non-deuterated fraction.

2.2.2 Conformational analysis

In solution rapid interconversion between the staggered conformers g^+ , g^t and g^- (Fig. 3) yields weighted time averaged vicinal coupling constants $J_{\text{H}(2)\text{H}(1\text{S})}$, $J_{\text{H}(2)\text{H}(1\text{R})}$, $J_{\text{H}(2)\text{H}(3\text{S})}$, and $J_{\text{H}(2)\text{H}(3\text{R})}$ which are related to the coupling constants in the individual rotamers and their mole fractions $x(g^+)$, $x(g^t)$ and $x(g^-)$:

$$J_{H(2)H(iS)H(iR)} = x(g^+)Jg^+_{H(2)H(iS)H(iR)} + x(g^t)Jg^t_{H(2)H(iS)H(iR)} + x(g^-)Jg^-_{H(2)H(iS)H(iR)}$$

for $i = 1,3$ with $x(g^+) + x(g^t) + x(g^-) = 1$. The rotamer populations can be solved with the coupling constants of the g^+ , g^t and g^- rotamers obtained from an empirical generalized Karplus equation developed by Haasnoot et al. [13].

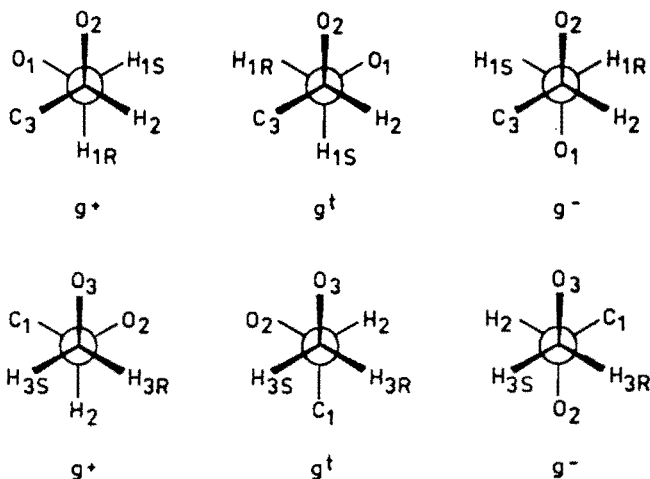


Fig. 3. Newman projections of the rotamers around C(1)-C(2) (upper trace) and C(2)-C(3) (lower trace). For clarity, the C(1)-C(2) rotamer in which the oxygens are trans located, is indicated as g^- , despite of the conventional rules.

As can be seen from the data in Table I, the rotameric distribution around the C(2)-C(3) bond of the P(IV) compounds 1a to 4a in various solvents is dominated by the gauche effect, i.e. the preference of vicinally orientated oxygens to adopt a gauche conformation [14] (C(2)-C(3): $x(g^+) = 0.40 - 0.47$, $x(g^t) = 0.37 - 0.47$ and $x(g^-) = 0.10 - 0.23$). Upon lowering the solvent polarity, the increase in the electrostatic charge repulsion between O(2) and O(3) leads to a conformational change for the C(2)-C(3)

Table I. $J_{\text{H}(2)\text{H}(1\text{S})\text{H}(1\text{R})}$ and $J_{\text{H}(2)\text{H}(3\text{S})\text{H}(3\text{R})}$ and corresponding rotamer populations around C(1)-C(2) and C(2)-C(3) for the P(IV) compounds in some solvents at room temperature.

Com- pound	Solvent	E_{T}^{a}	Conformational distribution around C(1)-C(2)					Conformational distribution around C(2)-C(3)				
			$J_{\text{HH}(\text{S})}$	$J_{\text{HH}(\text{R})}$	$x(\text{g}^+)$	$x(\text{g}^{\text{t}})$	$x(\text{g}^-)$	$J_{\text{HH}(\text{S})}$	$J_{\text{HH}(\text{R})}$	$x(\text{g}^+)$	$x(\text{g}^{\text{t}})$	$x(\text{g}^-)$
			Hz	Hz				Hz	Hz			
1a	C_6H_{14}	30.0	4.25	6.12	0.37	0.47	0.16	5.57	4.09	0.44	0.42	0.14
	CCl_4	32.5	4.15	5.93	0.40	0.45	0.15	5.42	4.10	0.45	0.40	0.15
	C_6D_6	34.5	4.17	5.97	0.39	0.45	0.16	5.70	4.00	0.43	0.44	0.13
	CDCl_3	39.1	4.43	5.78	0.39	0.42	0.19	5.58	4.49	0.40	0.40	0.20
	$(\text{CD}_3)_2\text{CO}$	42.2	4.19	6.24	0.37	0.48	0.15	5.50	4.17	0.44	0.41	0.15
	CD_3CN	46.0	4.24	6.00	0.38	0.46	0.16	6.02	3.95	0.40	0.47	0.13
	CD_3OD	55.5	4.06	6.58	0.34	0.52	0.14	5.50	3.74	0.47	0.43	0.10
2a	CDCl_3	39.1	4.26	5.81	0.40	0.43	0.17	5.56	4.50	0.41	0.39	0.20
	$(\text{CD}_3)_2\text{CO}$	42.2	4.00	6.63	0.34	0.53	0.13	5.77	4.35	0.40	0.42	0.18
	CD_3OD	55.5	3.68	6.10	0.41	0.50	0.09	5.96	3.95	0.41	0.46	0.13
3a	CDCl_3	39.1	4.68	5.34	0.40	0.35	0.25	5.46	4.78	0.40	0.37	0.23
	$(\text{CD}_3)_2\text{CO}$	42.2	4.76	5.48	0.40	0.36	0.24	5.32	4.49	0.43	0.37	0.20
	CD_3OD	55.5	4.71	5.37	0.41	0.36	0.23	5.33	4.39	0.44	0.38	0.18
4a	CDCl_3	39.1	- ^b	- ^b	-	-	-	5.77	3.75	0.44	0.46	0.10
5a	CDCl_3	39.1	4.84	6.56	0.36	0.44	0.20	6.13	5.13	0.37	0.38	0.25
	$(\text{CD}_3)_2\text{CO}$	42.2	4.81	6.82	0.34	0.46	0.20	6.24	5.12	0.36	0.39	0.25
	CD_3OD	55.5	4.80	6.56	0.36	0.44	0.20	- ^b	- ^b	-	-	-

^a Solvent polarity constant.

^b Coupling constants could not be determined due to the near equivalence of the protons involved.

bond in favour of the g^- conformer (with O(2) and O(3) trans located). This outcome is in good agreement with the observation on model nucleotides [6]. The C(1)-C(2) rotameric distribution, on the other hand, is governed by the tendency of the hydrocarbon chains to adopt a parallel orientation, which will be more pronounced in polar solvents, thereby excluding a large contribution of the g^- conformer (O(1) and O(2) trans located).

For compound **3a**, in which the sn-2 chain is linked by an ether bond to the glyceryl backbone, a slightly increased g^- population around C(2)-C(3) and C(1)-C(2) is observed compared to the 2-ester analogue **1a** (for CDCl_3 : C(2)-C(3): $x(g^-) = 0.23$ resp 0.20 ; C(1)-C(2): $x(g^-) = 0.25$ resp 0.19). This finding is obviously due to the enhanced electron density on O(2) in **3a** with respect to **1a**. When the 2-ester group is substituted by an alkyl moiety, as in **5a**, virtually no shifts in conformer populations are detectable around the C(2)-C(3) bond upon increasing solvent polarity. Identical distributions were also found for the C(1)-C(2) bond in various solvents. Apparently the 2-ester moiety plays a crucial role in alterations in the C(1)-C(2) conformational equilibrium.

Comparing the data of Table I and Table II it follows that a coordinational change from P(IV) into P(V)-TBP brings about a significant increase in g^- population around C(2)-C(3) (for CDCl_3 : P(IV): $x(g^-) = 0.10 - 0.23$; P(V): $x(g^-) = 0.18 - 0.33$), whereas the g^- population around C(1)-C(2) decreases (for CDCl_3 : P(IV): $x(g^-) = 0.17 - 0.25$; P(V): $x(g^-) = 0.08 - 0.12$). As the results point out, the coordinational change of phosphorus is transmitted into specific conformational changes in the glyceryl backbone. This conformational transmission effect originates from the enhanced electron density on O(3) in the P(V)-TBP, when the glyceryl moiety is located in the axis of the TBP, resulting in increased O(2)-O(3) and O(1)-O(3) repulsions with respect to the P(IV) counterpart. Fig. 4 demonstrates the coupled conformational

Table II. $J_{H(2)H(1S)(H(1R))}$ and $J_{H(2)H(3S)(H(3R))}$ values in Hz and the corresponding rotamer populations around C(1)-C(2) and C(2)-C(3) for the P(V)-TBP compounds at room temperature.

Com- pound	Solvent	E_T^a	Conformational distribution around C(1)-C(2)					Conformational distribution around C(2)-C(3)				
			$J_{HH(S)}$	$J_{HH(R)}$	$x(g^+)$	$x(g^t)$	$x(g^-)$	$J_{HH(S)}$	$J_{HH(R)}$	$x(g^+)$	$x(g^t)$	$x(g^-)$
			Hz	Hz				Hz	Hz			
1b	C_6H_{14}	30.0	3.52	6.53	0.37	0.55	0.08	5.21	5.37	0.37	0.32	0.31
	C_6D_6	34.5	3.60	6.60	0.37	0.55	0.08	5.28	5.36	0.38	0.31	0.31
	$CDCl_3$	39.1	3.60	6.63	0.38	0.50	0.12	5.38	5.47	0.36	0.36	0.28
	$(CD_3)_2CO$	42.2	3.62	6.78	0.35	0.55	0.10	5.45	5.06	0.38	0.35	0.27
	CD_3CN	46.0	3.74	6.59	0.36	0.54	0.10	5.70	5.03	0.36	0.38	0.26
2b	$CDCl_3$	39.1	3.60	6.63	0.37	0.55	0.08	5.38	5.47	0.35	0.32	0.33
3b	$CDCl_3$		3.81	6.00	0.41	0.48	0.11	6.24	5.35	0.27	0.42	0.31
4b	$CDCl_3$		- ^b	- ^b	-	-	-	5.75	4.44	0.40	0.42	0.18
5b	$CDCl_3$		5.31	6.26	0.35	0.38	0.27	5.91	5.27	0.38	0.36	0.26

^a Solvent polarity constant.

^b Coupling constants could not be determined due to the near equivalence of the protons involved.

changes which take place on increasing the coordination from P(IV) to a P(V)-TBP. The enhanced O(2)-O(3) repulsion shifts the rotameric distribution around the C(2)-C(3) bond towards g^- . Consequently, in the g^- conformation around C(1)-C(2), the repulsion between O(1) and O(3) increases. From Dreiding models it follows that in the particular arrangement in which a g^- conformation around C(1)-C(2) and C(2)-C(3) is adopted, the interatomic distance between O(1) and O(3) is comparable to the O(2)-O(3) distance in the g^+ or g^t conformer around the C(2)-C(3) bond (approximately 0.27 Å). Relaxation of this energetically unfavourable geometry results in a decreased g^- population around the C(1)-C(2) linkage, leading to a decrease in the intrachain distance.

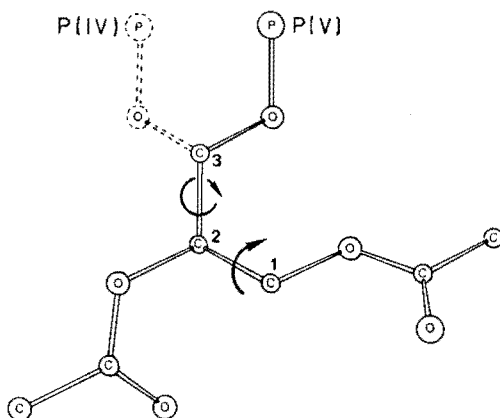


Fig. 4. ORTEP drawing of the glyceryl fragment. The bold lines represent the g^-, g^- arrangement of the glyceryl backbone. The dotted lines show the phosphoryl group trans with respect to C(1). The similarity in interatomic distances between O(1) and O(3) in the g^-, g^- arrangement and between O(2) and O(3) in the g^t conformer around C(2)-C(3) is obvious.

Consistent with the electrostatic nature of the oxygen-oxygen repulsion is the observation that in compound 5, where the 2-ester group is substituted by an alkyl moiety, no conformational changes could be detected around the C(2)-C(3) bond on going from a P(IV) to a P(V)-TBP geometry. Concerning the C(1)-C(2) bond a slight increase in g^- conformation is observed in the P(V)-TBP with respect to the P(IV) counterpart [15], which is in contrast to the results on the 2-ester analogues (vide supra).

The conformational changes about the C(2)-C(3) bond in the P(V)-TBP compounds 1b - 4b, on varying solvent polarity show a similar behaviour as was observed for the P(IV) derivatives.

It should be mentioned, however, that the coupling constants from which the rotamer distributions are derived, are measured under rapid phosphorus pseudo-rotation conditions, as could be judged from the magnetic equivalence of the pseudo-axially and pseudo-equatorially orientated methyl groups in the P(V)-TBP. This process leads to time averaged conformational distributions in which axially and equatorially located glyceryl fragments both participate. Therefore it can reasonably be expected that in P(V)-TBP compounds with the glyceryl moiety on a distinct axial position, the observed transmission effect will be even more pronounced.

None the less, the results presented here clearly demonstrate that conformational changes take place in the glyceryl backbone of phospholipids when the coordinational number is increased from P(IV) to P(V)-TBP and when varying external factors like solvent polarity. In order to investigate whether these conformational changes are carried over in any shifts in the conformational equilibria of the alkyl part of the acyl chain, a ^{13}C NMR analysis was performed. As was shown previously, ^{13}C NMR chemical shifts are a sensitive probe for changes in conformational equilibria [8]. The data in Table III reveal that

the ^{13}C chemical shifts do not reflect substantial changes in conformational equilibria in the alkyl part of the phospholipid upon a P(IV) to P(V)-TBP transition. The deshielding effect on C(2) and C(3) of the hydrocarbon chain is most likely due to a charge redistribution in the ester moiety as a consequence of the P(IV) into P(V)-TBP transition.

Table III. ^{13}C deshieldings upon a coordinational change of phosphorus from P(IV) to P(V)-TBP for compound **2** in CDCl_3 . Concentration: 140 mg/ml. Measurement conditions were kept as equal as possible. C(16) is the terminal methyl group.

Chain Carbon no	Deshielding
16	0
15	0
14	0
13 ^a	0
12 ^a	0
11-5	0.01
4	0.01
3	0.11 ^b
	0.06
2	0.19 ^b
	0.13

^a Resonances could not be assigned properly.

^b Downfield resonance.

When any conformational changes in the alkyl part would occur, they would be most easily brought about in the studied monomeric phospholipids. Therefore it is to be expected that in more condensed phases, with much larger interchain interactions, such conformational changes are even less probable. Thus one might very well surmise that

in condensed phases those conformational changes in head-group and/or glyceryl backbone which result in a change in the effective chain length difference between the sn-1 and sn-2 hydrocarbon chain, will be compensated almost exclusively by changes in the angle of tilt of the hydrocarbon chains relative to the bilayer normal [16]. The other possibility to change the effective chain length difference, that is by a dissimilar shift in the conformational equilibria in the sn-1 and sn-2 hydrocarbon chains, can be ruled out in view of the ^{13}C chemical shift data.

The present results are in good agreement with the observed invariability of the hydrocarbon chain conformation in dihexadecylphosphatidic acid upon proton dissociation [16]. One might reasonably expect that the negative charge on the phosphate headgroup is partly transferred to O(3), as will be theoretically and experimentally confirmed in chapter 3.

Furthermore, the outcome described in this chapter gives some further experimental support for the role of short living P(V)-TBP intermediates in the ion transport mechanism through membranes as was worked out by Merkelbach and Buck [3,4]. Their experimental results, based on the sodium transport rate through vesicles with incorporated gramicidin A as a function of the phospholipid composition suggest a correlation between the ease of formation of a P(V)-TBP and the ion transport rate. In case of phosphatidylserine a considerable rate acceleration was observed with respect to phosphatidylcholine. This finding was ascribed to the availability of the carboxy group of phosphatidylserine, serving as the axial fifth ligand, to build up a P(V)-TBP. To make an estimate of the amount of P(V)-TBP in the case of phosphatidylserine the hydrolysis of diaryl-2-carboxyphenyl phosphates catalyzed by the neighbouring group participation of the carboxylate anion was taken as a reference [17]. The equilibrium constant for the interconversion between the P(V)-TBP intermediate and the starting phosphate was 10^{-6} .

Transferring this value to the phosphatidylserine, it means that about $10^{-4}\%$ exists in a TBP form [18]. Therefore the P(V)-TBP can be considered as a realistic intermediate for triggering a phase transition. Such phase transition is envisaged as the result of a change in the angle of tilt of the hydrocarbon chains, which is brought about by the enhanced oxygen-oxygen repulsions in the P(V)-TBP [3]. A cooperative change in the angle of tilt of a number of phospholipid molecules will be needed to maximize the Van der Waals interactions between neighbouring acyl chains. This will lead at macromolecular level to the formation of a cluster with an average angle of tilt differing from the surrounding matrix and with a much longer lifetime than the P(V)-TBP intermediate. In this model a correlation is supposed between protein activation and the uptake in a cluster of different fluidity. A transfer of glyceryl backbone conformational changes into shifts in the gauche/trans conformational equilibria in the hydrophobic part of the phospholipid as an alternative for changing tilt angles was not taken into account. The present results indeed do rule out a change in the rotamer state of the hydrocarbon chains.

2.3 Experimental section

2.3.1 Spectroscopy

^1H NMR spectra were recorded at 300.13 MHz on a Bruker CXP 300 spectrometer at room temperature. Coupling constants were derived by iterative fitting of expansions of the H(1S)/H(1R) and H(3S)/H(3R) patterns, using the program PANIC-82 (Bruker Spectrospin). ^{31}P spectra were run on a Bruker HX-90R spectrometer with a Digilab FT-NMR-3 pulsing accessory. ^{13}C spectra were run at 75.47 MHz on a Bruker CXP 300 NMR spectrometer under proton noise decoupling at 37°C . 656 Transients were accumulated of spec-

tral width 1.5 kHz in 32k data points. All NMR samples were routinely dissolved in CDCl_3 , unless otherwise stated.

2.3.2 Materials

All solvents were reagent grade and were used as received or purified as required. All reactions involving P(III) or P(V) compounds were run under a dry and inert atmosphere. Horse liver alcohol dehydrogenase (EC 1.1.1.1) and diaphorase with the coenzyme FAD from pig heart (EC 1.6.4.3) were purchased from Boehringer Mannheim. NAD^+ , NADH and albumine were products of Sigma.

2.3.3 Synthesis

1,2-Isopropylidene-(3R)-sn-[3- ^2H]glycerol

1,2-Isopropylidene-(3R)-sn-[3- ^2H]glycerol was prepared from 1,2-isopropylidene-sn-glycerol [19,20], as was described by Wohlgemuth et al. [9]. Immediately before use the enzyme suspensions were centrifugated (3,000 rpm, 4 min. at 20° C) and the clear supernatant removed. The extent of deuteration amounted to 65% as judged by the ^1H NMR integral.

1,2-Dihexanoyl-(3R)-sn-[3- ^2H]glycerol

1,2-Isopropylidene-(3R)-sn-[3- ^2H]glycerol was protected by treatment with sodium, followed by benzyl chloride. The isopropylidene group was hydrolyzed in 10% acetic acid/water at 100°C and the resulting clear solution was concentrated [21,22]. Toluene was added and the solvent was evaporated. The product was dried in vacuum at 40°C. The 3-benzyl-(3R)-sn-[3- ^2H]glycerol thus obtained, was acylated by adding hexanoyl chloride to a solution of the benzylglycerol in dry toluene at 0°C. The solution was allowed to stand overnight at room temperature and the

product was worked up following usual procedures. Purification of the residue by column chromatography on silica using chloroform/acetone (96/4) as eluents, yielded pure 1,2-dihexanoyl-3-O-benzyl-(3R)-sn-[3-²H]glycerol which was converted into the 1,2-dihexanoyl-(3R)-sn-[3-²H]glycerol by hydrogenolysis in ethylacetate catalyzed by 10% Pd/C just before the next reaction [21]. All of the isolated intermediates and the product were identified by comparing the ¹H NMR chemical shifts with literature data.

(1,2-Dihexanoyl-(3R)-sn-[3-²H]glyceryl)dimethylphosphite

A solution of chlorodimethoxyphosphine [23] in anhydrous diethyl ether was added to a stirred and cooled (-10°C) solution of equivalent amounts of 1,2-dihexanoyl-(3R)-sn-[3-²H]glycerol and triethylamine in dry diethyl ether. The reaction mixture was stirred for 1.5 h at room temperature and the precipitated triethylamine hydrochloride was removed by filtration. After evaporation of the solvent an oily residue was obtained and used without further purification. ³¹P NMR: δ 140.7; ¹H NMR: δ 3.50 (d, 6H, OCH₃), 3.7 - 4.4 (m, H(3S), H(1S), H(1R)), 4.9 - 5.3 (m, 1H, H(2)).

(1,2-Dihexanoyl-(3R)-sn-[3-²H]glyceryl)dimethylphosphate (1a-d₁)

An ozone/oxygen stream was passed through a solution of (1,2-dihexanoyl-(3R)-sn-[3-²H]glyceryl)dimethylphosphite in dry dichloromethane at -78°C until a blue colour appeared. Without external cooling, the solution was then purged with an oxygen stream until room temperature was reached. Evaporation of the solvent yielded an oily residue which was chromatographed on a silica column using ethylacetate as eluents. ³¹P NMR: δ 1.3; ¹H NMR: δ 3.72 (d, 6H, OCH₃), 4.2 - 4.4 (m, H(3S), H(1S), H(1R)), 5.2 - 5.3 (m, 1H, H(2)). Anal. Calcd. for C₁₇H₃₂DPO₈: C, 51.38; H, 8.62. Found: C, 51.64; H, 8.46.

**2,2-Dimethoxy-2-(1,2-dihexanoyl-(3R)-sn-[3-²H]glycero)-
2,2-dihydro-4,5-dimethyl-1,3,2-dioxaphosphol-4-ene (1b-d₁)**

To a solution of (1,2-dihexanoyl-(3R)-sn-[3-²H]glyceryl)-dimethylphosphite in chloroform-d₁, being contained in a NMR tube, a small excess of butanedione was added at 0°C. The addition was completed within 1 hour, as judged by ³¹P NMR. ³¹P NMR: δ -49.6; ¹H NMR: δ 1.82 (s, 6H, CH₃ dioxaphospholene ring), 3.9 - 4.0 (m, H(3S), H(1S), H(1R)), 5.1 - 5.2 (m, 1H, H(2)).

**(1,2-Dihexanoylglyceryl)dimethylphosphate (1a) and
(1,2-dipalmitoylglyceryl)dimethylphosphate (2a) and their
P(V) Analogues (1b) resp (2b)**

These compounds were prepared starting from 1,2-isopropylidene-glycerol according to similar procedures as described for the synthesis of 1a-d₁ and 2b-d₁ and their P(V) derivatives 1b-d₁ and 2b-d₁. Addition of butanedione to (1,2-dipalmitoylglyceryl)dimethylphosphite in CDCl₃ yielded at first the corresponding phosphonium ion (³¹P NMR: δ 42.8) which slowly converted into the P(V)-derivative (³¹P NMR: δ -49.5).

1-Hexanoyl-2-hexylglycerol

1,3-Benzylideneglycerol was alkylated with 1-hexyl bromide according to a procedure described by Howe et al. [22]. Removal of the protective group by hydrogenolysis in dry ethylacetate catalyzed by 10% Pd/C, resulted in 2-hexyl-glycerol, which was acylated with 1 equivalent of hexanoyl chloride. The crude product was purified by column chromatography on silica using chloroform/methanol (30/1) as eluents. The isolated intermediates were identified by comparing the ¹H NMR chemical shifts with literature data. ¹H NMR: δ 0.87 (t, 6H, CH₃), 1.0 - 2.0 (m, 14H, CH₂), 2.33 (t, 2H, CH₂), 3.3 - 3.8 (m, 5H, CH₂O, CH, OH), 4.13 (d, 2H, CH₂O).

Dimethoxy-N,N-dimethylaminophosphine

To a stirred and cooled (-10°C) solution of chloro-dimethoxyphosphine (90 mmol, 11.5 g) in anhydrous diethyl ether (100 ml) a solution of dimethylamine (180 mmol, 8.1 g) in dry diethyl ether (40 ml) was added dropwise. The mixture was stirred at room temperature for 2 h. After removal of the precipitated dimethylamine hydrochloride by filtration, the solution was concentrated and the mixture distilled twice under reduced pressure, yielding 4.0 g of pure material: bp 32 - 35°C at 20 mm. ^{31}P NMR: δ 147.8; ^1H NMR: δ 2.62 (d, 6H, NCH₃), 3.42 (d, 6H, OCH₃).

(1-Hexanoyl-2-hexylglyceryl)dimethylphosphite

1-Hexanoyl-2-hexylglycerol (2 mmol, 0.5 g) was dissolved in an excess dimethoxy-N,N-dimethylaminophosphine (3 mmol, 0.4 g) and the solution was stirred at 65°C until no dimethylamine could be detected (1.5 h). The excess of the phosphine was removed in vacuo and the crude product was used immediately without purification. ^{31}P NMR: δ 140.7; ^1H NMR: δ 3.42 (d, 6H, OCH₃), 3.8 - 4.3 (m, 6H, OCH₂).

(1-Hexanoyl-2-hexylglyceryl)dimethylphosphate (3a)

This compound was synthesized according to similar procedures as described for the preparation of 1a-d₁. ^{31}P NMR: δ 1.3. ^1H NMR: δ 3.68 (m, 1H, H(2)), 3.78 (d, 6H, OCH₃), 4.0 - 4.3 (m, 4H, H(1R), H(1S), H(3R)).

2,2-Dimethoxy-2-(1-hexanoyl-2-hexylglycero)-2,2-dihydro-4,5-dimethyl-1,3,2-dioxaphosphol-4-ene (3b)

The P(V) derivative 3b was obtained according to a similar procedure as described for the synthesis of 1b-d₁. ^{31}P NMR: δ -49.5; ^1H NMR: δ 1.83 (s, 6H, CH₃ dioxaphospholene ring), 3.61 (d, 6H, OCH₃), 3.8 - 4.0 (m, 2H, H(3S), H(3R)), 4.3 - 4.1 (m, 2H, H(1S), H(1R)).

1-Hexyl-2-hexanoylglycerol

1,2-Isopropylidene-glycerol was alkylated with 1-hexyl bromide according to a procedure described by Howe et al. [22]. Subsequent removal of the isopropylidene group in refluxing 10% acetic acid/water yielded 1-hexylglycerol. After protection of the primary hydroxyl group with chlorotriphenylmethane in a solution of dry toluene and dry pyridine (1/1), and working up according to usual procedures, the resulting viscous oil was acylated with hexanoyl chloride. Removal of the trityl group was accomplished in a similar manner as was described by Buchnea [24]. All of the isolated intermediates were identified by comparing the ^1H NMR chemical shifts with literature data. ^1H NMR: δ 2.7 (br. s., 1H, OH), 3.2 - 3.9 (m, 6H, CH_2O), 4.8 - 5.2 (m, 1H, CH).

(1-Hexyl-2-hexanoylglyceryl)dimethylphosphite

This compound was obtained according to the procedure which was described for the preparation of (1,2-dihexanoyl-(3R)-sn-[3- ^2H]-glyceryl)dimethylphosphite and used without purification. ^{31}P NMR: δ 141.1; ^1H NMR: δ 3.3 - 3.6 (m, 2H, H(1R), H(1S)), 3.8 - 4.0 (m, 2H, H(3R), H(3S)), 5.1 - 5.2 (m, 1H, H(2)).

(1-Hexyl-2-hexanoylglyceryl)dimethylphosphate (4a)

This compound was prepared according to a procedure which was described for the synthesis of 1a-d₁. ^{31}P NMR: δ 0.4; ^1H NMR: δ 3.4 - 3.5 (m, 2H, H(1R), H(1S)), 4.1 - 4.3 (m, 2H, H(3R), H(3S)), 5.1 - 5.2 (m, 1H, H(2)).

2,2-Dimethoxy-2-(1-hexyl-2-hexanoylglycerol)-2,2-dihydro-4,5-dimethyl-1,3,2-dioxaphosphol-4-ene (4b)

This compound was obtained in a similar manner as described for 1b-d₁. ^{31}P NMR: δ -49.6; ^1H NMR: δ 1.83 (s, 6H, CH_3 , dioxaphospholene ring), 3.2 - 3.5 (m, 2H, H(3R), H(3S)), 5.1 - 5.2 (m, 1H, H(2)).

Diethyl 1,1-octanedicarboxylate

Diethyl 1,1-octanedicarboxylate was obtained in 70% yield from diethyl malonate and hexyl bromide according to a similar procedure as described by Mercier et al. [25]. Bp. 126°C at 0.5 mm. $^1\text{H NMR}$: δ 0.87 (t, 3H, CH_3), 1.23 (t, 6H, OCH_2CH_3), 1.26 (s, 10H, CH_2), 1.6 - 2.1 (m, 2H, CH_2), 3.23 (t, 1H, CH), 4.13 (q, 4H, OCH_2). Anal. Calcd. for $\text{C}_{14}\text{H}_{26}\text{O}_4$: C, 65.09; H, 10.14. Found: C, 65.08; H, 10.08.

1-Hydroxy-2-hydroxymethylnonane

A stirred suspension of LiAlH_4 (0.1 mol, 3.5 g) in dry diethyl ether (125 ml) was refluxed for 30 minutes, after which the suspension was cooled to 0°C, and the octane ester (0.04 mol, 10.5 g) dissolved in dry diethyl ether (100 ml), was added in 1 h. The reaction mixture was slowly heated to 35°C and, while stirring, maintained at this temperature. To destroy the excess of LiAlH_4 , water (100 ml) was added cautiously at 0°C. After the addition, the mixture was thoroughly extracted with diethyl ether. Evaporation of the dried organic layer afforded the colourless diol (6.2 g, 90% yield). $^1\text{H NMR}$: δ 0.88 (t, 3H, CH_3), 1.0 - 1.5 (m, 12H, CH_2), 3.5 - 3.9 (m, 5H, CH + CH_2O), 4.2 (br.s., 2H, OH). Anal. Calcd. for $\text{C}_{14}\text{H}_{26}\text{O}_4$: C, 68.92; H, 12.72. Found: C, 68.38; H, 12.84.

2-Deoxy-2-heptyl-3-hexanoylglycerol

1-Hydroxy-2-hydroxymethylnonane was acylated by adding hexanoyl chloride to a solution of the diol and pyridine in toluene at -10°C. After the reaction mixture was stirred at 35°C for 1 h, and the mixture was worked up following usual procedures. The oily residue, consisting of the mono- and diacylated alcohol, was purified by column chromatography on silica, using chloroform/methanol (96/4) as eluents, yielding the oily colourless product (3.5 g, 90% yield). $^1\text{H NMR}$: δ 0.88 (t, 3H, CH_3), 0.90 (t, 3H, CH_3), 1.2 - 1.4 (m, 16H, CH_2), 1.63 (q, 2H, $\text{CH}_2\text{CH}_2\text{O}$), 1.79 (m, 1H, CH), 2.02 (s, 1H, OH), 2.32 (t, 2H, CH_2COO),

3.5 - 3.6 (m, 2H, H(3R), H(3S)), 4.1 - 4.2 (m, 2H, H(1R), H(1S)). Anal. Calcd. for $C_{16}H_{32}O_3$: C, 70.54; H, 11.84. Found: C, 70.81; H, 11.91.

(2-Deoxy-2-heptyl-3-hexanoylglyceryl)dimethylphosphate (5a) and 2,2-dimethoxy-2-(2-deoxy-2-heptyl-3-hexanoylglycero)2,2-dihydro-4,5-dimethyl-1,3,2-dioxaphosphol-4-ene (5b)

These compounds were obtained via (2-deoxy-2-heptyl-3-hexanoyl-glyceryl)dimethylphosphite (^{31}P NMR: δ 140.7) according to similar procedures as described for the synthesis of 1a-d₁ resp 1b-d₁. The P(IV) derivate 5a was purified by column chromatography on silica Woehlm, using ethyl acetate as eluens. ^{31}P NMR: δ 1.46. 1H NMR: δ 3.76 (d, 6H, OCH₃), 3.7 - 3.8 (m, 2H, H(3R), H(3S)), 4.0 - 4.1 (m, 2H, H(1R), H(1S)). Anal. Calcd. for $C_{18}H_{37}PO_6$: C, 56.82; H, 9.80. Found C, 56.82; H, 9.83.

The P(V) derivative 5b: ^{31}P NMR: δ -49.2. 1H NMR: δ 1.82 (s, 6H, CH₃ dioxaphospholene ring), 3.58 (d, 6H, OCH₃), 3.7 - 3.9 (m, 2H, H(3R), H(3S)), 4.0 - 4.1 (m, 2H, H(1R), H(1S)).

References and notes

1. H. Hauser, I. Pascher, R.H. Pearson and S. Sundell, *Biochim. Biophys. Acta* 650 (1981) 21.
2. H. Hauser, W. Guyer, I. Pascher, P. Skrabal and S. Sundell, *Biochemistry* 19 (1980) 366.
3. I.I. Merkelbach, Ph.D. Thesis, Eindhoven University of Technology (1985).
4. I.I. Merkelbach and H.M. Buck, *Recl. Trav. Chim. Pays-Bas* 102 (1983) 283.
5. L.H. Koole, E.J. Lanters and H.M. Buck, *J. Am. Chem. Soc.* 106 (1984) 5451.
6. L.H. Koole, R.J.L. van Kooyk and H.M. Buck, *J. Am. Chem. Soc.* 107 (1985) 4032.

7. The stereospecific numbering (sn) indicates that the groups attached to the chiral center C(2) are numbered 1 to 3 in the conventional top to bottom sequence when the oxygen at C(2) is located on the left side of the glyceryl carbon chain in the usual Fischer projection. When in the sn convention the hydrocarbon chains are numbered 1 and 2 respectively, this corresponds with an L configuration in the Fischer notation. (see IUPAC-IUB Commission on Biological Nomenclature, Eur. J. Biochem. 79 (1977) 11).
8. R.J.E.M. de Weerd, J.W. de Haan, L.J.M. van de Ven, M. Achten and H.M. Buck, J. Phys. Chem. 86 (1982) 2528.
9. R. Wohlgemuth, N. Waespe-Šarčević and J. Seelig, Biochemistry 19 (1980) 3315.
10. H. Günther, M. Kellner, F. Biller and H. Simon, Angew. Chem. 85 (1973) 141.
11. The enantiomerically pure alcohol must be used, otherwise a diastereomeric mixture is obtained after the stereo-specific H/D-exchange, in which the H(3S) protons are magnetically inequivalent.
12. H. Batiz-Hernandez and R.A. Bernheim, Prog. Nucl. Magn. Res. Spec. 3 (1967) 67.
13. C.A.G. Haasnoot, F.A.A.M. de Leeuw and C. Altona, Tetrahedron 36 (1980) 2783.

In this generalized equation the standard Karplus relation is extended with a correction term which accounts for the influence of electronegative substituents on $^3J_{HH}$: $^3J_{HH} = 13.22\cos^2\varphi - 0.99\cos\varphi + \Sigma(0.87 - 2.46\cos^2(\xi_i\varphi + 19.9|\Delta\chi_i|))\Delta\chi_i$; φ is the dihedral angle between the protons, $\Delta\chi_i$ is the difference in electronegativity between the substituent (i) and hydrogen according to the electronegativity scale of Huggins and ξ_i is a substituent orientation parameter. Substituting the numerical values for the case the sn-2 chain is linked via an oxygen to the backbone, and relating the coupling constants of the g^+ , g^t and g^- conformers to the experimental coupling constants

gives:

$$x(g^+) = - 0.075 J_{H(2)H(i)} - 0.100 J_{H(2)H(j)} + 1.303,$$

$$x(g^t) = - 0.054 J_{H(2)H(i)} + 0.104 J_{H(2)H(j)} + 0.061,$$

$$x(g^-) = + 0.129 J_{H(2)H(i)} - 0.003 J_{H(2)H(j)} - 0.364,$$

and in case the sn-2 chain is linked via a methylene group to the backbone:

$$x(g^+) = - 0.085 J_{H(2)H(i)} - 0.085 J_{H(2)H(j)} + 1.332,$$

$$x(g^t) = - 0.025 J_{H(2)H(i)} + 0.110 J_{H(2)H(j)} - 0.166,$$

$$x(g^-) = + 0.110 J_{H(2)H(i)} - 0.026 J_{H(2)H(j)} - 0.166,$$

with $i = 1S, 3R$; and $j = 1R, 3S$.

14. S. Wolfe, Acc. Chem. Res. 5 (1972) 102.
15. In this P(V) compound the assignment of H(1S) and H(1R) most likely reverses, otherwise the g^- conformer will contribute to an improbably high extent, which is in sharp contrast with the well-known parallel alignment of the hydrocarbon chains [2].
16. F. Jähnig, K. Harlos, H. Vogel and H. Eibl, Biochemistry 18 (1979) 1461.
17. R.H. Bromilow, S.A. Khan and A.J. Kirby, J. Chem. Soc. Perkin II (1972) 911.
18. It must be emphasized that in the given example from literature [17] the excellent leaving group capacity of the aryl oxygen ligands also leads to the irreversible formation of P(IV) products, a situation which cannot occur in the regular phospholipids.
19. J. Lecocq and C.E. Ballou, Biochemistry 3 (1964) 976.
20. R.G. Jensen and R.E. Pitas, Adv. Lip. Res. 14 (1976) 213.
21. K. Bruzik, R. Jiang and M. Tsai, Biochemistry 22 (1983) 2478.
22. R.J. Howe and T.J. Malkin, J. Chem. Soc. (1951) 2663.
23. A.E. Lippman, J. Org. Chem. 30 (1965) 3217.
24. D. Buchnea, Lipids 6 (1971) 734.
25. C. Mercier, A.R. Addas and P. Deslongchamps, Can. J. Chem. 50 (1972) 1882.

CHAPTER 3

Conformational transmission in anionic phospholipids.

The influence of headgroup charge on the conformational distribution in the glyceryl backbone

Abstract

A conformational analysis of the glyceryl backbone was performed on neutral, monoanionic and dianionic phosphatidic acids in the monomeric state. The results point out that an increase in formal headgroup charge brings about similar shifts in the conformational equilibria as were found for a P(IV) into a P(V)-TBP transition. The conformational changes are attributed to the enhanced electron density on O(3) as is indicated by calculations based on MNDO.

3.1 Introduction

Various studies deal with the elucidation of mechanisms by which the interactions between phospholipid headgroups can be modified. The understanding of the principles that govern these interactions is of considerable interest, since it is at this level that the membrane interacts with its environment. Most studies are primarily focussed on intermolecular electrostatic interactions. However, it is very likely that changes in the electrostatic balance will affect the conformational distribution in phospholipids. In this chapter the intramolecular consequences will be described when extra negative charge is introduced in the phosphate moiety of the lipid.

It was shown that on going from a formal headgroup charge of -1 to -2 in phospholipids the hydrocarbon chains become more tilted, i.e. the angle with the bilayer normal

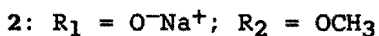
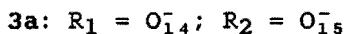
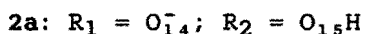
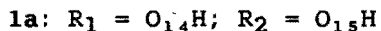
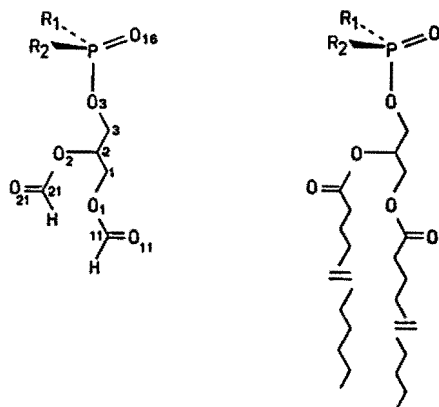


Fig. 1. Compounds 1a - 3a for the MNDO calculations and 1 - 3 for the experimental study.

increases [1,2]. This change in acyl chain packing was ascribed to an increase in effective headgroup area, due to the enhanced repulsive force between the phosphate moieties. However, it is very plausible that part of the extra headgroup charge will be delocalized on O(3) of the glyceryl backbone. Therefore, it is expected that the conformational equilibria in the glyceryl backbone will be shifted in an analogous direction as was found for the P(IV) \rightarrow P(V)-TBP transition. In order to estimate the charge transfer from the headgroup towards O(3), calculations based on MNDO were performed on phosphatidic acid (1a) and its deprotonated forms (2a and 3a) (Fig. 1). The theoretical result is compared with the experimentally obtained conformational distributions of a triesterified phospholipid compound 1 and its mono- and dianionic analogues 2 and 3.

3.2 Results and discussion

3.2.1 MNDO calculations

Calculations were carried out with the QCPE version of the MNDO program [3]. This program does not include d-orbital functions for phosphorus. However, a number of ab initio studies revealed that the principal concept of bonding is adequately described without the introduction of d-functions [4].

The geometries 1a-3a were fully optimized with respect to all variables, i.e. bond length, bond angles and torsion angles. The results of the calculations are listed in Table I. As can be seen, the net atomic charge on O(3) increases from -0.48 to -0.57 on abstracting a proton from phosphatidic acid. In the dianionic form the charge on O(3) is virtually not changed compared to the monomeric form.

Table I. Net atomic charge on some relevant atoms in compounds 1a-3a.

	neutral 1a	mono- anionic 2a	di- anionic 3a
O(3)	-0.480	-0.568	-0.582
O(2)	-0.345	-0.327	-0.310
O(1)	-0.347	-0.349	-0.353
O(21)	-0.346	-0.390	-0.433
O(11)	-0.355	-0.375	-0.395
O(14)	-0.475	-0.750	-0.863
O(15)	-0.488	-0.529	-0.875
O(16)	-0.634	-0.757	-0.889
P	1.366	1.324	1.285

3.2.2 Conformational analysis

Experimental support for the calculations was obtained by performing a ^1H NMR conformational analysis on the disodium salt of dipalmitoylphosphatidic acid (1) and the mono- and dimethylated analogues (2) and (3) respectively. In order to prevent aggregation of the charged lipids, the compounds were dissolved in CD_3OD . In this solvent the lipids are present in their monomeric forms [6], which could be confirmed by the linewidth of the ^{31}P resonance (< 0.04 ppm) [7].

The rotameric populations around C(1)-C(2) and C(2)-C(3) were calculated as in chapter 2 with the empirically generalized Karplus equation [8]. The assignment of the protons involved was the same as in (dihexanoylglyceryl)dimethylphosphate [9].

The data in Table II reveal that with the introduction

Table II. Conformational distribution around C(2)-C(3) and C(1)-C(2) in CD₃OD at 298 K in relation to the headgroup charge.

	1	2	3
(charge)	(0)	(-1)	(-2)
<u>C(2)-C(3):</u>			
J _{H(2)H(3R)} (Hz)	3.95	- ^a	5.37
J _{H(2)H(3S)} (Hz)	5.96	- ^a	5.66
x(g ⁺)	0.41		0.33
x(g ^t)	0.46		0.36
x(g ⁻)	0.13		0.31
<u>C(1)-C(2):</u>			
J _{H(2)H(1S)} (Hz)	3.68	3.28	2.90
J _{H(2)H(1R)} (Hz)	6.10	6.52	6.98
x(g ⁺)	0.41	0.40	0.38
x(g ^t)	0.50	0.56	0.62
x(g ⁻)	0.09	0.04	0.00
³¹ P (ppm)	1.3	4.2	6.6

^a could not be determined due to the near equivalence of the protons involved.

of formal charge in the phospholipid headgroup the conformational equilibria in the glyceryl backbone shift in the same direction as in the case of the P(IV) → P(V)-TBP transition; i.e. an increase in the g⁻ contribution around the C(2)-C(3) bond (O(2) and O(3) trans orientated) and a decrease in the g⁻ population around the C(1)-C(2) bond. Apparently, the extra negative charge in the phosphate headgroup in anionic phospholipids is accommodated according to the same mechanism as in the P(V)-TBP lipid. Unfortunately the conformational distribution around the C(2)-C(3) bond in the monomethylphosphatidic acid could not be resolved due to the near magnetic equivalence of

the protons involved.

A similar conformational distribution around C(2)-C(3) in the dianionic lipid is observed as in the corresponding P(V)-TBP lipid model under pseudorotating conditions.

Apparently, the increase in the O(3) electron density on going from the neutral to the dianionic state, corresponds to the extra charge density on O(3) in a pseudorotating P(V)-TBP structure with respect to the neutral phosphate.

As was demonstrated in chapter 2, the conformational distribution around the C(1)-C(2) bond is related to the O(1)-O(3) repulsion. An enhanced electron density on O(3) was found to result in a decreased O(1)-O(2) trans contribution. The same trend is observed in phosphatidic acid. A stepwise increase in formal headgroup charge from 0 to -2, results in a virtually constant decrease in the O(1)-O(2) trans population. However, the calculations do not indicate a substantial enhancement in the negative charge on O(3), upon going from the monoanionic to the dianionic form. This discrepancy between the computed and experimental results most probably originates from the shielding effect that the solvent molecules (methanol) exert on the charge in the anionic headgroups. As a consequence, the actual electron density on O(3) increases more gradually on raising the headgroup charge. Hence, the difference in charge on O(3) between the mono- and dianionic forms, as reflected in the respective conformational distributions around C(1)-C(2), will be more pronounced than theoretically predicted.

In natural phospholipids the headgroup charge can readily be modulated by divalent ions. It has been demonstrated that for instance Ca^{2+} ions can replace water molecules [10]. As a consequence, this replacement might result in an enhanced electron density in the phosphate moiety which, in turn, can be transferred to O(3), as the present results clearly point out.

The consequent conformational changes in the glyceryl backbone may very well induce different chain packing

modes in more ordered systems. This was indeed demonstrated by studies on lipid model compounds in which the rotational state of the backbone is restricted. Recently, it was found that the replacement of the glyceryl backbone by a cyclopentane 1,2,3-triol moiety in various diastereomeric forms, brings about a different chain packing mode for the O(2)-O(3) trans orientation compared to the O(2)-O(3) gauche orientations [11]. Furthermore, vesicles composed of these model phospholipids with O(2)-O(3) in the trans configuration, showed an increased permeability to sodium ions with respect to vesicles with the cis analogue. The findings on conformationally restricted lipids underline the importance of the rotamer state of the glyceryl backbone. The results presented in this and the previous chapter on the conformational transmission in phospholipids indicate the mechanisms by which the conformational equilibria may be modified.

3.3 Experimental section

3.3.1 Methods

¹H NMR spectra were recorded at 300.13 MHz on a Bruker CXP 300 spectrometer at room temperature. Chemical shifts were related to the signal of CD₂HOD at $\delta = 3.35$. ³¹P spectra were run on a Bruker AC 200 at 81.01 MHz with a 16k data set. The chemical shifts were related to 85% H₃PO₄ as an external standard.

3.3.2 Materials and synthesis

Solvents and reagents were reagent grade. The disodium salt of dipalmitoylphosphatidic acid was a Sigma product. (Dipalmitoylglyceryl)dimethylphosphate was synthesized according to established procedures outlined in chapter 2

starting from racemic dipalmitoylglycerol. The monomethylated derivative was obtained by refluxing the triesterified phosphate in dry methyl ethyl ketone with NaI [12].

References and notes

1. F. Jähnig, K. Harlos, H. Vogel and H. Eibl, *Biochemistry* 18 (1979) 1459.
2. H. Vogel, M. Stockburger and H. Träuble, *Proc. 5th Int. Conf. Raman Spectrosc.* (1976) 176.
3. M.J.S. Dewar and W. Thiel, *J. Am. Chem. Soc.* 99 (1977) 4899.
4. R.A.J. Janssen, G.J. Visser and H.M. Buck, *J. Am. Chem. Soc.* 106 (1984) 3429.
5. This value agrees well with the electron density of -0.59 on the axially located oxygen in a pentamethoxyphosphorane in a P(V)-TBP structure as calculated with MNDO, see N.K. de Vries and H.M. Buck, *Phosphorus and Sulfur*, 31 (1987) 267.
6. H. Hauser, W. Guyer, I. Pascher, P. Skrabal and S. Sundell, *Biochemistry* 19 (1980) 366.
7. A.C. McLaughlin, P.R. Cullis, J.A. Berden and R.E. Richards, *J. Magn. Reson.* 20 (1975) 146.
8. C.A.G. Haasnoot, F.A.A.M. de Leeuw, H.P.M. de Leeuw and C. Altona, *Recl. Trav. Chim. Pays-Bas* 98 (1979) 576.
9. G.H.W.M. Meulendijks, W. van Es, J.W. de Haan and H.M. Buck, *Eur. J. Biochem.* 157 (1986) 421.
10. M.B. Abramson, R. Katzman and H.P. Gregor, *J. Biol. Chem.* 239 (1964) 70.
11. M.A. Singer, M.K. Jain, H.Z. Sable and A.J. Hancock, *Biochim. Biophys. Acta* 731 (1983) 373.
12. D.A. McMillen, J.J. Volwerk, J. Ohishi and O.H. Griffith, *Biochemistry* 25 (1986) 182.

CHAPTER 4*

Conformational transmission in condensed lipid model compounds with four coordinated phosphorus and five coordinated silicon headgroups

Abstract

A ^{13}C CP-MAS NMR study is presented on the conformational transmission in a set of condensed diether lipid model compounds (oxy-lipids) with a four coordinated phosphorus (P(IV)) and five coordinated silicon (silatranes, Si(V)) as headgroups. The silatranes were chosen as realistic substitutes for P(V) lipids. The lipid models were referenced to analogues in which the O(2) is replaced by a methylene group (deoxy-lipids). An indication of the conformational preference of the glyceryl backbone was obtained by studying the lipid models in solution with ^{13}C and ^1H NMR or by making comparisons with the rotational state in strongly related lipid compounds. In the solid state the ^{13}C chemical shifts prove valuable probes for monitoring packing differences. The solid state results indicate tightly packed chain methyl groups in the oxy-silatrane lipid compared to the deoxy counterpart, whereas no differences in packing were found between the oxy- and deoxy-phosphates. Furthermore, a comparison between the oxy-silatrane and the oxy-phosphate lipid, reveals a similar packing difference as was found between both silatrane lipids. The observed differences in chain end arrangements were ascribed to the enhanced electron density on O(3) in the silatranes with respect to the P(IV) lipids, resulting in

* G.H.W.M. Meulendijks, J.W. de Haan and H.M. Buck, submitted for publication.

a O(2)-O(3) trans orientation in the oxy-silatrane. A mechanism is presented to account for the propagation of the headgroup change to the chain end region which is based on a reorientation of the glyceryl backbone with respect to the chain direction.

4.1 Introduction

In the preceding chapters it was demonstrated that increasing the electron density on O(3), results in specific rotations in the glyceryl backbone of phospholipid model compounds. However, these investigations were performed on lipid models in the monomeric phase. In order to mimic the ordered situation in the bilayer, the conformational transmission effects have to be studied in the condensed phase. Unfortunately however, attempts to solidify the P(V)-TBP phospholipid model failed, due to the intrinsic instability of the P(V)-TBP lipid [1]. Recently, it was demonstrated that related compounds with the P(V)-TBP phosphorus replaced by a five coordinated TBP-silicon (silatranes, Si(V)), also show conformational transmission effects [2,3]. This phenomenon was ascribed to the transfer of electron density from the nitrogen lone pair via the Si \leftarrow N transannular interaction [4], to the axially located oxygen in the Si-TBP. Considering the resemblance in conformational transmission effects, a five coordinated silicon derivative of dihexadecylglycerol was selected as a substitute for the P(V)-TBP lipid (Fig. 1). This novel artificial lipid could readily be obtained in a pure, solid state. Furthermore, the strong Si \leftarrow N dipole gives the silatrane lipid an amphiphilic character, therein resembling the natural occurring lipids.

In the condensed phase a precise and detailed conformational analysis, based on the scalar ^1H coupling constants, is still beyond the possibilities of the presently known NMR techniques. Therefore the ^{13}C nucleus is selected as an attractive probe for monitoring packing differences. The probe is non-perturbing and various sites in the lipid molecule can be studied in one experiment. Moreover, it was recently demonstrated by De Weerd et al., that the ^{13}C chemical shift is very sensitive to (dis)ordering effects in vesicular systems [5]. However, in order to gain detailed structural information about packing changes

in the condensed phase with ^{13}C NMR, cross-polarization (CP) and magic angle spinning (MAS) are a prerequisite to obtain narrow resonances in a reasonable time [6].

Although the conformational distributions found in solution, cannot a priori be extrapolated to the solid state, they do indicate which conformations are preferred. Therefore, ^1H and ^{13}C NMR analyses are performed on the model compounds in solution first.

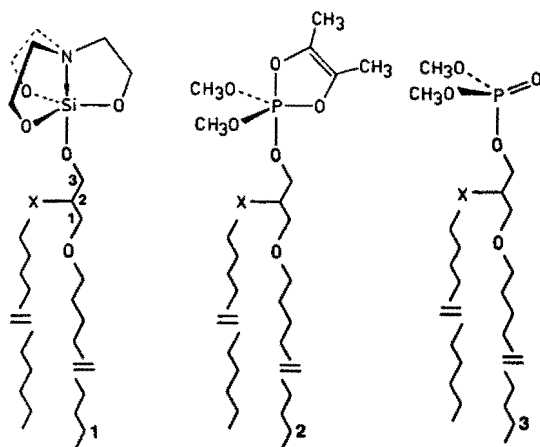


Fig. 1. Lipid model compounds 1A-3A ($\text{X}=\text{O}$) and 1B-3B ($\text{X}=\text{CH}_2$). The phosphoranes 2A and 2B could only be studied in an organic solvent.

Even more than in solution, the choice of the solid reference compounds is restricted to isosteric derivatives of the silatrane lipid, otherwise the observed packing differences cannot unequivocally be attributed to conformational changes. Therefore, a 2-deoxy-silatrane lipid is considered as a most suitable reference, since in this compound the vicinal electrostatic backbone repulsion with O(3) is absent. Based on the experimental findings for the P(V)-TBP counterparts in solution, it is expected that the g^- population around the C(2)-C(3) bond in the deoxy-silatrane will be substantially decreased with respect to the situation in the 2-oxy-silatrane [7].

To gain further support for the nature of the conformational transmission effect the corresponding triesterified phosphates have also been studied. It has been demonstrated that related oxy-phosphates have virtually the same conformational distribution around C(2)-C(3) in solution as the deoxy analogues [7]. Thus between both phosphates no marked differences are to be expected in the ^{13}C chemical shifts for the solid state.

4.2 Results

4.2.1 Conformational transmission in solution

The conformational analysis based on ^1H coupling constants was performed as outlined recently [7]. The diastereotopic protons attached to C(3) were assigned according to the findings on the P(IV) or P(V)-TBP derivative of 1,2-sn-dihexanoylglycerol [7]. The conformational distributions around C(2)-C(3) in the deoxy-silatrane and oxy-phosphate thus obtained, are compiled in Table I, along with the data on some compounds related to the oxy-silatrane and deoxy-phosphate. No conformational analyses were possible for these latter compounds, due to the near equivalence of the protons involved. However, it is possible to make a prediction about the preferred conformation around C(2)-C(3) in the oxy-silatrane by comparing the ^{13}C chemical shift dependence for C(3) on the nature of the headgroup in the lipid models with that for the corresponding C(5') nucleus in the related tetrahydrofurfuryl systems. In order to relate the ^{13}C chemical shift to the size of the conformational transmission effect, the set of lipid models was extended with a P(V)-TBP oxy and deoxy counterpart. The conformational distribution around C(2)-C(3) in the oxy-phosphorane is virtually the same as around the corresponding C(4')-C(5') bond in the P(V)-TBP tetrahydrofurfuryl system (Table I). The data in Table I

Table I. Conformational distributions^a around C(2)-C(3) for the lipid model compounds at 300 K in chloroform-d₁ and around the corresponding C(4')-C(5') bond in the tetrahydrofurfuryls in acetone-d₆^b. C(x) denotes the ¹³C chemical shift (in ppm) for C(3) in case of lipid models and C(5') in case of tetrahydrofurfuryl systems.

	x(g ⁺)	x(g ^t)	x(g ⁻)	C(x)
<u>Si(V)</u>				
tetrahydrofurfuryl ^c	0.30	0.18	0.52	66.4
oxy-dihexadecyl 1A	-	-	-	62.7
deoxy-dihexadecyl 1B ^h	0.33	0.44	0.23	64.0
<u>P(V)-TBP</u>				
tetrahydrofurfuryl ^d	0.25	0.14	0.61	67.49
tetrahydrofurfuryl ^e	0.32	0.35	0.33	69.9
oxy-dihexadecyl 2A ^j	0.36	0.35	0.29	66.6
deoxy-dihexadecyl 2B	-	-	-	67.8
<u>P(IV)</u>				
tetrahydrofurfuryl ⁱ	0.40	0.43	0.17	70.6
oxy-dihexadecyl 3A ^k	0.44	0.41	0.15	67.2
deoxy-dihexadecyl 3B	-	-	-	68.3
2-hexyl-3-hexanoylglyceryl ^f	0.40	0.37	0.23	
2-deoxy-2-heptyl-3-hexanoylglyceryl ^f	0.37	0.38	0.25	

^a x(g⁺) represents the fractional population of the conformation in which the vicinal orientated C and O are located gauche⁺. These atoms are located trans in the g^t arrangement and gauche⁻ in the g⁻ conformation. This g⁻ arrangement corresponds with the conformer in which the vicinal oxygens are located trans. ^b the conformational distribution in acetone-d₆ does not substantially deviate from that in chloroform-d₁, since the solvent polarities are very much alike. ^c data taken from [2]. ^d data taken from [8] for axially located tetrahydrofurfuryl. ^e data taken from [8] not corrected for phosphorus pseudorotation. ^f data taken from chapter 2. ^g data taken from [9]. ^h J_{H(2)H(3R)} = 5.11 Hz; J_{H(2)H(3S)} = 6.67 Hz. ⁱ data taken from [8]. ^j J_{H(2)H(3R)} = 5.20 Hz; J_{H(2)H(3S)} = 5.29 Hz. ^k J_{H(2)H(3R)} = 4.11 Hz; J_{H(2)H(3S)} = 5.52 Hz.

reveal that within the tetrahydrofurfuryl series P(IV), P(V)-TBP, Si(V)-TBP the electron density on O(5') increases (reflected in an enhanced g^- contribution around C(4')-C(5')) with a concomitant shielding of the C(5') nucleus. Especially the C(5') in Si(V) is clearly shielded with respect to the P(V) (3.5 ppm). Exactly the same pattern appears for the lipid models. Also in the oxy-silatrane a shielding is observed for the C(3) nucleus with respect to the oxy-phosphorane (3.9 ppm), similar to that for the tetrahydrofurfuryls. Since the short range substitution effect (due to replacing phosphorus by silicon) contributes for ca. 1 ppm [10], the remaining part of the shielding of C(3) thus originates from an enhanced electron density on O(3) and the directly related conformational changes in the oxy-silatrane compared to the oxy-phosphorane. This result indicates that in the oxy-silatrane lipid the g^- conformation around C(2)-C(3) will be strongly preferred, completely analogous with the tetrahydrofurfuryl silatrane. Accordingly, in the deoxy-silatrane in which the 1,4 electrostatic repulsion is absent (vide supra), the g^- population is drastically decreased to 23% and approximates the value found in the oxy-phosphate.

Although the conformation in the deoxy-phosphate could not be elucidated, a close similarity in rotational behaviour is assumed for the oxy- and deoxy-phosphate on the one hand and (2-hexyl-1-hexanoylglycerol)dimethoxyphosphate and its deoxy counterpart on the other hand [7]. Therefore, between both phosphate lipids studied here, no major conformational differences will exist.

4.2.2 Conformational transmission in the solid state

Fig. 2 shows the ^{13}C CP-MAS NMR spectrum of the silatrane compound of L-1,2-sn-dihexadecylglycerol along with the 2-deoxy counterpart. The solid state chemical shifts of the silatrane and phosphate lipids are assigned accord-

ing to the findings for the compounds in solution (Table IV, page 67) and are compiled in Table II. Although the solid state spectra are characterized by broad lines, some interesting differences in chemical shift appear between the L and DL forms of the oxy-silatrane and between the oxy- and deoxy-silatrane. In the optically pure oxy-silatrane, the inner methylene carbons of the chains and the ultimate methyl carbon have shifted downfield by ca. 0.6 ppm with respect to the racemic modification and resonate at 33.7 and 15.8 ppm respectively. A similar chemical shift for the inner methylene carbons was found in the deoxy-silatrane. It has been well established that hydrocarbon chains with a chemical shift ranging from 33.6 to 34.3 are arranged in a triclinic lattice with parallel chain planes, whereas chains resonating at ca. 33.0 ppm are packed in one of the other crystallographic structures, i.e. orthorhombic, pseudo-hexagonal or monoclinic with perpendicular chain planes [11-13]. Therefore we conclude that the L-oxy- and DL-deoxy-silatrane are packed in triclinic cells, whereas the DL-oxy-silatrane and the phosphates are packed in another lattice (which one is of less importance since the chemical shifts of the inner

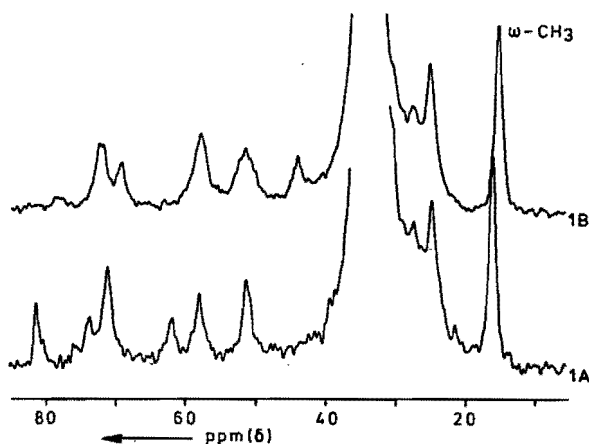


Fig. 2. ^{13}C CP-MAS NMR spectra of the L-oxy- (1A) and DL-deoxy- (1B) silatrane lipids.

Table II. The solid state ^{13}C chemical shifts^a (in ppm) for the enantiomerically pure and racemic silatranes and phosphates. The experimental conditions are compiled in the experimental section. α and ω indicate the first and terminal chain carbon, respectively. The lattices are denoted with NT: non-triclinic and T: triclinic.

	silatrane			phosphate		
	2-oxy		2-deoxy	2-oxy		2-deoxy
	DL-form	L-form	DL-form	DL-form	L-form	DL-form
	NT	T	T	NT	NT	NT
C(3)	61.80	61.53	68.84	67.03	67.01	69.19
C(2)	83.29	81.14	41.45	78.10	77.99	40.05
C(1)	73.61 ^b	70.87 ^b	72.23 ^b	71.72 ^b	71.73	70.80
α sn-1	73.61 ^b	70.87 ^b	71.54 ^b	71.72 ^b	71.73	70.80
sn-2	75.63 ^b	73.42 ^b		71.00 ^b	71.73	
internal	33.12	33.67	33.68	33.08	33.09	33.13
ω -1	24.83	24.62	24.76	24.37	24.30	24.30
ω	15.13	15.77	14.85	14.40	14.39	14.41
POCH ₃				54.64	54.63	54.76
SiOCH ₂ ^c	58.05	57.67	57.53			
NCH ₂ ^c	51.45	51.20	51.20			
$^{29}\text{Si}^c$	-95.11	-95.19	-96.30			

^a estimated accuracy \pm 0.05

^b resonances could not be assigned properly.

^c in agreement with the values reported in [14,15].

chain carbons are identical in all three cells). Hence the chemical shift differences between DL- and L-oxy-silatranes result from the different lattices in which the chains are packed.

It is very unlikely that the substitution of the 2-oxygen by a methylene group would bring about a different crystallographic form (the bond length and angle are

quite similar in both compounds). This supposition is supported by recent X-ray and electron diffraction studies in which no change in the type of chain (sub)cells was found when the ester linkage in 1,2-sn-dipalmitoylphosphatidylcholine was replaced by ether bonds [16,17]. Therefore, one has to compare lipids within one type of crystallographic cell for a proper evaluation of the observed ^{13}C chemical shift differences.

Thus comparing L-oxy- and DL-deoxy-silatrane both with triclinic lattices, a marked shielding of 7.3 ppm is observed for C(3) in the oxy form. The ca. 40 ppm difference for C(2) is mainly due to the short range substitution effect and appears as well between the oxy- and deoxy-phosphate lipids. A remarkable deshielding of 0.9 ppm occurs for the ultimate methyl groups in the oxy-silatrane with respect to the deoxy counterpart. Such a large shift difference has never been observed within one crystallographic class. The deshielding effect originates from an increase in packing density in this area, since it is well documented that the ^{13}C nuclei of two approaching methyl groups become less shielded due to the mutual depolarization effect of the C-H bonds of the respective groups [18]. In addition, the optimum cross-polarization contact time for the terminal methyl groups decreases from 1.5 ms to 1.0 ms on going from the deoxy- to the oxy-silatrane (Table III). This result also indicates that in the oxy compound the methyl groups are more ordered, since the resonance intensities of carbons in more mobile regions in a molecule reach their maximum at longer contact times compared to the signals of carbons in restricted areas [6]. In contrast with the chemical shift differences found in the silatranes, no differences in the chain region are observed between the oxy- and deoxy-phosphate. Apparently, in these latter compounds the chain packing is not affected by the substitution in the glyceryl backbone. In line with this result is the observation that both phosphates have the same optimum contact times for the methyl groups.

Table III. Optimum contact time^a in ¹³C CP-MAS NMR (in ms) for solid silatranes and phosphates. The lattices are denoted with NT: non-triclinic, and T: triclinic.

	<u>Silatrane</u>		<u>Phosphate</u>	
	<u>oxy</u>	<u>deoxy</u>	<u>oxy</u>	<u>deoxy</u>
	L-form	DL-form	L-form	DL-form
	T	T	NT	NT
internal	0.7	0.8	1.7	1.7
ω -CH ₃	1.0	1.5	4.0	4.0

^a Estimated accuracy \pm 0.2 ms.

Between the DL-oxy-silatrane and the DL-oxy-phosphate a similar shift difference for the ultimate methyl groups is observed as between the triclinic forms of the oxy- and deoxy-silatrane. Within the former set of lipids the head-group areas are very much alike, as indicated by Dreiding models (ca. 46 Å² for the silatrane and 41 Å² for the phosphate) and the alkyl chains are arranged in non-triclinic lattices. Therefore, the comparable chemical shift differences for the terminal methyl groups within both sets suggest a similar packing difference between L-oxy- and DL-deoxy-silatrane on the one hand and between DL-oxy-silatrane and DL-oxy-phosphate on the other hand.

4.3 Discussion

The combined results in the solution and condensed phases suggest that substantial changes in the chain end region can be brought about by changing the conformational state of the glyceryl backbone. The close resemblance in the C(3) chemical shift in the oxy-silatrane in solid

state and solution seems indicative for a similar conformation of the molecule in both phases. In the solid phase a difference in the rotational state of the backbone between the oxy-silatrane and the deoxy-silatrane clearly appears from the drastically deshielded (7.4 ppm) C(3) nucleus in the deoxy-silatrane with respect to the oxy-silatrane. This deshielding is partly due to a short range substitution effect. From a comparison of the C(3) chemical shifts in the oxy- and deoxy-phosphate in solution, with similar backbone conformations, it is estimated that this effect contributes ca. 1 ppm to the deshielding of C(3). The remaining part must then be brought about by conformational differences. It is well established that such a large deshielding effect on C(3) can originate from a conformational change around a C(3)-C-C-X bond (with X = O,C) from a gauche into a trans arrangement [19]. Thus the deoxy-silatrane should have one C(3)-trans interaction more compared to the C(3) in the oxy-silatrane. This, in combination with the findings regarding the preferred conformation in solution (vide supra), is related to the observed different chain end packing in the solid L-oxy- and deoxy-silatrane, as follows (see Fig. 3). In the solid state a g^- conformation around the C(2)-C(3) bond in the oxy-silatrane and a packing for the rest of the lipid similar to the one in the deoxy-silatrane, would induce steric repulsions between the silatrane cage and the sn-2 chains of neighbouring lipids. Such a g^- conformation can be accommodated when in addition the glyceryl backbone is situated more parallel to the layer plane. This orientation however, does not result in a more densely packed chain end, unless the reorientation is accompanied by a conformational change around the C(1)-C(2) bond from a g^t into a g^+ arrangement. In addition, small changes in the torsion angles of the first part of the sn-2 chain are necessary to restore the parallel alignment of the chains. Consequently, the characteristic bend at the beginning of the sn-2 chain is largely eliminated, resulting in

a reduced effective chain length difference between the sn-1 and sn-2 chain. Hence the average packing densities of the methyl groups increase.

In accordance with this mechanism is the observed shielding of C(3) in the oxy-silatrane, since the net effect of the conformational change around the C(1)-C(2) bond is a transition from a C(3)-O(1) trans orientation in the deoxy-silatrane into a C(3)-O(1) gauche arrangement in the oxy counterpart. Indeed, as a consequence of this transition, with a substitution and a conformational

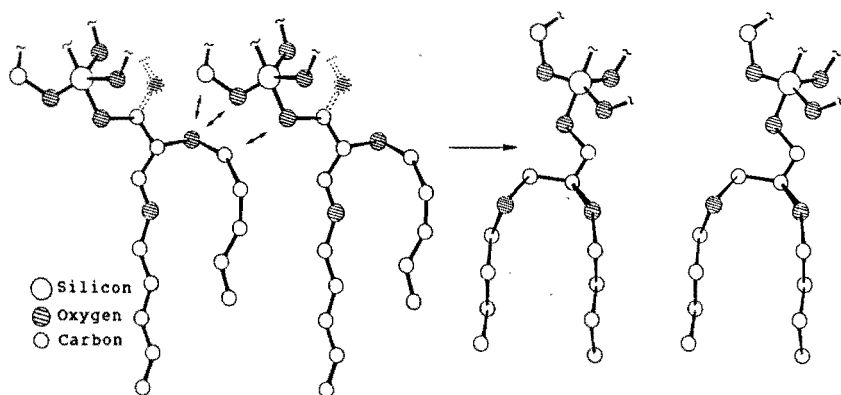


Fig. 3. Conformational transmission in the condensed phase. Left part: The silatrane cage in a gauche (dashed lines) and anti (drawn lines) conformation with respect to the sn-2 chain. This latter arrangement induces steric repulsions between the headgroup and the sn-2 chains of neighbouring molecules. Right part: oxy-silatrane lipid with the glyceryl backbone in a layer parallel orientation and the O(2) and O(3) vicinal oxygens orientated trans. The chain methyl groups are clearly more densely packed in such an arrangement than in the case depicted in the left part.

effect (vide supra), a shielding of ca. 7.3 ppm is realistic [20].

In line with this extended conformational transmission model is the observation that between DL-oxy-silatrane and DL-oxy-phosphate, both in a solid, non-triclinic structure, a similar packing difference was found for the ultimate methyl group as between the L-oxy- and deoxy-silatrane, both in a triclinic form. Both findings can be traced back to the conformational transmission effect. The lower electron density on O(3) in the oxy-phosphate relative to the oxy-silatrane results in a decreased g^- conformation around the C(2)-C(3) bond in the oxy-phosphate. A similar packing change occurs when the enhanced electron density in a silatrane lipid compared to the oxy-phosphate cannot lead to an increased g^- population by the absence of a vicinally orientated oxygen as in the deoxy-silatrane.

Finally, support for this model comes from the oxy- and deoxy-phosphates, with a similar rotational state in solution, showing virtually the same chemical shifts and optimum contact times for the hydrocarbon chains in the solid state.

Thus it is demonstrated that conformational transmission effects originating in the headgroup can be transferred to the chain end region, simply by a reorientation of the glyceryl backbone. A change in the glyceryl backbone orientation from a more perpendicular to a more parallel arrangement with respect to the bilayer plane was also assumed in the high pressure induced transition in dioleoylphosphatidylcholine, thereby allowing an optimal packing of the cis-double bonds [21]. As a result of the rearrangement of the glyceryl backbone, a condensing effect on the methyl groups was found with i.r.-spectroscopy, analogous to the observations for the silatranes.

4.4 Concluding remarks

It has already been demonstrated that silatranes are very suitable substitutes for P(V)-TBP models in solution. In this chapter evidence is presented for conformational transmission effects in the solid state. In the solid phase remarkable differences were observed in the chain end packing between L-oxy- and deoxy-silatrane and between DL-oxy-silatrane and DL-oxy-phosphate. In both sets of lipid models the differences can be attributed to conformational transmission effects. The underlying mechanism is based upon an enhanced electron density on O(3) in the silatrane compounds relative to the phosphate counterparts. As a consequence the O(2)-O(3) backbone repulsion in the oxy-silatrane is increased, leading to a preference for the g^- conformation relative to the oxy-phosphate but also compared to the deoxy-silatrane in which the conformational transmission is inhibited. Steric restrictions in the solid state however, prevent an O(2)-O(3) trans-arrangement, without a reorientation of the backbone taking place at the same time. Apparently, the electronic repulsion is sufficiently strong to bring about a different chain packing mode, in which at least the methyl groups are more densely packed.

4.5 Experimental section

4.5.1 NMR spectroscopy

The solution ^1H , ^{13}C and ^{31}P NMR spectra were obtained at 200.13, 50.32 and 81.02 MHz respectively, using a Bruker AC-200 NMR spectrometer. In order to facilitate the elucidation of very complicated ^1H patterns, some spectra were recorded on an AM-500 NMR spectrometer at the Dutch National NMR Facility in Nijmegen. Samples were routinely dissolved in CDCl_3 and the chemical shifts were related to

TMS in case of the ^1H and ^{13}C shifts and to H_3PO_4 as external standard in case of the ^{31}P shifts. The solid state ^{13}C and ^{29}Si CP-MAS NMR spectra were recorded at 75.48 and 59.63 MHz respectively on a Bruker CXP-300 NMR spectrometer equipped with a double air-bearing CP-MAS probe. The samples were stored in Kel-F capsules [22] which were sealed and used in aluminium oxide MAS rotors. By using these capsules moisture was kept out, and the sample amount could in principle be as low as a few milligrams without spinning instability problems. The temperature was about 300 K. The chemical shifts were related to TMS (in case of ^{13}C via adamantane). The cross-polarization measurements were carried out with flipback of the proton magnetization and spin temperature inversion. The CP-MAS parameters were: time domain of 1k data points; spectral width 17.2 kHz for ^{13}C and 20 kHz for ^{29}Si ; pulse width 6 μs ; contact and acquisition time 2.5 ms and 29 ms, respectively for ^{13}C , and 6 ms and 10 ms, respectively for ^{29}Si ; pulse delay 2 s for the silatranes and 3 s for the phosphates. The samples were rotated at 3 kHz. The reported chemical shifts were averaged values of at least two measurements with a deviation of less than 0.05 ppm.

4.5.2 Synthesis

The enantiomerically pure precursor 1,2-*sn*-dihexadecylglycerol was synthesized according to the method of Yamauchi et al. [23] starting from D-mannitol. The racemic modification of the alcohol was obtained by the same procedure but in this case starting from racemic 2,2-dimethyl-1,3-dioxolane-4-methanol (Janssen Chimica).

2-Hydroxymethylnonadecanol

To a stirred suspension of 1.8 g (75 mmol) NaH in 30 ml of dry DMF was added 7.2 g (45 mmol) diethyl malonate. After keeping the solution at 85°C for 1 h, 7.2 g (23

mmol) heptadecyl bromide was added dropwise at room temperature. The mixture was allowed to stand for 72 h, after which 200 ml H₂O was added. Then the solution was brought to pH = 5 with 6N hydrochloric acid. Extraction with diethyl ether, subsequent treatment with H₂O, and thorough drying of the organic layer, yielded 2.2 g of crude product which was used without further purification in the next reaction step. To a solution of 1.8 g (47 mmol) LiAlH₄ in anhydrous diethyl ether was added 8.2 g (21 mmol) of the alkylated diethyl malonate at 0°C. After refluxing the solution for 1 h the mixture was worked up according to standard procedures, resulting in 5.9 g (90%) of 2-hydroxymethyl nonadecanol. ¹H NMR: δ 0.88 (t, 3H, CH₃), 1.25 (m, 32H, CH₂), 1.7 - 2.1 (m, 3H, CH + OH), 3.75 (m, 4H, CH₂O).

2-Deoxy-2-heptadecyl-3-hexadecylglycerol

Alkylation was performed according to Yamauchi [23] with 1.8 g (6 mmol) alcohol and 3.5 g (9 mmol) hexadecyl tosylaat [24]. Purification was obtained by recrystallization from ethyl acetate. ¹H NMR: δ 0.88 (t, 6H, CH₃), 1.28 (m, 48H, CH₂), 1.56 (m, 4H, βCH₂), 2.18 (m, 1H, CH), 3.3 - 3.8 (m, 7H, CH₂O + OH).

(2,3-Dihexadecylglyceryl)silatrane 1A and (2-deoxy-2-hexadecyl-3-heptadecylglyceryl)silatrane 1B

The silatranes were synthesized according to a procedure developed by Voronkov et al. [25] with slight modifications. Triethanolamine and tetraethyl orthosilicate were distilled before use. The alcohol was dried in vacuo over P₂O₅. Equimolar amounts of the reagents and a catalytic amount of KOH were mixed in toluene. The mixture was stirred for 24 h at 100°C during which the formed ethanol was azeotropically removed. After removing the solvent the crude product was crystallized twice from hot hexane.

1A: ¹H NMR: δ 0.88 (t, 6H, CH₃), 1.25 (m, 48H, CH₂) 1.58

(m, 4H, β CH₂), 2.84 (t, 6H, SiOCH₂), 3.38 - 3.80 (m, 9H, CH, CH₂O), 3.82 (t, 6H, NCH₂).

1B: ¹H NMR: δ 1.80 (m, 1H, CH), 2.83 (t, 6H, SiOCH₂), 3.27 - 3.68 (m, 6H, CH₂O), 3.83 (t, 6H, NCH₂).

The solid state-²⁹Si and the solution-¹³C NMR chemical shifts are compiled in Tables II and IV, respectively.

2,2-Dimethoxy-2-(2,3-dihexadecylglycero)2,2-dihydro-4,5-dimethyl-1,3,2 dioxaphosphol-4-ene 2A and 2,2-dimethoxy-2-(2-deoxy-2-heptadecyl-3-hexadecylglycero)-2,2-dihydro-4,5-dimethyl-1,3,2-dioxaphosphol-4-ene 2B

The phosphoranes were prepared according to procedures described in chapter 2.

2A: ¹H NMR: δ 0.88 (t, 6H, CH₃), 1.26 (m, 52H, CH₂), 1.54 (m, 3H, CH+ β CH₂), 1.82 (s, 6H, CH₃), 3.4 - 3.7 (m, 6H, OCH₂), 3.60 (d, 6H, POCH₃), 3.91 (m, 2H, POCH₂). ³¹P NMR: δ -48.87.

2B: ¹H NMR: δ 1.55 (m, 1H, CH), 1.82 (s, 6H, CH₃), 3.38 (t, 4H, OCH₂), 3.58 (d, 6H, POCH₃), 3.87 (m, 2H, POCH₂). ³¹P NMR: δ -48.74.

The ¹³C solution NMR chemical shifts of both phosphoranes are compiled in Table IV.

(2,3-Dihexadecylglyceryl)dimethylphosphate 3A and (2-deoxy-2-hexadecyl-3-heptadecylglyceryl)dimethylphosphate 3B

The phosphates were prepared via essentially the same procedure as outlined in chapter 2.

3A: ¹H NMR: δ 0.88 (t, 6H, CH₃), 1.25 (m, 52H, CH₂), 1.54 (m, 4H, β CH₂), 3.77 (d, 6H, POCH₃), 3.35 - 3.68 (m, 7H, OCH₂ + CH), 3.98 - 4.24 (m, 2H, POCH₂). ³¹P NMR: δ 1.95.

3B: ¹H NMR: δ 1.89 (m, 1H, CH), 3.38 (m, 4H, OCH₂), 3.78 (d, 6H, POCH₃), 4.05 (t, 2H, POCH₂). ³¹P NMR: δ 2.06.

The ¹³C solution NMR chemical shifts are compiled in Table IV.

Table IV. The solution ^{13}C NMR chemical shifts (in ppm) for the silatranes Si(V), phosphoranes P(V)-TBP and the phosphates P(IV) in CDCl_3 . α and ω represent the first and terminal chain carbon, respectively. The coupling constants with phosphorus (in Hz) are given in parenthesis.

	<u>silatrane</u>		<u>phosphorane</u>		<u>phosphate</u>	
	1A	1B	2A	2B	3A	3B
	2-oxy	2-deoxy	2-oxy	2-deoxy	2-oxy	2-deoxy
C(3)	62.74	64.02	66.64	67.81	67.25	68.30
			(11.2)	(11.1)	(6.1)	(6.2)
C(2)	79.78	41.45	78.14	40.18	77.33	39.76
			(9.1)	(8.2)	(7.2)	(7.5)
C(1)	72.41	72.23	71.45	71.20 ^a	71.46	71.90
α sn-1	71.47	71.02	71.00	71.31 ^a	69.70 ^a	70.14
sn-2	70.46		70.33		70.80 ^a	
internal	29.81	29.85	29.82	29.78	29.77	29.79
ω -1	22.78	22.83	22.82	22.86	22.77	22.78
ω	14.18	14.26	14.15	14.20	14.18	14.20
POCH_3			54.87	54.99	54.37	54.27
			(10.8)	(10.5)	(5.8)	(5.9)
$\text{SiOCH}_2^{\text{b}}$	57.83	57.93				
NCH_2^{b}	51.41	51.37				

^a resonances could not be assigned properly.

^b in agreement with the values reported in [15].

References and Notes

1. Attempts to solidify the P(V)-TBP lipid model compounds resulted in a rearrangement of the headgroup to a four coordinated derivative. The structure of the resulting product and mechanism are not clear at the moment, but a compressive force on the headgroup,

caused by optimizing the Van der Waals contacts between the hydrocarbon chains, might be the reason for this coordinational transition. Moreover, it was found that the addition of 2 equivalents of octadecane stabilizes the P(V)-TBP geometry, probably as a result of cancelling the mismatch between the cross-sectional area of the headgroup and the hydrocarbon chains.

2. M.H.P. van Genderen and H.M. Buck, Recl. Trav. Chim. Pays-Bas 106 (1987) 449.
3. M.H.P. van Genderen and H.M. Buck, Magn. Reson. Chem. 25 (1987) 872.
4. J.W. Turley and F.P. Boer, J. Am. Chem. Soc. 90 (1968) 4026.
5. R.J.E.M. de Weerd, J.W. de Haan, L.J.M. van de Ven, M. Achten and H.M. Buck, J. Phys. Chem. 86 (1982) 2523.
6. C.S. Yannoni, Acc. Chem. Res. 16 (1982) 201.
7. G.H.W.M. Meulendijks, W. van Es, J.W. de Haan and H.M. Buck, Eur. J. Biochem. 157 (1986) 421.
8. L.H. Koole, E.J. Lanters and H.M. Buck, J. Am. Chem. Soc. 106 (1984) 5451.
9. N.K. de Vries and H.M. Buck, Phosphorus and Sulfur 31 (1987) 267-279.
10. This estimation is based upon comparisons of the α - ^{13}C chemical shifts of various silicon and phosphorus compounds.
11. M. Takenaka, T. Yamanobe, T. Komoto, I. Ando and H. Sato, Solid State Communications 61 (1987) 563.
12. D.L. VanderHart, J. Magn. Reson. 44 (1981) 117.
13. T. Yamanobe, T. Sorita, T. Komoto, I. Ando and H. Sato, J. Mol. Struct. 131 (1985) 267.
14. M. Ya Myagi, A.V. Samoson, E.T. Lippmaa and M.G. Voronkov, Doklady Phys. Chem. 25 (1980) 345.
15. J.M. Bellama, J.D. Nies and N. Ben-Zvi, Magn. Reson. Chem. 24 (1986) 748.
16. D.L. Dorset, Biochim. Biophys. Acta 898 (1987) 121.
17. M.J. Ruocco, D.J. Siminovitch and R.G. Griffin, Biochemistry 24 (1985) 2406.

18. D.M. Grant and B.V. Cheney, *J. Am. Chem. Soc.* 89 (1967) 5315.
19. J.D. Roberts, F.J. Weigert, J.I. Kroschwitz and N. Reich, *J. Am. Chem. Soc.* 92 (1970) 1338.
20. E.L. Eliel, W.F. Bailey, L.D. Kopp and D.W. Cochran, *J. Am. Chem. Soc.* 97 (1975) 322.
21. D.J. Siminovitch, P.T.T. Wong and H.H. Mantsch, *Biochemistry* 26 (1987) 3277.
22. W.T. Ford, S. Mahanray and H. Hall, *J. Magn. Reson.* 65 (1985) 156.
23. K. Yamauchi, F. Une, S. Tabata and M. Kinoshita, *J. Chem. Soc. Perkin Trans I* (1986) 765.
24. D.A. Shirley and W.H. Reedy, *J. Am. Chem. Soc.* 73 (1951) 458.
25. M.G. Voronkov and G.I. Zelchan, *Khim. Geteros. Soed.* 1 (1965) 210.

CHAPTER 5*

A ^{13}C CP-MAS NMR study on the chain packing in anhydrous and hydrated DL- and L-dipalmitoylphosphatidylcholine

Abstract

With ^{13}C CP-MAS NMR it is demonstrated that the anhydrous forms of DL- and L-DPPC show pronounced packing differences in both the headgroup region and the hydrocarbon part of the bilayer. In DL-DPPC the acyl chains and more specifically their end groups are more ordered than in the L-modification. The anhydrous L- and DL-DPPC structures show a completely different behaviour towards the addition of one equivalent of water. DL-DPPC is far less hygroscopic and forms small domains of dihydrated and anhydrous DPPC as was concluded from the combined results of the NMR and a DSC study. The dihydrated form of DL-DPPC is arranged according to a similar structure as is observed for anhydrous L-DPPC. On the other hand, L-DPPC did not show any packing changes in the acyl chains on going from the anhydrous state to the hydrated forms. These results reveal that stereospecific interactions can be responsible for different lipid packing modes and hence in their behaviour towards the uptake of water.

* G.H.W.M Meulendijks, J.W. de Haan, A.H.J.A. Vos, L.J.M. van de Ven and H.M. Buck, submitted for publication.

5.1 Introduction

There is strong experimental evidence that various membrane processes are regulated by a controlled change in the fluidity of parts in the membrane (domains) [1-3]. The action of some anaesthetics on ion-channels is supposed to occur via an alteration in the packing of the lipids which surround the channel [4-6]. A change in the lipid structure can already be induced by a local dehydration of phospholipids. For instance, it has been shown that the transmembrane channel gramicidin can locally withdraw water from phosphatidylcholines [7]. With the removal of the water molecules, the lipid formal charges become more exposed, and hence the intermolecular electrostatic headgroup interactions will be intensified, resulting in a smaller effective cross-sectional headgroup area and an increased polarity in the headgroup region. A change in the polar headgroup conformation or properties can very well affect the packing of the lipid acyl chains, which in turn might influence the activity of some membrane proteins.

It has been shown using Raman spectroscopy, that the reversed process, i.e. the hydration of anhydrous bilayers, induces a marked change in the motional and conformational properties of the headgroup [8]. Moreover, the addition of about four equivalents of water to dipalmitoylphosphatidylcholine (DPPC) resulted in a drastic increase in the intrachain (gauche/anti) and interchain (lattice) disorders. Therefore, the hydration of anhydrous bilayers can be considered (like the P(IV) \rightarrow P(V)-TBP transition, see chapters 2 and 4) as an initiating step in the transmission of a conformational headgroup change into alterations in the chain packing. In contrast to these findings a recent ^{13}C CP-MAS NMR study revealed that no substantial changes in the conformational equilibria of the acyl chains take place upon hydrating anhydrous DPPC [9]. This discrepancy between the Raman and NMR results might origi-

nate from the difference in optical purity of the used DPPC. Whereas the Raman study was based on racemic DPPC, the NMR study was performed on the enantiomerically pure L-form. In order to verify this supposition and to gain insight in the extent to which the acyl chain packing is perturbed upon hydration, a detailed ^{13}C CP-MAS NMR study is performed on DL- and L-DPPC bilayers in the gel phase. This study also shows that the CP-MAS NMR technique, in addition to its already well-known application in protein and carbohydrate research [10], can be successfully used for monitoring packing changes in ordered phospholipids.

5.2 Results

5.2.1 Anhydrous DL- and L-DPPC

The anhydrous character of the sample was confirmed by elemental analysis and DSC*, which showed a double phase transition at 395 K. The ^{13}C CP-MAS NMR spectrum of polycrystalline, anhydrous DL-DPPC is shown in Fig. 1 along with the solution spectrum. In Table I the ^{13}C chemical shifts are collected, and assigned according to those in the solution spectra.

Some distinct features in the solid state spectrum of DL-DPPC can be attributed to specific packing properties of the phospholipid. The carbonyl resonances are 2.8 ppm apart, versus 0.3 ppm when DPPC is solubilized in chloroform/methanol. The large shift difference in the solid bilayer is ascribed to the environmental difference of the sn-2 ester moiety compared to the sn-1 group. As a result of the well-known bend in the sn-2 chain, the ester moiety is situated at the interface between the polar headgroups

* DSC: differential scanning calorimetry.

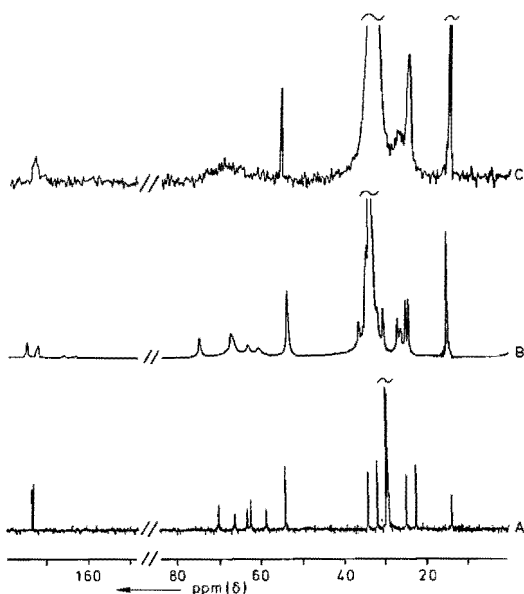


Fig. 1. The ^{13}C spectrum of DL-DPPC in $\text{CDCl}_3/\text{CD}_3\text{OD}$ (A) and the CP-MAS spectra of anhydrous DL-DPPC (B) and DL-DPPC with two equivalents of water (C).

and the non-polar chains, whereas the sn-1 carbonyl is buried in the hydrophobic core. From solvent polarity dependencies of the chemical shifts of ester groups, the assignment is made that the downfield signal originates from the sn-2 carbonyl moiety [11]. Interestingly, the penultimate ($\omega-1$) as well as the $\omega-2$ methylene groups show two separate signals for both chains, whereas only one resonance for the $\omega\text{-CH}_3$ groups is observed. This observation originates from differently packed chain ends, since it is well documented that the ^{13}C nuclei of two approaching methyl(ene) groups become less shielded due to the mutual depolarization effect on the C-H bonds of the respective groups [12].

It should be noticed that despite pronounced differences in the hydrocarbon chain and backbone resonances between anhydrous L- and DL-DPPC, the shifts of the head-group carbons in both forms are almost identical. The NCH_3 resonance at 53.4 ppm found in L- and DL-DPPC, seems an

Table I. ^{13}C Chemical shifts for anhydrous DL-DPPC and L-DPPC in solution ($\text{CDCl}_3/\text{CD}_3\text{OD}$ 3:2) and in solid state. α and ω represent the first and terminal carbon of the hydrocarbon chain respectively.

	<u>solid state</u>		<u>solution</u>	
	DL-DPPC	L-DPPC	DL-DPPC	
<u>headgroup</u>				
CH ₂ N	66.5 ^a	66.6	67.43	
CH ₂ OP	60.3	60.4	59.90	
N(CH ₃) ₃	53.25	53.50	55.17	
<u>backbone</u>				
CHO	74.38	71.02	71.27	
CH ₂ OP	66.5 ^a	64.7	64.46	
CH ₂ O	62.80	63.0	63.63	
<u>acyl chain</u>				
C=O	sn-2	175.30	173.65	174.69
	sn-1	172.55	172.77	174.33
α	sn-2	36.17	- ^b	35.14
	sn-1	35.55	- ^b	34.99
β	sn-2	26.87	27.81	25.80
	sn-1	26.10	27.33	25.76
internal		33.12	33.00	30.59
ω -2 ^c	sn-2	34.54	- ^b	32.80
	sn-1	34.02	- ^b	32.80
ω -1 ^c	sn-2	24.88	24.63	23.55
	sn-1	24.28	24.10	23.55
ω		15.03	14.50	14.12

^a coinciding signals.

^b unresolved resonances.

^c for assignment see discussion.

additional indication of their anhydrous character. The other resonances in L-DPPC show a remarkable resemblance with those for the dihydrated DL-DPPC form (vide infra). The chemical shifts for L-DPPC agree well with those previously found [9].

5.2.2 Addition of water to anhydrous DL-DPPC

The controlled addition of two equivalents of water to anhydrous DL-DPPC changes the spectrum drastically (see Fig. 1 and Table II). The sn-2 carbonyl resonance has shifted upfield and has collapsed with the sn-1 carbonyl group resulting in a broad featureless signal in the hydrated form. Another intriguing observation is the pronounced downfield shift of ca. 1 ppm of the choline methyl carbons and the considerable upfield shift of ca. 3 - 4 ppm of the CHO- glyceryl carbon. The upfield shift of the sn-2 carbonyl group is attributed to the shielding of the formal charges in the headgroup and the concomitant decrease in dielectric constant in the interface region [13]. In addition, this effect brings about an upfield shift of the CHO- glyceryl carbon. The pronounced downfield shift of ca. 1 ppm for the choline methyl groups upon hydration of both forms of DPPC also indicates a decreased dielectric constant in this region. Consequently, the C-N and C-H bonds become less polarized, but due to the larger polarizability of the C-H bonds, the net effect is a deshielding of the carbon nucleus [14]. The internal methylene groups of the chains and, more pronounced, the chain methyl resonances move upfield on the addition of 2 equivalents of water, which indicates an increased gauche contribution and/or a larger intermolecular distance between the hydrocarbon chains in the matrix. The sn-1 and sn-2 ω -1 methylene groups can no longer be distinguished and resonate at approximately the same frequency as the upfield signal in the anhydrous state. Furthermore, the glyceryl backbone and headgroup resonances are considerably broadened, probably as a consequence of molecules experiencing different, non-interchangeable environments [15].

An interesting phenomenon occurred when anhydrous DL-DPPC was exposed to a humid atmosphere until 1 equivalent of water was absorbed. The ^{13}C NMR spectrum of this

phase turned out to be a superposition of resonances of the anhydrous and dihydrated forms of DPPC (within the experimental error). To check whether the monohydrated phase was homogeneous, a DSC analysis was performed. In the temperature range from 305 to 410 K only one phase transition was observed at 350 K. Furthermore, a monohydrated sample of DPPC prepared by slow solvent crystallization from chloroform/methanol according to Chapman [16], yielded similar ^{13}C NMR and DSC results as above. Moreover, when an anhydrous sample was exposed to an atmosphere of ca 60% humidity and aliquots were taken in regular time intervals, a decrease in intensity was observed of the $\delta = 53.25$ and 15.03 signals (originating from the choline and chain methyl groups respectively) in favour of the 54.32 and 14.40 intensities, respectively.

5.2.3 Addition of water to anhydrous L-DPPC

The hydration of L-DPPC was studied previously with ^{13}C CP-MAS NMR by De Haan et al. [9]. For a proper evaluation of the packing changes between both forms of DPPC it is essential that the samples are prepared according to exactly the same procedure, otherwise the preparation technique itself might impose a distinct crystallographic form on the phospholipid [13]. Therefore, the effects of water addition to L-DPPC are reinvestigated.

On hydrating L-DPPC in a humid atmosphere it is observed that L-DPPC appears to be much more hygroscopic than the racemic modification. However, the data in Table II reveal that apart from a deshielding of the choline methyl carbons, no pronounced changes in chemical shifts are detected between the anhydrous and the monohydrated form of L-DPPC. Thus, in contrast to the situation in DL-DPPC, only one signal for the choline and chain methyl groups is found on the addition of one equivalent of water. The present findings confirm the previous results [9].

Table II. The ^{13}C -chemical shifts of the resolvable resonances in anhydrous and hydrated DPPC. Experimental parameters are given in the experimental section. α and ω represent the first and terminal carbon of the hydrocarbon chain respectively.

	DL-DPPC			L-DPPC	
	anhydrous	2-H ₂ O	4-H ₂ O	anhydrous	1-H ₂ O ^a
C=O sn-2	175.30	172.0	172.7	173.65	173.3
sn-1	172.55	172.0	172.7	172.77	173.3
CHO	74.38	< 70	< 70	71.0	71.0
N(CH ₃) ₃	53.25	54.32	54.41	53.50	54.25
internal	33.12	33.01	32.97	33.00	33.01
ω -1 ^b sn-2	24.88	24.14	24.15	24.63	24.37
sn-1	24.28	24.14	24.12	24.10	24.37
ω CH ₃	15.03	14.40	14.40	14.50	14.40

^a similar shifts are found for 2-H₂O and 4-H₂O.

^b for assignment see discussion.

Increasing the water content further to four water molecules per lipid, does not affect the chemical shift significantly (data not shown).

5.3 Discussion

For anhydrous DL-DPPC an end group packing model can be derived from the different chemical shifts in the sn-1 and sn-2 chain of the ultimate as well as the penultimate

methylene group and the overlapping methyl resonances in both chains. In this model (see Fig. 2) the $\omega-1$ and $\omega-2$ methylene groups of the sn-1 chain have less Van der Waals contacts with neighbouring chains than the analogous methylene groups in the sn-2 chain. As a result, the assignment can be made that the sn-2 $\omega-1$ and $\omega-2$ methylene groups resonate downfield with respect to the sn-1 methylenes [12]. The ultimate methyl groups of both chains have similarly packed environments, due to a partial interdigitation of the opposed monolayers. Hence, no separate signals are found for these carbons.

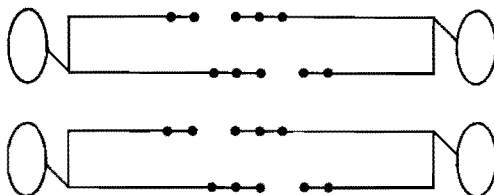


Fig. 2. Chain end packing model for anhydrous bilayers of DL-DPPC. The $\omega-1$ and $\omega-2$ methylene groups of the sn-2 chain are completely surrounded by neighbouring methyl(ene) groups, whereas the $\omega-1$ and $\omega-2$ methylenes in the sn-1 chain have less direct neighbours in the surrounding sn-2 chains and/or indirect neighbours which are situated one bond distance further from this direct neighbour.

On addition of 2 equivalents of water to anhydrous DL-DPPC, changes are observed in the headgroup and acyl chain regions. The upfield shift of the ^{13}C NMR resonances of the internal methylenes, the sn-2 $\omega-1$ methylene and the methyl groups upon hydration, is ascribed to an increase in the effective headgroup area as the result of a weakening of intermolecular electrostatic $\text{PO}^- \cdots \text{N}^+\text{CH}_3$ interactions. Due to the resulting mismatch in the cross-sectional area between the headgroups and the chains, a rearrange-

ment of the chains will occur either by changing the angle of tilt or by increasing the number of gauche conformers or both. The results indicate that it is mainly the former mechanism which is operative in filling up the resulting space. The introduction of gauche conformers would shift the internal methylene groups more upfield than the methyl groups as can be deduced from simple statistical considerations [17]. Since this is clearly not supported by our results, the changes in the end group chemical shifts are predominantly attributed to a change in the angle of tilt. From the chemical shift data, it is difficult to depict the exact arrangement of the chains that causes the (near) equivalence of both chains and the pronounced upfield shift of the chain end region compared to the anhydrous state. Nevertheless, the chemical shifts indicate a less densely packed environment.

The appearance of the subspectrum of the dihydrated form of DL-DPPC as soon as anhydrous DL-DPPC is exposed to a humid atmosphere indicates that the monohydrate phase of DPPC is not homogeneous with respect to the water distribution. Apparently, the so called monohydrate phase of DL-DPPC consists of separate domains of anhydrous and dihydrated DPPC which can be distinguished by ^{13}C NMR. The single phase transition in the DSC spectrum suggests that the domains are too small to be detected separately with DSC. The possibility of a dihydrated phase homogeneously mixed with anhydrous DPPC at a molecular level, can definitely be ruled out, since at least some cooperativity in packing properties is needed to bring about exactly the same chemical shifts in a mixed phase as in the separate phases. Thus, it is postulated that the monohydrate phase of DL-DPPC prepared under the conditions described here, does in fact not exist on a molecular level.

The packing of anhydrous L-DPPC differs significantly from that in the anhydrous DL-modification as is revealed by comparing the chemical shifts of specifically the sn-2 C=O, CHO and ω -methyl carbons. Given the fact that exactly

the same sample preparation and drying techniques were used, it is concluded that the discrepancy in packing properties is caused at least partially by stereospecific interactions. Apparently, these interactions allow a more tightly packed arrangement for DL-DPPC with respect to the L-form as is demonstrated by the downfield shift of the internal methylene groups and the ω -methyl groups of DL-DPPC with respect to the L-form. This finding is supported by the DSC measurements which show a phase transition for the DL-form some 20°C higher than for the L enantiomer [16].

The close resemblance in chemical shift differences between the anhydrous and hydrated DL-DPPC phases on the one hand and between anhydrous DL- and L-DPPC on the other hand, suggests a common origin. As argued above, the reason for these similar differences might very well be the tilting of the hydrocarbon chains in L-DPPC and hydrated DL-DPPC with respect to the non-tilted chains in anhydrous DL-DPPC. An independent confirmation can be found in the electron diffraction study on anhydrous L- and DL-DPPC of Sakurai et al. [18]. They concluded that the chains in L-DPPC are tilted with respect to the bilayer plane, whereas in the DL-form essentially no tilting occurs. Thus the addition of 2 equivalents of water to anhydrous DL-DPPC brings about a complete unlocking of a tightly packed structure to a more disordered arrangement as in anhydrous or hydrated L-DPPC. On the contrary, in bilayers of anhydrous L-DPPC 2 equivalents of water can be accommodated without structural rearrangements in the hydrocarbon chains. Although the unlocking in anhydrous DL-DPPC is not accompanied by a substantial increase in gauche conformations in the acyl chains of DL-DPPC, as was suggested by Raman spectroscopy [8], there are certainly some marked differences in acyl chain and headgroup packing between the anhydrous and hydrated phase. Therefore it is concluded that the discrepancy between the previous Raman investigation [8] and the recently performed ^{13}C NMR study [9] in

which no changes in packing differences were detected, can be ascribed to differences in optical purity of the used DPPC.

It is interesting to compare the present results with a detailed study on chiral aggregation phenomena in bilayers of DL and L-DPPC in water [19]. Despite the high purity of the phospholipids, no specific interactions could be demonstrated by various techniques between racemic DPPC and its enantiomers. This finding is consistent with the present results on hydrated DPPC samples. However, the findings in this chapter also clearly point out that packing differences due to stereospecific interactions have to be taken into account in tightly packed anhydrous systems. Apparently, on hydrating anhydrous bilayers of DPPC, all chirally induced packing differences are overruled by the concomitant structural change in the lipid molecules. Vice versa, since dehydration of phospholipids is presumably an important step in various membrane processes [7,20], stereochemical control might be effectuated by different packing arrangements between phospholipids and other chiral molecules in the membrane bilayer. It was argued that in this way the membrane can act as a stereospecific screen towards molecules of wrong chirality [19].

5.4 Concluding remarks

The results clearly indicate that a conformational change in the headgroup of anhydrous DPPC bilayers induced by water molecules, results for DL-DPPC in a more disordered structure. This change in packing seems related to an increase in the angle of tilt, resulting in a very similar structure as was found for anhydrous L-DPPC on the basis of the ^{13}C chemical shifts. On the contrary, the hydrocarbon chain arrangement of anhydrous L-DPPC is not affected by the addition of water. Apparently, in DL-DPPC a

tight packing is possible for which two equivalents of water are necessary to disturb the structure. The addition of only one equivalent results in small domains of dihydrated and anhydrous DL-DPPC. In anhydrous L-DPPC such tight packing cannot be realized, and hence water can be accommodated without structural rearrangements in the hydrocarbon chains.

5.5 Experimental section

5.5.1 Materials

DL- and L-Dipalmitoylphosphatidylcholine were obtained from Sigma (99% pure) and treated with chloroform. Application of high vacuum ($< 10^{-5}$ Torr) and elevated temperatures (about 40°C) during 48 h yielded anhydrous DPPC, according to elemental analysis, DSC [16] and the ^{13}C NMR results (one signal for NCH_3). Hydration of DPPC was accomplished either by controlled addition of double distilled water and centrifuging above the main phase transition temperature or by standing in a humid atmosphere until equilibrium was reached [21]. In order to maintain the anhydrous and hydrated compounds in an exactly defined composition the samples were stored in Kel-F capsules [22] which were immediately sealed and subsequently used in aluminium oxide MAS rotors. By following this procedure moisture was kept out and any evaporation of water from hydrated forms (due to electromagnetic heating) was prevented.

5.5.2 NMR spectroscopy and DSC analysis

The ^{13}C CP-MAS spectra were recorded at 75.48 MHz on a Bruker CXP-300 NMR spectrometer equipped with a double air-bearing CP-MAS probe. The cross polarization measure-

ments were carried out with flipback of the proton magnetization and spin temperature inversion. The sample amount was 0.1 - 0.2 g and the temperature was about 30°C. The chemical shifts are related via adamantane to TMS. Typically 1,000 scans of 1k data points were accumulated and zero-filled to 16k points prior to Fourier transformation. The spectral width was 16 kHz and the pulse width employed was 6 μ s. The contact time was 2.5 ms. The pulse delay varied between 10 and 20 s, depending on the main phase transition temperature. The acquisition time was 29 ms. The samples were rotated at 2.5 - 2.7 kHz in order to prevent unwanted pressure induced phase transitions [9]. The reported chemical shifts are average values of at least two independently prepared samples (starting from solvent evaporation) with a deviation of < 0.05 ppm, provided that the samples have the same experimental history.

The solution spectrum was recorded on a Bruker CXP-300 NMR spectrometer at room temperature. The DPPC was dissolved in CDCl₃/CD₃OD 2:1 v/v and the chemical shifts were related to TMS.

The DSC recordings were made on a Perkin Elmer DSC-7 calorimeter at a scan rate of 10 K/min.

References

1. J.H. Davis, *Biochim. Biophys. Acta* 737 (1983) 117, and references therein.
2. J. Seelig and P.M. Macdonald, *Acc. Chem. Res.* 20 (1987) 221.
3. T. Ming Fong and M.G. McNamee, *Biochemistry* 25 (1986) 830.
4. A. Makriyannis, D.J. Siminovitch, S.K. Das Gupta and R.G. Griffin, *Biochim. Biophys. Acta* 859 (1986) 49.
5. E.C. Kelusky, Y. Boulanger, S. Schreier and I.C.P. Smith, *Biochim. Biophys. Acta* 856 (1986) 85.
6. B.J. Forest and J. Mattai, *Biochemistry* 24 (1985) 7148.

7. J.A. Killian and B. de Kruyff, *Biochemistry* 24 (1985) 7890.
8. S. Fowler Bush, R.G. Adams and I.W. Levin, *Biochemistry* 19 (1980) 4429.
9. J.W. de Haan, R.J.E.M. de Weerd, L.J.M. van de Ven, F.A.H. den Otter and H.M. Buck, *J. Phys. Chem.* 89 (1985) 5518.
10. H. Saitô, *Magn. Reson. Chem.* 24 (1986) 835, and references therein.
11. S. Uegi and H. Nakamura, *Tetrahedron Letters* (1976) 2549.
12. D.M. Grant and B.V. Cheney, *J. Am. Chem. Soc.* 89 (1967) 5315.
13. P.M. Green, J.T. Mason, T.J. O'Leary and I.W. Levin, *J. Phys. Chem.* 91 (1987) 5099.
14. I. Morishima, K. Yoshikawa, K. Okada, T. Yonezawa and K. Goto, *J. Am. Chem. Soc.* 95 (1973) 165.
15. J. Scheafer and E.O. Stejskal, *Topics in Carbon 13 NMR Spectrosc.* 3 (1980) 283.
16. D. Chapman, R.M. Williams and B.D. Ladbroke, *Chem. Phys. Lipids* 1 (1967) 445.
17. J.W. de Haan, L.J.M. van de Ven, A.R.N. Wilson, A.E. van den Hout-Lodder, C. Altona and D.H. Faber, *Org. Magn. Reson.* 8 (1976) 477.
18. I. Sakurai, S. Sakurai, T. Sakurai, T. Seto, A. Ikegami and S. Iwayanagi, *Chem. Phys. Lipids* 26 (1980) 41.
19. E.M. Arnett and J.M. Gold, *J. Am. Chem. Soc.* 104 (1982) 636.
20. M. Rossignol, T. Uso and P. Thomas, *J. Membr. Biol.* 87 (1985) 269.
21. E. Mushayakara, N. Albon and F.W. Levin, *Biochim. Biophys. Acta* 686 (1982) 153.
22. W.T. Ford, S. Mahanray and H. Hall, *J. Magn. Reson.* 65 (1985) 156.

CHAPTER 6*

The different influences of ether and ester phospholipids on the conformation and transport properties of gramicidin A. A molecular modelling and experimental study

Abstract

The effects of the type of chain linkage (e.g. ether or ester) in phosphatidylcholines on the transport properties of gramicidin A were studied using efflux measurements through vesicle walls. A marked suppression of the permeability was found when ether lipids are added to a bilayer composed of ester lipids. With molecular modelling techniques the interactions between both types of lipids and gramicidin were approximated. It was found theoretically, that replacement of the ester function in dipalmitoylphosphatidylcholine (DPPC) by an ether moiety induces a shift in the rotameric distribution of the Trp₁₅ side chain in gramicidin A. Concomitantly, the channel entrance is contracted by ca. 0.4 Å. The perturbation can be related to the strong hydrogen bond formed between the lipid carbonyl group and the indole proton of the Trp₁₅ residue of gramicidin. In the ether lipid-gramicidin assembly a weaker H-bond is formed between Trp₁₅ and the phosphate moiety. Thus, the experimental finding can be explained in terms of changes in channel stability and conformation. Furthermore, a mechanism is proposed, based on the hydrogen bridge, by which changes in the phospholipid headgroup can affect the activity of gramicidin.

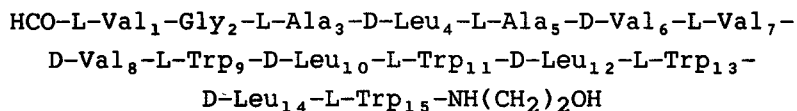
* G.H.W.M. Meulendijks, T. Sonderkamp and H.M. Buck, submitted for publication.

6.1 Introduction

Numerous studies have been conducted on protein-lipid interactions, but only few address the subject from the lipid side, i.e. are lipids capable of modifying the conformation of membrane proteins. Phospholipids in particular, are very well suited to transfer information from the easily accessible headgroups to the hydrophobic part of the membrane [1]. Recently, a mechanism was outlined by which a geometrical change in the phospholipid headgroup can be transmitted via intramolecular electrostatic forces to the hydrocarbon chains [2,3]. It can be imagined that by adopting a different phospholipid conformation, the structure of embedded proteins may very well be modified. For instance, it has been argued, based on theoretical investigations, that the channel forming polypeptide gramicidin A can be influenced by the lipid environment via conformational changes in the side chains resulting in different conductivities through the channel [4].

Gramicidin A is an extensively investigated polypeptide, but little is known about its molecular interactions with lipids. Although this antibiotic does not affect the permeability of parent cell-membranes but rather that of membranes in invading bacteria [5], it accurately mimics important characteristics of channel transport in higher organisms [6].

Gramicidin A consists of 15 alternating D- and L-amino acids:



The N-terminal part is blocked by a formyl group and the C-terminal part by an ethanolamine group [7]. The active form is a dimer with the formyl ends facing each other. The monomers are linked by 6 hydrogen bonds, and

the channel is embedded in the hydrophobic core of the membrane [8]. The dimer assumes in the membrane a left handed β -helical conformation with a length of ca. 26 Å and an internal pore of about 4 Å in diameter [9]. It has been established that only partially hydrated, monovalent cations can be translocated through the channel [10]. The loss of hydration energy is compensated by complexation with the carbonyl groups of the peptide backbone [11]. By using specifically ^{13}C -enriched carbonyls in gramicidin A analogues, it was demonstrated that the carbonyl groups of the four tryptophanes (Trp) and the one of leucine (Leu) at position 14 are involved in the binding with the ion [12].

Conductance studies on gramicidin analogues with various side chains have indicated that changes in the side chain conformational distributions can affect the channel conductance [13]. Furthermore, the importance of the rotational state of the side chains on the mean life time of the channel and hence the transport properties, is also apparent from a previous theoretical study on gramicidin analogues in vacuo [4,14]. When considering lipid-gramicidin interactions, the conformational distribution of the Trp_{15} side chain is of interest in particular. This residue is situated in the vicinity of the lipid-water interface and moreover, the molecular structure of the channel entrance might easily be influenced by a change in the rotameric state of this side chain [4].

In this chapter a theoretical and experimental study is performed on gramicidin-lipid interactions to arrive at a mechanism by which conformational changes can be transferred from the lipid to the polypeptide. It is conceivable that alterations in the gramicidin conformation are effectuated by a change in the relative orientation of the lipid carbonyl group and the nearby aromatic Trp_{15} side chain. To gather support for this idea gramicidin properties are compared in case the peptide is surrounded by phospholipids in which the hydrocarbon chains are linked via ester bonds to the glyceryl backbone as opposed to

lipids with ether linked chains (and no carbonyl group). Following this approach, information is obtained as to what extent ester lipids can influence the conformation of gramicidin, simply by turning away the carbonyl group from the polypeptide. Such reorientation might be the result of conformational changes in the glyceryl backbone of the lipid, which in turn can easily be induced by changes in phospholipid headgroups [2,3].

Therefore, a set of large unilamellar vesicles (LUVs) is prepared containing ester and ether lipids and the gramicidin-mediated sodium efflux is monitored using ^{23}Na NMR spectroscopy.

With molecular modelling techniques the gramicidin-lipid interactions are theoretically approached. The gramicidin conformation in the presence of an ester lipid is compared with the one in the presence of an ether lipid. It is found that the carbonyl group in acyl lipids can interact via a hydrogen bond with the Trp₁₅ side chain of the gramicidin channel, thereby affecting the rotational state of this residue. The importance of this H-bond is underlined by similar calculations on systems consisting of ether or ester lipids and a gramicidin A analogue in which the tryptophanes are substituted by phenylalanines (Phe), lacking a hydrogen capable of hydrogen bond formation with the lipids (gramicidin M⁻).

Molecular modelling, based on AMBER force field calculations (Assisted Model Building with Energy Refinement), was originally developed for nucleotides and proteins [15]. Since no data on phospholipids are included in the AMBER program yet, force field constants for specific lipid groups have to be supplemented to enable the theoretical study of lipid-protein interactions.

6.2 Procedures for calculational studies

6.2.1 Starting conformations

A monomer of gramicidin A was built with the modelling program CHEM-X [16]. The conformation was set to a left handed β -helix with 6.3 residues per turn [17]. The atomic charges of the peptide residues were taken from the Brookhaven Protein Database. This structure was minimized with the AMBER program (vide infra). The molecular structure of dipalmitoylphosphatidylcholine (DPPC) was obtained by adding the choline moiety of D-glycero-1-phosphorylcholine to dimyristoylphosphatic acid. Both structures are available from the Cambridge Crystallographic Database. The hydrocarbon chains were extended with two methylene units each. The torsion angles of the DPPC thus obtained, were set according to values in the crystal structure of the dihydrate of DMPC [18]. The atomic charge distribution

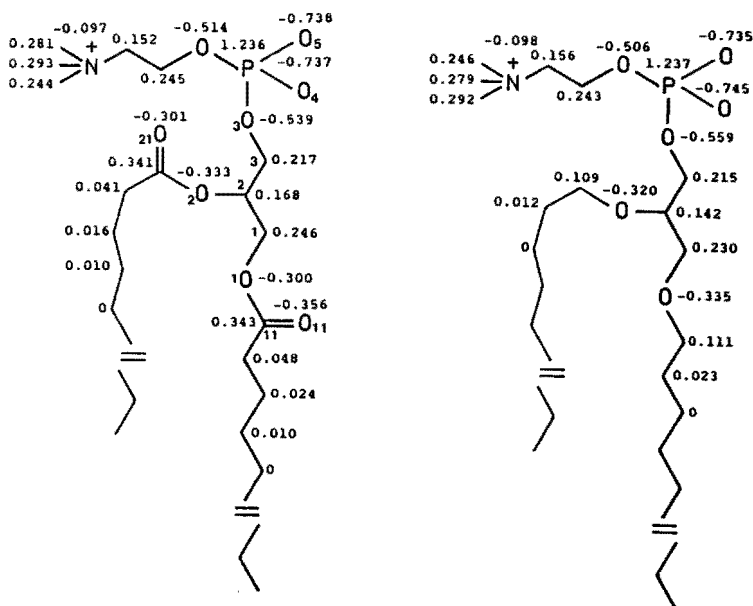


Fig. 1. Charge distribution in DPPC and DHPC derived from calculations based on MNDO.

Table I. Relevant torsion angles^{a,b} in DPPC, DHPC, DMPC.2H₂O.

	α_1	α_2	α_3	α_4	α_5	α_6	θ_1	θ_2	θ_3	θ_4
DMPC ^c	177	-74	-47	-150	54	176	168	-82	166	51
DPPC ^d	171	-78	-63	-121	66	173	175	-65	177	56
DPPC ^e	167	-76	-67	-123	66	174	171	-68	-175	64
DHPC ^f	179	-71	-69	-122	65	173	171	-67	-168	70
	β_1	β_2	β_3	β_4	β_5	γ_1	γ_2	γ_3	γ_4	γ_5
DMPC ^c	120	179	-134	67	180	102	176	180	180	-170
DPPC ^d	123	170	-155	61	-175	81	-178	-175	175	-179
DPPC ^e	94	-173	-147	61	-170	160	-175	127	-175	177
DHPC ^f	88	-173	-177	65	-172	66	-172	-180	-177	-179

^a Notation according to [18]. ^b Torsions in degrees. ^c Torsions in the crystal structure of DMPC.2H₂O [18]. ^d Torsions in DPPC minimized without gramicidin A. ^e Torsions in DPPC in the vicinity of gramicidin A. ^f Torsions in DHPC in the vicinity of gramicidin A.

stants and r the distance between two bonded atoms or in case of R_{ij} between the atoms i and j ; θ , bond angle; ϕ , dihedral angle; q , charge; n , multiplicity of the torsion potential and γ , phase angle. With e_q the equilibrium value is denoted.

Additional force field parameters for the lipid had to be included in the AMBER parameter set. The values of the lacking constants were based on molecular mechanics calculations on lipids and analogous compounds. In the parameter set thus obtained, small adjustments were made until the AMBER refined torsion angles of the central DPPC molecule in an assembly of in total seven DPPC lipids, arranged in a hexagonal lattice, agree with the crystallographic data on dimyristoylphosphatidylcholine (DMPC) (Table I) [18]. The optimized, supplemented parameters are compiled in Table II. A distant dependent dielectric

Table II. Supplemented force field parameters to the AMBER parameter set^a.

bond	r_{eq} (Å)	K_r (kcal/(mol.Å ²))		
C-HC	1.09 ^b	331.0 ^{c1}		
CH-OS	1.32 ^d	400 ^d		
C2-OS	1.32 ^d	400 ^d		
C-OS	1.33 ^f	527 ^f		
angle	θ_{eq} (deg)	K_θ (kcal/(mol.rad))		
HC-C-N	120 ^{c2}	35.0 ^{c2}		
HC-C-O	120 ^{c2}	35.0 ^{c2}		
C2-C2-OH	109.5 ^{c3}	80.0 ^{c3}		
C2-C-OS	109.0 ^e	98 ^e		
C-OS-CH	114.0 ^e	64 ^e		
C-OS-C2	114.0 ^e	64 ^e		
C3-N3-C2	108.0 ^e	90 ^e		
OS-C-O	124.0 ^e	190 ^e		
C2-OS-CH	111.8 ^{c4}	100 ^{c4}		
C3-N3-C3	108.0 ^e	90 ^e		
C2-CH-C2	112.4 ^{c5}	63 ^{c5}		
C3-C2-C2	112.4 ^{c5}	63 ^{c5}		
torsion	$V_N/2$ (kcal)	γ	n	
C2-C-OS-CH	3.50 ^e	0 ^e	1 ^e	
CH-C-OS-C2	3.50 ^e	0 ^e	1 ^e	
C2-C-OS-C2	3.50 ^e	0 ^e	1 ^e	
CH-OS-C-O	6.00 ^f	180 ^f	2 ^f	
C2-OS-C-O	6.00 ^f	180 ^f	2 ^f	
CH-C2-OS-C	1.00 ^e	0 ^e	1 ^e	
C2-CH-OS-C	0.35 ^e	0 ^e	1 ^e	
OS-C-C2-C2	0.80 ^e	0 ^e	3 ^e	

^a Notation according to [15].

^b Analogously to values taken from [21].

^c Analogously to values taken from [22]: 1. CT-HC 2. HC-CT-OH
 HC-C-C HC-CA-C 3. CH-C2-OH CH-CH-OH C2-CH-OH 4. C2-OS-C2
 C2-OS-C3 5. CH-C2-C2 CH-C2-C3 C2-C2-C2 CH-C2-CH.

^d For C-OS r_{eq} was taken as an average value from the data in [22] and [23].

^e Optimized values starting from data in [24].

^f Value taken from [24].

constant $\epsilon = R_{ij}$ was used for all calculations, which means that the solvent effect is implicitly taken into account [15,22,25]. The energy is refined by applying a minimization function with analytical gradients until the root mean square of the energy is less than 0.1 kcal/Å. To make the calculation problem manageable for the computer, the united atom model is used. In this model the hydrogen atoms in CH, CH₂ and CH₃ groups are omitted and their mass and charge are added to the carbon atoms to which they were originally bonded [15].

6.3 Results

6.3.1 Molecular modelling

The helical torsion angles of the gramicidin backbone ϕ_L , ψ_L and ϕ_D , ψ_D , initially set at resp. (-140, 130) and (100, -120) [17], show after the AMBER energy refinement a rather large systematical variation with respect to the starting values (Table III). Whereas ϕ_L and ϕ_D decrease from the formyl end towards the channel opening, ψ_L and ψ_D show a steady increase in this direction, starting from D-Val₆. The calculated diameter of the cavity is 3.9 Å and is obtained by subtracting the Van der Waals diameter for the carbonyl-oxygen (i.e. 1.6 Å) from the distance between

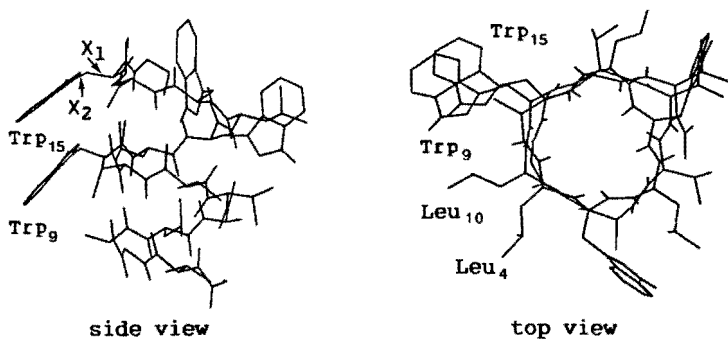
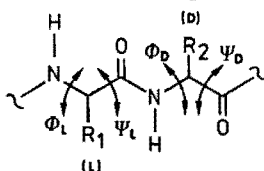


Fig. 2. AMBER-minimized gramicidin structure.

Table III. Helical torsion angles^a of the gramicidin (GA) backbone after energy refinement with AMBER.

	ϕ			ψ		
	GA	GA/DPPC	GA/DHPC	GA	GA/DPPC	GA/DHPC
L-Val ₁	-137	-135	-143	76	76	70
Gly ₂	157	150	153	-151	-156	-155
L-Ala ₃	-108	-87	-85	85	75	68
D-Leu ₄	145	149	149	-139	-135	-139
L-Ala ₅	-133	-130	-125	97	107	110
D-Val ₆	138	124	120	-176	166	165
L-Val ₇	-100	-88	-87	103	102	99
D-Val ₈	131	136	136	-146	-133	-125
L-Trp ₉	-114	-126	-117	124	120	126
D-Leu ₁₀	107	108	98	-124	-114	-109
L-Trp ₁₁	-132	-140	-142	141	143	141
D-Leu ₁₂	98	95	97	-101	-92	-95
L-Trp ₁₃	-161	-168	-166	152	152	152
D-Leu ₁₄	77	75	73	-96	-89	-88
L-Trp ₁₅	-163	-159	-167	129	129	128

^a Torsions in degrees, notation according to [26]:



the innermost carbonyl-oxygens in the helix core. The calculated length for a monomer is 12 Å. Both features are in close agreement with reported values [9,12]. The AMBER minimized geometry shows regarding the stacking of the Trp side chains 9 and 15, a strong resemblance with other calculated gramicidin structures as well (Fig. 2) [17].

The minimized DPPC-gramicidin A assembly (Fig. 3) shows some interesting features with respect to the lipid-

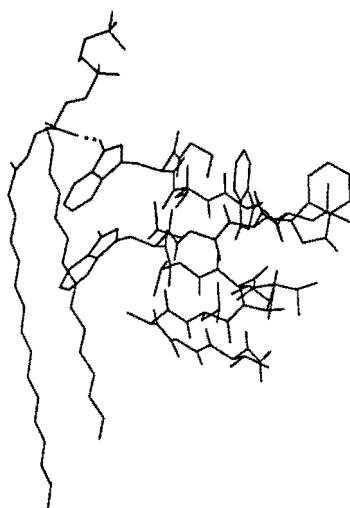


Fig. 3. AMBER-minimized gramicidin A-DPPC assembly. The H-bond between Trp₁₅ and C=O(21) is denoted with ..

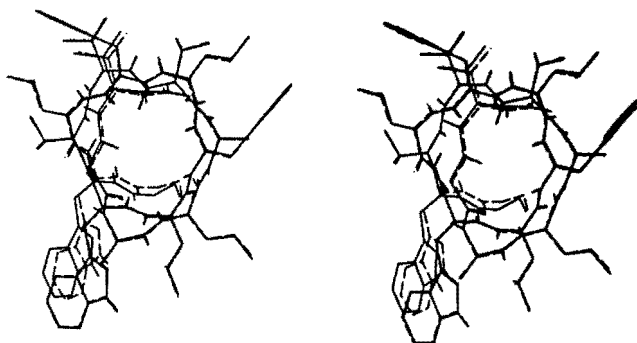


Fig. 4. Stereo view of AMBER-minimized gramicidin A-DPPC (—) and gramicidin A-DHPC (---). For clarity both lipids have been removed.

peptide interaction. The indole hydrogen of Trp₁₅ proves a well suited interaction site for the phospholipid. Two hydrogen bonds are formed: a strong one with the lipid carbonyl of the sn-2 chain with an energy comparable to the intramolecular H-bonds, and a very weak H-bond with the phosphate moiety (Table IV). From the side chain torsional angles χ_1 and χ_2 (for definitions see Fig. 2) in Table V it is concluded that the hydrogen bond induces a change

Table IV. Calculated energies^a of some inter- and intramolecular H-bonds in the studied gramicidin A-phospholipid assemblies. HNE and HN denote the indole hydrogen of the tryptophane residue and the amide hydrogen respectively. The nomenclature of the lipid atoms is indicated in Fig. 1.

Origin of bonds	Energy
HNE(Trp ₁₅)-O(21) (DPPC)	-0.466
HNE(Trp ₁₅)-O(4) (DPPC)	-0.002
HNE(Trp ₁₅)-O(4) (DHPC)	-0.005
HNE(Trp ₁₅)-O(5) (DHPC)	-0.227
HN(Val ₈)-O=C(Val ₁)	-0.500
HN(Trp ₁₅)-O=C(Trp ₁₃)	-0.122
HN(Trp ₁₅)-O=C(Trp ₁₃) with DPPC	-0.094
HN(Trp ₁₅)-O=C(Trp ₁₃) with DHPC	-0.333

^a energies in kcal/mol. These values are only valid for mutual comparisons and have no absolute meaning.

of 3° in χ_1 and 18° in χ_2 of the Trp₁₅ side chain, with respect to the situation in vacuo. The specific rotation results in a less stacked arrangement of Trp₁₅ and Trp₉. The conformational distributions in other side chains are virtually not affected in the presence of a lipid molecule (data not shown). When DPPC is replaced by the ether lipid DHPC, some pronounced changes occur in particular in the channel entrance area (Fig. 4). The ether lipid interacts with gramicidin A via an H-bond as well, but in this case, an H-bond is formed between Trp₁₅ and the charged oxygens in the phosphate moiety of DHPC. However, this interaction is weaker than the one between DPPC-carbonyl and Trp₁₅ (Table IV). As a consequence, in the DHPC-gramicidin system the torsion angles χ_1 and χ_2 of the Trp₁₅ side chain are changed with ca. 7° and 5° respectively with respect to the DPPC-protein assembly (Table V).

Table V. Side chain torsion angles^a in gramicidin A after energy refinement.

	χ_1			χ_2		
	GA	GA/DPPC	GA/DHPC	GA	GA/DPPC	GA/DHPC
L-Trp ₉	66	71	73	-71	-75	-72
L-Trp ₁₅	68	65	58	-54	-72	-67

^a Torsions in degrees.

An interesting effect of substituting DPPC by DHPC is the small contraction of ca. 0.4 Å of the channel entrance. Such a conformational change in this part of the protein backbone originates from a ca. 10° change in the helix torsion angle ϕ of Trp₉, Trp₁₅, and Leu₁₀ (Table III). Furthermore the contraction seems related to the lowering of the intramolecular H-bond energy between the amide proton of Trp₁₅ and the carbonyl group of Trp₁₃ (Table IV).

In order to verify that the lipid induced conformational changes in the gramicidin channel entrance, are not the result of different dipole-dipole interactions between the lipids and the protein, exactly the same procedure was followed for gramicidin M⁻ as was outlined for the A modification. The phenylalanines in gramicidin M⁻ are also aromatic like the tryptophanes, but lack a hydrogen capable of forming H-bonds with the lipids. The relative starting positions of the lipids and gramicidin M⁻ before AMBER minimization, were identical to those in the lipid-gramicidin A assemblies. It appeared that the torsion angles in gramicidin M⁻ are virtually not affected upon the lipid substitution (data not shown). This outcome underlines the conclusion that the H-bond formation in DPPC is essential in affecting the conformational state of gramicidin A.

In order to check whether the conclusions drawn from molecular modelling on gramicidin-lipid systems, are

subject to the force field parameter set used, all calculations were also performed with the non-optimized set (vide supra). Despite small variations in the torsion angles of the gramicidin channel and H-bond energies, all conclusions remain valid.

6.3.2 Ion efflux measurements

Fig. 5 shows a typical example of a series of ^{23}Na NMR spectra, obtained after the addition of gramicidin A to a homogeneous preparation of Large Unilamellar Vesicles (LUVs) with a sodium gradient over the vesicle walls. The vesicles consist of a matrix of dioleoylphosphatidylcholine (DOPC) with 10 mol-% additions of DPPC or DHPC. This specific composition is chosen to keep the lipid mixture above the phase transition temperature (ca. 0°C for 10 mol-% DPPC [27]), a prerequisite in the vesicle preparation technique used [28]. Moreover, it is to be expected that vesicle size and fluidity are not much affected on substituting DPPC by DHPC at this concentration [29,30].

It was observed that immediately after the addition of gramicidin to the vesicles, Na^+ -efflux is very fast until after ca. 10 minutes a stabilization is reached and the

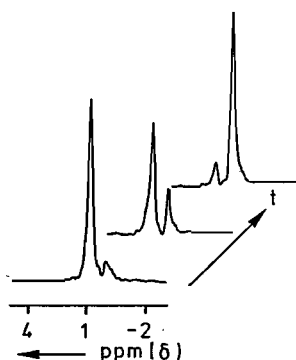


Fig. 5. A series of ^{23}Na NMR spectra during the time course of an efflux experiment. The downfield signal originates from Na^+ -ions in the vesicles.

transport decreases exponentially. It was argued that during this latter process, the lithium gradient is dissipated by a Na^+ for Li^+ exchange out of and into the vesicles respectively [31]. After this stage, there is still a sodium gradient, which causes a Na^+ -efflux at the expense of creating a new Li^+ -gradient until the diffusion potential of both ions has become equal. However, the latter process starts only after a few hours and is very slow for the vesicles used in this study. Therefore only the transport rate between ca. 10 and 100 minutes is considered.

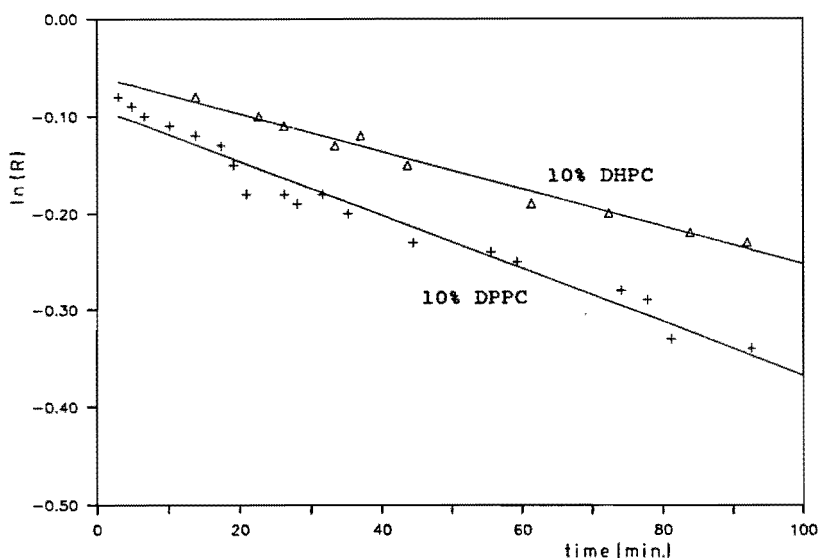


Fig. 6. The evaluated kinetics of an experiment. R is the ratio of the integrals for $(\text{Na}_{\text{int}}/\text{Na}_{\text{ext}})_{t=t'}$ and $(\text{Na}_{\text{int}}/\text{Na}_{\text{ext}})_{t=0}$.

In Fig. 6 the time course of the Na^+ -efflux is plotted for vesicles with DHPC or DPPC. The efflux (R) is given as the ratio of the integrals for the internal and external sodium resonances relative to the situation just before the addition of the gramicidin solution. This figure clearly demonstrates that DHPC suppresses the efflux rate with

respect to DPPC. The outcome of this plot is quantified in Table VI from which it can be seen that the Na⁺ transport rate decreases by ca. 25% on going from DPPC to DHPC.

Table VI. Scaled^a Na⁺-efflux rate (k_i) through (DOPC) vesicle walls with 9:1 mol additions of DPPC and DHPC. The actual number of gramicidin channels ranged from 3 - 4 per vesicle^b. Measurements were carried out at 298 K.

	F_{lipid}^c	$k_i * 10^4 [s^{-1}]$
DPPC	0.44	3.7
DHPC	0.49	2.7

^a See experimental section for definition. The estimated error was less than 10%.

^b Calculated from the amount of lipids in the sample and the known quantity of added gramicidin, thereby assuming 1000 Å vesicles with 85000 phospholipids per vesicle [28].

^c Average fraction of initial quantity of lipid found in the vesicles as determined after phosphate analysis.

6.4 Discussion

The AMBER refined gramicidin A channel (either in vacuo or in the presence of lipids) reveals in its basic features as pore diameter and channel length, a great similarity with the structure computed by Urry et al. [17]. However, the torsion angles of the helical backbone show a considerable, systematic variation along the channel direction. From the data in Table III and Fig. 2, it can be concluded that the carbonyls near the channel entrance are turned more inward the channel pore than those at the formyl end. This result suggests that the ion binding site, which is located near the channel opening [12], is already present in the gramicidin molecule and is not formed on the entry of an ion. Indeed, CD-studies have in-

licated that virtually no changes in the helical pore diameter occur upon ion binding [32]. Although the effect of water on the gramicidin conformation is not explicitly taken into account, the damping effect of the water molecules on electrostatic interactions is simulated by taking a distant dependent dielectricum [15,22,25].

The most striking result of the present calculations is the formation of a strong hydrogen bond between the carbonyl group of DPPC and the hydrogen of the indole ring of Trp₁₅ in the AMBER minimized gramicidin-lipid assembly. This H-bond brings about a change in the conformational distribution of the Trp₁₅ side chain in particular. Such an altered side chain conformation is accommodated by changes in specific torsion angles in the helical backbone at the entrance of the helix, resulting in a small widening of the channel opening with respect to the conformation in the DHPC-gramicidin assembly. This effect was not found with gramicidin M⁻ upon replacing DPPC by DHPC, which strongly indicates that the conformational changes are due to H-bond formation.

A change in the vicinity of the ion binding location will most likely affect the conductivity of the gramicidin. Indeed, the experimental kinetic study on the gramicidin-mediated ion transport demonstrates a lowering of the efflux rate when DPPC is replaced by DHPC. The rather small effect can partly be attributed to the presence of only 10% of DHPC in the vesicle wall. A misinterpretation could arise when the gramicidin channel is preferentially surrounded by DOPC molecules (also ester lipids). Since the H-bond contributes only for a very small extent to the total energy of the assembly according to the calculations (ca. 0.5 kcal/mol to 22 kcal/mol), this supposition seems very unlikely. Therefore, the change in ion transport apparently originates from different interactions of both types of lipids with the gramicidin.

With the present results no direct relation of the changed ion transport to a specific feature of the altered

gramicidin conformation can be deduced. Of course, it is very tempting to relate the slower transport through vesicle walls containing ether lipids to the smaller channel diameter. In addition, the absence of a strong hydrogen bond with Trp₁₅ can destabilize the gramicidin dimer conformation in the phospholipid bilayer. Since only the dimer enables the translocation of ions, a decreased life time will thus result in a less effective transport. In fact, such an interpretation was previously suggested for the observed decrease in stability of the gramicidin dimer conformation in an ether lipid environment compared with an ester lipid surrounding [33]. Stability was discussed in terms of a specific interaction between the lipid carbonyl and the carboxyl terminus of the channel, but unfortunately these findings were only very briefly reported so the precise arguments are unclear. Examination of the gramicidin top-view however (Fig. 2), reveals that steric interference from the leucine side groups, makes it very improbable that lipids are situated near the channel end and form an H-bond with the hydroxyl group of the carboxyl terminus. The present results indicate a more likely interaction site with the protein, based on the vicinity of the lipid carbonyl and the easily accessible hydrogen of Trp₁₅.

To the best of our knowledge the theoretically found H-bond has not yet been experimentally observed. Nevertheless, various studies indicate the importance of the indole moiety (with the hydrogen involved) for a proper functioning of the peptide. Recently, it was found that on photo-oxidation of the Trp-residues, the indole moiety loses the proton and within milliseconds, oxidation products are formed. The resulting irreversible loss in conductivity was ascribed to conformational changes near the tryptophan containing channel entrance [34]. Finally, it was firmly established that a gramicidin analogue in which the hydrogen bonding feature is blocked by the substitution of the indole hydrogens by formyl groups, has lost its ability to induce a non-bilayer arrangement (H_{II}

phase) [35,36].

The present results show that the Trp₁₅ side chain orientates to the most basic site available in the lipid to form an H-bond with maximum energy stabilization. This change in the rotational state of Trp₁₅ consequently alters the conformation of the channel entrance. On the other hand, the H-bond in the DPPC-gramicidin complex is dominated by the orientation of the lipid-carbonyl group, which in turn is a result of the conformational equilibrium in the glyceryl backbone of the lipids. Thus, via the H-bond interaction, conformational changes in the lipid surrounding of gramicidin may be transferred into conformational changes in the polypeptide. We propose the following sequence of such alterations starting in the lipid headgroup, which ultimately will result in a change in the transport properties of gramicidin. As outlined in the chapters 2 and 3, the rotameric distribution of the glyceryl backbone in the lipid can easily be changed by an increase in the headgroup charge or by a geometrical change in the headgroup from P(IV) into P(V)-TBP [2,3]. Both processes lead to a shift of the sn-2 carbonyl group towards the hydrophobic core. In order to optimize the H-bond interaction, the Trp side chain has to adopt a new conformation. Preliminary calculations reveal that such a change will result in a widening of the channel opening in gramicidin, with respect to an assembly with P(IV) lipids before modification. Analogous to the experimental observations for gramicidin surrounded by DPPC or DHPC lipids, it is expected that the change in the channel entrance will result in a faster ion transport. Thus, the present findings have resulted in a refinement of the recently proposed mechanism by which a phospholipid headgroup change can be transmitted via a cascade of conformational changes from the lipid to the protein [2,3].

6.5 Concluding remarks

The present investigations show that ester lipids have a promoting influence on the gramicidin-mediated efflux through vesicle walls, with respect to the ether lipids. A molecular modelling study reveals a difference between the two types of lipids in their capacities of forming an H-bond with gramicidin. The ester lipid forms a strong H-bond with Trp₁₅ of the polypeptide, and consequently the channel entrance is larger than in the ether lipid-gramicidin system. However, further experiments are necessary to confirm the presence of this specific H-bond interaction between ester lipids and gramicidin. If so, an effective mechanism exists, via which conformational changes in the surrounding lipid environment can ultimately be carried over in alterations in the ion efflux rate.

6.6 Experimental section

6.6.1 Materials

Phospholipids used in these experiments, Trizma base, the sodium salt of deoxycholic acid and gramicidin D* were purchased from Sigma Chemical Co. They were used without further purification. Sephadex resins used for gel filtrations were obtained from Pharmacia Inc. All other chemicals were of analytical reagent grade.

6.6.2 Methods

Large Unilamellar Vesicles (LUVs) of 1000 Å diameter were prepared from a thoroughly dried phospholipid film of

* Gramicidin D is a mixture of gramicidins A, B, and C in a molar ratio of approximately 80/5/15. The gramicidins B and C differ from A in the amino acid at position 11 being phenylalanine and tyrosine in the B and C modifications respectively.

typically 18 mg, according to the method described by Enoch and Strittmatter with slight modifications [28]. The lipid film was suspended in a NaCl-tris acetate buffer (100 mM in NaCl and 100 mM in tris acetate; pH = 8.1) containing 10 mM deoxycholate in a lipid/deoxycholate molar ratio of 2. The suspension was sonicated for 3 min in a Bransonic 12 ultrasonic bath, after which the opaque colour has changed to opalescent. After the formation of the LUVs, deoxycholate was removed by passing the sample over two subsequent gel filtration columns (respectively 60 vol. and 30 vol. of Sephadex G-25M; flow rate 100 ml/h) and the collected LUV samples were concentrated to 1 ml by means of an ultrafiltration step (Millipore, Immersible CX-30). In order to prepare a sample for the ^{23}Na NMR cation transport studies, external Na^+ was replaced by Li^+ in a third gel filtration step (20 vol. of Sephadex G-50M) [37]. Extreme care should be taken to avoid any sodium contamination at this point, since also small amounts can severely disturb the created sodium gradient. Elution was performed with 20 mM tris acetate buffer (pH 8.1) containing 50 mM LiCl with a flow rate of 10 ml/h. The aqueous solution trapped in the LUVs thus obtained, was 100 mM in NaCl, whereas the surrounding aqueous solution was 50 mM in LiCl. After the ion exchange, the collected samples were again concentrated to 1 ml by means of ultrafiltration.

6.6.3 Ion efflux measurements

^{23}Na NMR cation transport studies were performed according to the method of Pike et al. [31]. After the LUV sample was transferred to a NMR-tube (diameter 10 mm), 1 ml of 50 mM LiCl in D_2O was added, as well as 90 μl of a 0.16 M solution of a dysprosiumnitrilotriacetate complex (pH 7.0) as Na^+ shiftreagent [38,39], resulting in a final concentration of 3 mM. In this concentration the shift

reagent induces an upfield shift of 0.75 ppm of the outer Na^+ -signal with respect to the inner resonance. The ^{23}Na NMR spectra were recorded on a Bruker CXP-300 NMR spectrometer at 79.4 MHz. 256 FIDs (Free Induction Decays) were accumulated in 102.4 s. The relaxation time of the nuclei was about 0.1 s. The temperature of the measurements was 298 K. By recording five spectra in ca. 30 min., vesicles were checked for leakiness. The ion transport was induced by the addition of 6 μl of a 61.3 mM solution of gramicidin in methanol, resulting in a final concentration in the NMR-tube of 0.18 μM in gramicidin. This amounts to ca. 8 gramicidin molecules per vesicle (vide infra). Methanol has no influence on the sodium transport as was checked in a control experiment. The Na^+ -efflux started immediately after the addition of gramicidin and a series of spectra were recorded automatically. A typical kinetic experiment consisted of 20 spectra recorded with 10 s intervals, followed by 10 spectra with 60 s intervals and ultimately 20 spectra with 120 s intervals. The NMR data were plotted as $\ln(R)$ versus time with R the ratio of fractional area inside at $t = t'$ and the fractional area inside at $t = 0$. The fractional area was defined as the ratio of integrals for $\text{Na}_{\text{intern}}$ and $\text{Na}_{\text{extern}}$. The results represent the average of at least two different vesicle preparations.

6.6.4. Determination of the number of gramicidin channels per vesicle

The number of gramicidin channels per vesicle was calculated from the actual concentration of phospholipids and the number of phospholipid molecules in a 1000 Å vesicle [28]. The diameter of the pure DOPC-LUVs was checked by inclusion measurements with cytochrome c [40]. It is assumed that 10 - 20 mol-% additions of phospholipids do not alter the mean diameter of the vesicles substantially [29]. Phospholipid concentrations were deter-

mined as inorganic phosphate by a modification of the procedure of Bartlet as reported by Litman [41]. The extinction was recorded at 830 nm on a Hitachi 150-20 UV/VIS photospectrometer. Since the phospholipid concentration varies per vesicle preparation and a fixed quantity of gramicidin is added, the number of channels per vesicle is not constant for different preparations. None the less, comparisons can be made when the rate constants are scaled to a fixed number of gramicidin molecules per vesicle (i.e. 12), making use of the quadratic relation between the actual number of gramicidin molecules per vesicle and the observed rate constant [10]:

$$k_{\text{obs}}/n^2 = k_i/12^2$$

with n the determined number of gramicidin molecules per vesicle and k_i the scaled rate constant.

References

1. Y. Boulanger, S. Schreier and I.C.P. Smith, *Biochemistry* 20 (1981) 6824.
2. I.I. Merkelbach and H.M. Buck, *Recl. Trav. Chim. Pays-Bas* 102 (1983) 283.
3. G.H.W.M. Meulendijks, W. van Es, J.W. de Haan and H.M. Buck, *Eur. J. Biochem.* 157 (1986) 421.
4. D.W. Urry, C.M. Venkatachalam, K.U. Prasad, R.J. Bradley, G. Parenti-Castelli and G. Lenaz, *Int. J. Quantum Chem. Quantum Biology Symp.* 8 (1981) 385.
5. L. Masotti, P. Cavatorta, G. Sartoz, E. Casali and A.G. Szabo, *Biochim. Biophys. Acta* 862 (1986) 265.
6. R. Buchet, C. Sandorfy, T.L. Trapane and D.W. Urry, *Biochim. Biophys. Acta* 821 (1985) 8.
7. R. Sarges and B. Witkop, *Biochemistry* 4 (1965) 2491.
8. O.S. Andersen, *Ann. Rev. Physiol.*, 46 (1984) 531, and references therein.

9. D.W. Urry, Proc. Natl. Acad. Sci. USA 69 (1972) 1610.
10. S.B. Hladky, V.B. Myers and D.A. Haydon, Biochim. Biophys. Acta 274 (1972) 313.
11. D.W. Urry, Top. Curr. Chemistry 128 (1985) 175.
12. D.W. Urry, K.U. Prasad and T.L. Trapane, Proc. Natl. Acad. Sci. USA 79 (1982) 390.
13. F. Heitz, C. Cavach, G. Spach and Y. Trudelle, Biophys. Chem. 24 (1986) 143.
14. D.W. Urry and C.M. Venkatachalam, J. Comput. Chem. 5 (1984) 64.
15. S.J. Weiner, P.A. Kollman, D.A. Case, U. Chandra Singh, C. Ghino, G. Alagona, S. Profeta and P. Weiner, J. Am. Chem. Soc. 106 (1984) 765.
16. CHEMX/CHEMGRAF, created by E.K. Daries, Chemical Crystallography Laboratory, Oxford University, developed and distributed by Chemical Design Ltd., Oxford.
17. C.M. Venkatachalam and D.W. Urry, J. Comput. Chem. 4 (1983) 461.
18. R.H. Pearson and I. Pascher, Nature 281 (1979) 499.
19. M.J.S. Dewar and W. Thiel, J. Am. Chem. Soc. 99 (1977) 4899.
20. S. Weinstein, B.A. Wallace, J.S. Morrow and W.R. Veatch, J. Mol. Biol. 143 (1980) 1.
21. N.L. Allinger, J. Am. Chem. Soc. 99 (1977) 8127.
22. S.J. Weiner and P.A. Kollman, J. Comput. Chem. 7 (1986) 230.
23. A.E. Dorigo and K.N. Houk, J. Am. Chem. Soc. 109 (1987) 3698.
24. J.J.C. Teixeira-dias and R. Fausto, J. Mol. Structure, 144 (1986) 199.
25. R.A. Moss, T.F. Hendrickson, R. Ueoka, K.Y. Kim and P.K. Weiner, J. Am. Chem. Soc. 109 (1987) 4363.
26. IUPAC-IUB Commission on Biological Nomenclature, J. Mol. Biol. 52 (1970) 1.
27. K. Furuya and T. Mitsui, J. Phys. Soc. Japan 46 (1979) 611.

28. H.G. Enoch and P. Strittmatter, *Proc. Natl. Acad. Sci. USA* 76 (1979) 145.
29. S. Massari and R. Colonna, *Biochim. Biophys. Acta* 863 (1986) 264.
30. H. Hauser, *Biochim. Biophys. Acta* 646 (1981) 203.
31. M.M. Pike, S.R. Sanford, J.A. Balschi and C.S. Springer, *Proc. Natl. Acad. Sci. USA* 79 (1982) 390.
32. B.A. Wallace, W.R. Veatch and E.R. Blout, *Biochemistry* 20 (1981) 5754.
33. B.A. Wallace, *Biophys. J.* 49 (1986) 295.
34. D.D. Busath and R.C. Waldbillig, *Biochim. Biophys. Acta* 736 (1983) 28.
35. J.A. Killian, K.N.J. Burger and B. de Kruyff, *Biochim. Biophys. Acta* 897 (1987) 269.
36. F.J. Aranda, J.A. Killian and B. de Kruyff, *Biochim. Biophys. Acta* 901 (1987) 217.
37. L.T. Mimms, G. Zamphigi, Y. Nozaki, C. Tanford and J.A. Reynolds, *Biochemistry* 20 (1981) 833.
38. I.I. Merkelbach, Ph.D. Thesis, Eindhoven University of Technology (1985).
39. M.M. Pike and C.S. Springer, *J. Magn. Reson.* 46 (1982) 348-353.
40. A.D. Bangham, M.W. Hill and N.G.A. Miller, *Methods Membr. Biol.* 1 (1974) 115.
41. B.J. Litman, *Biochemistry* 12 (1973) 2545.

CHAPTER 7

Gramicidin-mediated ion transport in dependence on the phospholipid composition

Abstract

The gramicidin-mediated sodium efflux through vesicle walls was studied as a function of the lipid composition with ^{23}Na NMR. It was found that in vesicles containing 10 mol-% dipalmitoylphosphatidylserine (DPPS), the ion transport rate was accelerated by a factor 3.5 with respect to related vesicles in which the serine moiety is replaced by an isobutoxy group. Both lipids are isosteric and anionic. The observed rate enhancement is attributed to the presence of the ammonium and carboxylate functionality in the serine moiety of DPPS. Furthermore, kinetic experiments show that addition of small amounts of dipalmitoylphosphatidylcholine (DPPC) to highly fluidic vesicle membranes made up of dioleoylphosphatidylcholine, causes a pronounced enhancement of the transport rate. At higher concentrations of DPPC however, a constant level was reached. Thus it appears that the gramicidin-mediated transport rate is affected by the fluidity of the membrane. An optimal membrane fluidity is proposed for which the transport rate is at its maximum. Both results, fluidity dependence and the serine moiety as a catalyst for the ion transport, give further experimental support for the role of conformational transmission effects in phospholipids in triggering biochemical processes.

7.1 Introduction

Evidence is rapidly growing that lipids can act as intermediates in the regulation of membrane processes [1]. Very recently, an intriguing hypothesis was reported in which a transient coordinational increase round phosphorus from the naturally occurring four (P(IV)) to a five coordinated state in a trigonal bipyramidal arrangement (P(V)-TBP), was considered to trigger domain formation in bilayers [2,3]. Experiments on the gramicidin-mediated ion transport through vesicle walls give information about the influence that P(V)-TBP structures may have on the efflux rate [3]. Specifically, a rate acceleration was found for vesicles containing phosphatidylserine. This observation was ascribed to the intramolecular participation of the serine group in the formation of the P(V)-TBP geometry (see chapter 1).

In this chapter the gramicidin-mediated transport experiments are further refined in order to obtain more definite conclusions on the actual role of P(V)-TBP intermediates in the regulation of protein activity. Therefore, a set of large unilamellar vesicles (LUVs) of dioleoylphosphatidylcholine (DOPC) was prepared with 10 mol-% additions of dipalmitoylphosphatidylserine (DPPS), dipalmitoylglycerol (DPG) and (dipalmitoylglyceryl)isobutylphosphate (DPiBP), respectively. The latter lipid is a suitable reference compound for DPPS, since both lipids are anionic and have a similar size of the headgroup, but DPiBP lacks the possibility of forming a P(V)-TBP intermediate intramolecularly. DOPC is used as a matrix, since binary mixtures of DOPC with various lipids have been well characterized regarding their fluidity and miscibility [4]. Furthermore DOPC is synthetically pure, whereas for instance egg-yolk phosphatidylcholine* (EYPC) is a complex

* EYPC is composed mainly of 34% DPPC, 12% DSPC (S: stearyl, $C_{17}H_{35}COO$), 31% DOPC and 17% DEPC (E: elaidoyl, $C_{17}H_{33}COO$, with a trans double bond).

mixture of phosphatidylcholines with various types of chains. As a consequence, by using EYPC as a matrix, extra interactions between lipids among themselves and with gramicidin have to be considered compared with DOPC.

An essential part in the conformational transmission concept is the formation of domains with a fluidity different from the bulk membrane. In order to test the influence of the fluidity parameter on the ion transport by gramicidin, LUVs made up of DOPC were prepared with increasing amounts of DPPC, thus lowering the fluidity of the membrane [5]. After a gradient in sodium concentration was created over the vesicle wall, the gramicidin-mediated efflux was monitored by ^{23}Na NMR.

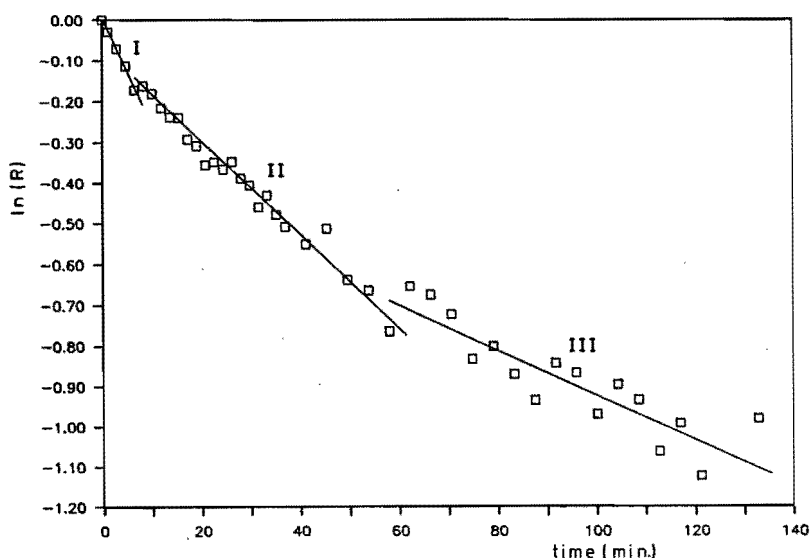


Fig. 1. Typical time-course of a gramicidin-mediated efflux experiment with $\ln(R)$ plotted versus time. R is the ratio of the integrals for $(\text{Na}_{\text{int}}/\text{Na}_{\text{ext}})_{t=t'}$ and $(\text{Na}_{\text{int}}/\text{Na}_{\text{ext}})_{t=0}$. The different stages (see text) in the sodium efflux process can clearly be seen.

7.2 Results and discussion

The experimental data were evaluated as described in detail in chapter 6. As was already pointed out there, a very fast sodium transport occurred during the first 10 minutes of the efflux process (stage I, see Fig. 1). Such an initial stage however, was not observed in previous efflux measurements with vesicles composed of EYPC [3,6]. At the moment no conclusive interpretation for this finding can be given. None the less, one can argue that the incorporation of gramicidin molecules in the more fluid DOPC vesicles used in this study, might bring about a local, transient disrapture of the lipid matrix through which sodium ions might leak spontaneously. From the second stage (dissipation of the Li^+ gradient by a Na^+ for Li^+ exchange) the rate constants for the sodium efflux are abstracted. For DOPC vesicles containing 20 mol-% DPPC, a third stage can clearly be distinguished. During this latter process the Na^+ gradient is further dissipated at the expence of creating a new Li^+ gradient until the diffusion potential of both ions has become equal. However, the scattering in efflux data in this stage, due to a low signal for internal Na^+ is substantial, giving less accurate results. Furthermore, in some vesicles this third process starts only after a few hours and is very slow. Therefore, the kinetic data for this stage are not used.

Comparisons between the efflux rates through vesicle walls with various lipid compositions can only be made when the number of gramicidin channels per vesicle is the same. Therefore, the calculated rate constants were scaled to 6 channels per vesicle, making use of the well-known quadratic relation between the number of monomers and the rate constant [7], (see chapter 6, experimental section). From a comparison of the scaled values (k_1) (see Table I), it is apparent that DPPS shows a 3.5 fold increase in the gramicidin-mediated Na^+ efflux rate with respect to DPiBP. This result is in line with the findings of Merkelbach et

Table I. Scaled rate constants (k_i)^a for the gramicidin-mediated sodium transport as a function of the lipid composition of DOPC-vesicles (in mol-%). Measurements were carried out at 298 K.

composition	F_{lipid}^b	n^c	$k_i * 10^4 [s^{-1}]$
10% DPPS	0.22	4	5.7
10% DPiBP	0.22	4	1.6
10% DPG	0.23	4	2.2
100% DOPC	0.32	3	2.7
10% DPPC ^d	0.44	2	3.7
15% DPPC	0.19	4	3.8
20% DPPC	0.27	3	4.3

^a See text for definition. The estimated error was less than 10%.

^b Average fraction of initial quantity of lipid found in the vesicles as determined after phosphate analysis. ^c Calculated from the amount of lipids in the sample and the known quantity of added gramicidin, thereby assuming 1000 Å vesicles with 85000 phospholipids per vesicle [6]. ^d Data taken from chapter 6.

al. who reported a pronounced rate acceleration in EYPC vesicles with 10% phosphatidylserine from bovine brain (PS) with respect to pure EYPC vesicles [3]. The present results allow a more direct comparison, since a well defined matrix was used to which pure synthetic lipids were added. In addition, the reference compound DPiBP, has a cross-sectional headgroup area similar to DPPS and possesses also a formal negative charge. Therefore, the promoting influence of DPPS apparently originates from the presence of an $^+NH_3$ and COO^- functionality in the headgroup. This conclusion is in close agreement with the idea that the intramolecular presence of a nucleophilic group can enhance the formation of P(V)-TBP intermediates [3].

There are however, a few other factors that have to be considered. Since it is well known that P(V)-TBP compounds in protic solvents readily hydrolyse [8], it may be sug-

gested that after the P(V)-TBP build-up, the diacylglycerol DPG is released in a fast hydrolysis step. This alcohol can impose major structural changes on phospholipid bilayers [9], which in turn may affect the gramicidin-mediated ion transport rate. The efflux data on vesicles consisting of DOPC and DPG (Table I) clearly show that the rate acceleration in vesicles containing DPPS, is not due to the released DPG. This experimental result supports the view that P(V)-TBP intermediates can play a role in membrane processes.

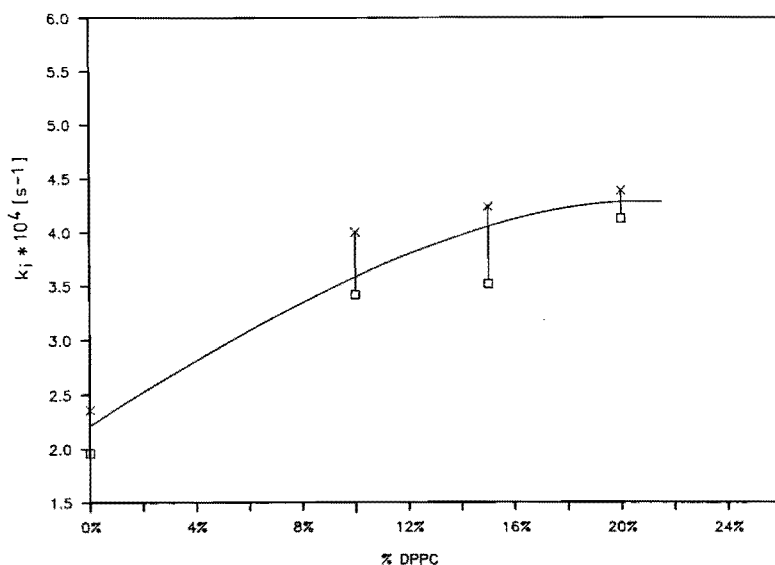


Fig. 2. Scaled rate constants (k_i) for the gramicidin-mediated sodium transport through DOPC-vesicle walls on addition of DPPC.

A change in the lipid conformation can be transferred to the protein via two different mechanisms. In chapter 6 it was argued that a reorientation of the lipid carbonyl group to a more layer inward position, may affect the rotational state of the channel entrance of the gramicidin channel, resulting in a decreased transport rate. Another

mechanism to influence the permeability properties of the channel is based on a (local) alteration in the membrane fluidity. The data in Table I and the plot in Fig. 2 clearly show that the addition of small amounts of DPPC to DOPC vesicles results in a fast increase in the gramicidin-mediated ion transport rate. At higher DPPC concentrations however, the curve seems to level off. The specific path of this curve is unlikely to be brought about by the formation of DPPC domains in a DOPC matrix, thereby concentrating the gramicidin in the more fluid DOPC phase [10]. The phase diagram of the DOPC-DPPC system unequivocally shows that for the DPPC concentrations used in this study (≤ 20 mol-%), no phase separation occurred at the measurement temperature [4]. Furthermore it is known that gramicidin induces a broadening of the phase transition temperature (T_f) of at most ca. 7°C for a gramicidin/DPPC ratio of 10^{-2} [11] (cf. 10^{-6} in the present study). Therefore we expect that in the ternary system gramicidin/DOPC/DPPC, no phase separation will occur.

In contrast, in an analogous experiment with EYPC vesicles, it was found that the addition of DPPC hampers the transport rate [3]. The results from both investigations clearly demonstrate that the gramicidin-mediated ion transport depends on the fluidity of the membrane, contrary to the findings of a circular dichroism study which showed no detectable effect of the fluidity on the gramicidin conformation [12]. The discrepancy between the EYPC and DOPC vesicles regarding the trend of the fluidity effect, can be explained by the difference in the fluidity of the membranes of 'pure' EYPC and DOPC. The presently used pure DOPC membrane shows a phase transition some 20°C below that of 'pure' EYPC ($T_f = 0^\circ\text{C}$) [13]. Thus at the temperature of the experiment (298 K), there exists a considerable difference in fluidity between both types of membranes. Therefore, it is visualized that the addition of DPPC to DOPC vesicles shifts the fluidity to the optimum value for gramicidin-mediated ion transport,

whereas for EYPC vesicles, the addition of DPPC is found to increase the gap between actual and optimum fluidity. Such a fluidity dependent behaviour has already been demonstrated for large proteins [14]. For gramicidin an optimal fluidity may be determined by a compromise between the lateral diffusion rate of monomers to form an ion conducting dimer [15] on the one hand, and a certain rigidity of the bilayer to maintain the functional dimer conformation on the other hand. The requirement of an ordered matrix of lipids for gramicidin channel formation, was also concluded from the observation that in the presence of monomeric phospholipids the ion conducting dimer conformation is not formed [12]. The present results are consistent with a temperature study on the gramicidin conductance in planar bilayers with a similar gramicidin/lipid ratio as was used in this study [10]. A monotonic decrease in conductance was found on increasing the temperature. Since the fluidity of the membrane, the equilibrium constant for the gramicidin dimerization and the single pore conductance (both latter factors are directly related to the transport rate) all have positive temperature coefficients, the observed net negative coefficient can be interpreted as the result of an overruling, hampering effect of the increased fluidity on the conductance.

7.3 Concluding remarks

It is shown that the phospholipid composition substantially affects the gramicidin-mediated ion transport rate through vesicle walls. In particular, the presence of DPPS has a promoting influence which could be attributed to the presence of the ammonium and carboxylate functionality in the serine moiety. The mere presence of an effective negative headgroup charge did not contribute to the rate enhancement, nor did the diacylglycerol which may be released upon hydrolysis of DPPS. Furthermore, grami-

cidin-mediated transport depends on the fluidity of the bilayer. An optimal membrane fluidity appears to exist for which the transport rate is at its maximum. Both conclusions give further experimental support for the role of P(V)-TBP intermediates in regulating membrane activity.

7.4 Experimental section

The materials, equipment, procedures and calculation methods are described in detail in chapter 6. The ^1H , ^{13}C and ^{31}P NMR spectra were recorded on a Bruker AC-200 NMR spectrometer. The chemical shifts were referenced to TMS (^1H , ^{13}C) and external H_3PO_4 (^{31}P).

1,2-sn-Dipalmitoylglycerol was synthesized according to known procedures [16] and DPiBP was obtained following the phosphoroamidite-method as described recently for phospholipids [17]. Freshly distilled isobutanol was used in this procedure in stead of choline tosylate. The protecting phosphate-methyl group was removed by refluxing the triesterified phosphate precursor in 200 ml of dry methyl ethyl ketone (MEK) to which 1.25 eq NaI was added [18]. After 30 minutes the mixture was cooled in ice and centrifuged. The solvent was discarded and the residue washed with ice-cold MEK. This procedure was repeated until a white solid was obtained. Further purification with MPLC (eluens, chloroform/methanol/water: 66/33/4) yielded pure DPiBP. ^1H NMR (CDCl_3): δ = 0.89 (d, 6H, CH_3), 0.97 (d, 6H, CH_3 -iBu), 1.27 (m, 48H, CH_2), 1.62 (m, 4H, βCH_2), 1.97 (m, 1H, CH -iBu), 2.34 (m, 4H, αCH_2), 3.64 (m, 2H, CH_2 -iBu), 4.01 (t, 2H, $\text{C}(3)\text{H}_2$), 4.32 (m, 2H, $\text{C}(1)\text{H}_2$), 5.24 (m, 1H, $\text{C}(2)\text{H}$). ^{31}P NMR (CDCl_3): δ = 3.33. ^{13}C NMR (CDCl_3): δ = 14.1 (ω - CH_3), 19.1 (CH_3 -iBu), 22.7 (ω -1- CH_2), 24.9 (βCH_2), 30.0 (CH_2 -bulk), 31.9 (ω -2- CH_2), 34.2 (αCH_2), 62.9 ($\text{C}(3)$), 70.8 (CHO), 74.1 (CH, iBu), 173.7 (C=O).

References

1. C. Huang and J.T. Mason, *Biochim. Biophys. Acta* 864 (1986) 423.
2. I.I. Merkelbach and H.M. Buck, *Recl. Trav. Chim. Pays-Bas* 102 (1983) 283.
3. I.I. Merkelbach, Ph.D. Thesis, Eindhoven University of Technology (1985).
4. K. Furuya and T. Mitsuy, *J. Phys. Soc. Japan* 46 (1979) 611.
5. W.J. van Blitterswijk, B.W. van der Meer and H. Hilkmann, *Biochemistry* 26 (1987) 1746.
6. M.M. Pike, S.R. Simon, J.H. Balschi and C.S. Springer Jr., *Proc. Nat. Acad. Sci. USA* 79 (1982) 810.
7. S.B. Hladkey and D.A. Haydon, *Biochim. Biophys. Acta* 274 (1972) 294.
8. D. Swank, C.N. Caughlan, F. Ramirez, O.P. Madan and C.P. Smith, *J. Am. Chem. Soc.* 89 (1967) 6503.
9. S. Das and R.P. Rand, *Biochem. Biophys. Res. Comm.* 124 (1984) 491.
10. G. Boheim, W. Hanke and H. Eibl, *Proc. Natl. Acad. Sci. USA* 77 (1980) 3403.
11. D. Chapman, B.A. Cornell, A.W. Elias and A. Perry, *J. Mol. Biol.* 113 (1977) 517.
12. B.A. Wallace, W.R. Veatch and E.R. Blout, *Biochemistry* 20 (1981) 5754.
13. B.D. Ladbroke and D. Chapman, *Chem. Phys. Lipids* 3 (1969) 304.
14. T.M. Fong and M.G. McNamee, *Biochemistry* 25 (1986) 830.
15. E.J. Bamberg, P. Läuger, *J. Membr. Biol.* 11 (1973) 177.
16. K. Bruzik, R. Jiang and M. Tsai, *Biochemistry* 22 (1983) 2478.
17. K.S. Bruzik, G. Salamończyk and W.J. Stec, *J. Org. Chem.* 51 (1986) 2368.
18. J.F.W. Keana, M. Shimizu and K.J. Jernstedt, *J. Org. Chem.* 51 (1986) 2297.

Summary

In this thesis investigations are described concerning the concept of conformational transmission in phospholipids as a mechanism for regulating the activity of membrane embedded proteins. Conformational transmission is induced by increasing the electron density on O(3) in the glyceryl backbone, for instance by a coordinational transition around phosphorus from four (P(IV)) to five (P(V)). Previously, a model was proposed which relates the headgroup change to a reorganisation of the lipid hydrocarbon chains. Consequently this rearrangement can result in the onset of domain formation in a membrane. A protein incorporated in a domain, may alter its conformation, which will affect the activity.

In chapter 2 the conformational distributions in the glyceryl backbone of a number of monomeric P(IV) phospholipid model compounds are compared with those of their P(V) trigonal bipyramidal (TBP) counterparts. It was shown using ^1H NMR coupling constants, that in the P(V)-TBP compounds the conformational equilibrium around C(2)-C(3) is shifted towards an increased O(2),O(3) trans contribution, whereas around C(1)-C(2) the O(1),O(2) trans contribution was substantially lowered. Both these equilibria are mutually dependent and are affected by the solvent polarity. The absence of conformational transmission effects when O(2) is substituted by a methylene group in the P(IV) and P(V)-TBP compounds, can be considered as additional support for the model.

In chapter 3 it is demonstrated that conformational changes similar to those occurring upon a P(IV) \rightarrow P(V)-TBP transition, can also be effectuated by increasing the formal headgroup charge. This was concluded on the basis of a ^1H conformational analysis on neutral, monoanionic and dianionic phospholipids in the monomeric state.

Chapter 4 deals with the effects of conformational

transmission on the packing of hydrocarbon chains in the condensed phase. Therefore, a set of lipid model compounds with headgroups containing a P(IV) or a five coordinated silicon (Si(V)) were investigated. From ^1H and ^{13}C NMR data it was established that the Si(V) lipids are realistic models for the P(V)-TBP analogues, which could not be solidified. The solid state ^{13}C CP-MAS chemical shifts show that the chain ends of a Si(V) lipid with an oxygen attached to C(2) (oxy-Si(V)) are clearly more densely packed than in a Si(V) counterpart in which the sn-2 chain is linked via a methylene group to C(2) (deoxy-Si(V)). Furthermore, a similar packing difference is found between the oxy-forms of the Si(V) and P(IV) lipids. However, the oxy-P(IV) and its deoxy counterpart show the same packing. These observations are ascribed to the enhanced O(2)-O(3) repulsion in the oxy-Si(V) compared with the one in the oxy-P(IV) on the one hand, and the O(3)-CH₂ repulsion in the deoxy-Si(V) on the other hand.

In chapter 5 conformational transmission was brought about by the addition of water to anhydrous dipalmitoylphosphatidylcholine (DPPC) bilayers. With ^{13}C CP-MAS NMR clear differences between the hydrocarbon chain structure were observed in anhydrous, racemic DPPC on the one hand and the corresponding dihydrate on the other hand. Optically pure DPPC did not show these differences. Moreover, the addition of one equivalent of water to anhydrous, racemic DPPC resulted in the formation of small domains of anhydrous and dihydrated DPPC.

In chapter 6 the different transport properties are described of the polypeptide gramicidin in an ester as opposed to an ether phospholipid surrounding. The sodium efflux from vesicles consisting of these lipids was measured using ^{23}Na NMR. It was demonstrated that ester lipids have a promoting influence on the transport rate. A molecular modelling study indicated that this effect may originate from a strong hydrogen bond between the carbonyl group in DPPC and the terminal tryptophane residue of the

gramicidin. This specific interaction is related to a somewhat widened channel entrance in the ester lipid-gramicidin assembly with respect to gramicidin surrounded by an ether lipid. These findings have resulted in the description of a detailed mechanism for the transmission of conformational changes in the phospholipids to changes in the gramicidin conformation.

Finally, in chapter 7 the possible role for the conformational transmission effect on the gramicidin-mediated sodium transport is further experimentally investigated. It was found that vesicles containing the anionic lipid dipalmitoylphosphatidylserine (DPPS) show a pronounced increase in the sodium efflux compared with vesicles containing a lipid in which the serine moiety is replaced by an isobutoxy group. The promoting influence of DPPS is ascribed to the presence of a carboxylate functionality in the headgroup, which could build up a P(V)-TBP intermediate intramolecularly. Furthermore, it was observed that decreasing the fluidity of dioleoylphosphatidylcholine vesicle walls by adding DPPC, results in a pronounced increase in the transport rate until at ca. 20 mol-% DPPC a constant level is reached. In combination with the outcome described in chapter 6, these results show that (i) lipids can affect the gramicidin-mediated ion transport and (ii) this dependence can be explained by the conformational transmission concept.

Samenvatting

In dit proefschrift wordt een onderzoek beschreven naar het conformatietransmissie-concept in fosfolipiden als een mechanisme om de activiteit van membraaneiwitten te reguleren. Conformatietransmissie wordt geïnduceerd door de electronendichtheid op O(3) in de glycerylbackbone te verhogen, bijvoorbeeld door een coördinatieverhoging rond fosfor van vier (P(IV)) naar vijf (P(V)). Een reeds eerder opgesteld model relateert deze verandering in de fosfolipide-kopgroep aan een reorganisatie van de koolwaterstofketens. Dit kan het begin zijn van domeinvorming in een membraan. Een eiwit dat in een domein opgenomen wordt, zou hierbij van conformatie veranderen, hetgeen van invloed is op de activiteit.

In hoofdstuk 2 zijn de conformatie-evenwichten in de glycerylbackbone van een aantal monomere P(IV) lipide-modelverbindingen vergeleken met die in de P(V) trigonaal bipyramidale (TBP) vorm. Aangetoond is met behulp van hoge resolutie ^1H NMR, dat in de P(V)-TBP verbindingen het conformatie-evenwicht rond C(2)-C(3) verschoven is naar een toegenomen O(2),O(3) trans bijdrage, terwijl rond C(1)-C(2) de O(1),O(2) trans bijdrage aanzienlijk vermindert is. Beide evenwichten zijn onderling afhankelijk en worden beïnvloed door de polariteit van het oplosmiddel. Het ontbreken van conformatietransmissie effecten wanneer O(2) vervangen wordt door een methyleengroep in de P(IV) en P(V)-TBP verbindingen, kan beschouwd worden als ondersteuning voor het model.

In hoofdstuk 3 wordt aangetoond dat overeenkomstige veranderingen zoals die optreden bij een P(IV)→P(V)-TBP overgang ook bewerkstelligd kunnen worden door de formele lading van de lipide-kopgroep te verhogen. Dit werd geconcludeerd op basis van een ^1H -conformatie-analyse aan neutrale, monoanionische en dianionische fosfolipiden in de monomere fase.

In hoofdstuk 4 worden de effecten bestudeerd van conformatietransmissie op de pakking van de koolwaterstofketens in de gecondenseerde fase aan hand van een serie lipiden met in de kopgroep een P(IV) of een vijf-gecoördineerd silicium (Si(V)). Uit ^1H en ^{13}C NMR analyses van deze verbindingen is vastgesteld dat de Si(V) lipiden realistische modelsystemen zijn voor de P(V)-TBP analoga, die echter niet in vaste vorm verkregen konden worden. De vaste stof ^{13}C CP-MAS chemical shifts tonen duidelijk aan dat de ketenuiteinden van een Si(V) lipide met een zuurstof aan C(2) (oxy-Si(V)) dichter gepakt zijn dan in een Si(V) verbinding waarin de sn-2 keten via een methyleengroep met C(2) verbonden is (deoxy-Si(V)). Bovendien wordt een overeenkomstig verschil in pakking gevonden tussen de oxy-vormen van de Si(V) en P(IV) lipiden. Daarentegen blijken de oxy- en deoxy-P(IV) een onderling gelijke pakking te bezitten. Deze waarnemingen worden toegeschreven aan een verhoogde O(2)-O(3) repulsie in de oxy-Si(V) vergeleken met die in de oxy-P(IV) enerzijds, en de O(3)-CH₂ repulsie in de deoxy-Si(V) anderzijds.

In hoofdstuk 5 wordt conformatietransmissie geïnduceerd door de additie van water aan dubbellen van anhydrysch dipalmitoylfosfatidylcholine (DPPC). Met ^{13}C CP-MAS NMR worden duidelijke verschillen in ketenpakkingen waargenomen tussen anhydrysch, racemisch DPPC enerzijds en het corresponderende dihydraat anderzijds. De optisch zuivere vorm vertoont deze verschillen niet. Bovendien bleek dat toevoegen van een equivalent water aan anhydrysch, racemisch DPPC resulteert in de vorming van kleine domeinen van de anhydrysche en digehydrateerde vormen.

De verschillende transporteigenschappen van het polypeptide gramicidine in een ester- en ether-fosfolipide omgeving zijn beschreven in hoofdstuk 6. De natrium-efflux werd gemeten met behulp van ^{23}Na NMR aan vesicles die uit deze lipiden bestaan. Gebleken is dat ester-lipiden een duidelijk versnellende invloed hebben op de transportsnelheid. Een Molecular Modelling studie gaf aan dat dit moge-

lijk veroorzaakt wordt door de sterke waterstofbrug tussen de carbonylgroep in de ester-lipiden en de eindstandige tryptofaanzijgroep van het gramicidine. Deze specifieke interactie resulteert in een enigszins verwijde kanaalopening in het ester-lipide-gramicidine systeem ten opzichte van gramicidine omgeven door een ether-lipide. Deze bevindingen hebben geresulteerd in een gedetailleerd mechanisme betreffende de transmissie van conformatieveranderingen in het fosfolipide naar veranderingen in de gramicidine-conformatie.

Tenslotte wordt in hoofdstuk 7 de mogelijke rol van het conformatietransmissie effect op het iontransport door gramicidine nader onderzocht. Gevonden is dat vesicle-membranen met het anionische lipide dipalmitoylfosfatidylserine (DPPS), een duidelijk sneller natriumtransport te zien geven dan overeenkomstige vesicles met een lipide waarin het serine fragment vervangen is door een isobutoxygroep. De versnellende invloed van DPPS wordt toegeschreven aan de aanwezigheid van een carboxylaat functionaliteit die, via een intramoleculaire aanval op de P(IV) kopgroep, een P(V)-TBP intermediair zou kunnen opbouwen. Verder werd waargenomen dat het geleidelijk verlagen van de fluiditeit van een dioleoylfosfatidylcholine vesicle-membraan door het toevoegen van DPPC, resulteert in een toename van de transportsnelheid totdat bij ca. 20 mol-% DPPC een plateau bereikt wordt. Deze resultaten, gecombineerd met die uit hoofdstuk 6, laten zien dat (i) lipiden het gramicidine-gekatalyseerd iontransport kunnen beïnvloeden en (ii) deze afhankelijkheid verklaard kan worden met het conformatietransmissie model.

Curriculum vitae

De schrijver van dit proefschrift werd geboren op 2 februari 1959 te Helmond. Na het behalen van het VWO-B diploma aan het Dr. Knippenberg-college te Helmond in 1977, werd in datzelfde jaar begonnen met de studie Scheikundige Technologie aan de Technische Universiteit Eindhoven. Het afstudeerwerk werd verricht bij de vakgroep Organische Chemie onder leiding van P.M. van Lier en Prof.dr. H.M. Buck. In november 1983 werd het doctoraal examen in de scheikundige technologie, met daarin opgenomen een eerstegraads onderwijsbevoegdheid scheikunde, met lof afgelegd.

Van 1 december 1983 tot 1 maart 1988 was hij werkzaam als wetenschappelijk assistent bij de vakgroep Organische Chemie van de Technische Universiteit Eindhoven. In deze periode werd het onderzoek zoals beschreven in dit proefschrift, uitgevoerd onder leiding van Prof.dr. H.M. Buck.

Dankwoord

Dit proefschrift is tot stand gekomen dankzij de medewerking van velen, waarvoor mijn welgemeende dank. Enkel van hen wil ik met name noemen.

Prof.dr. H.M. Buck en dr.ir. J.W. de Haan wil ik danken voor hun waardevolle suggesties en de enthousiaste wijze waarop zij mijn werkzaamheden gevolgd hebben.

Ook wil ik diegenen bedanken, die hun afstudeerwerk verricht hebben in het kader van mijn promotie-onderzoek: drs. Wilma van Es-Spiekman, ir. Hans de Ruiters, ir. Ad Vos, ir. Roman Nielen, ir. Joost Dubois en ir. Trudi Sonderkamp, en de externe stagairs Martien van Geffen, Rian Verberne, Marian Keulen, Frans van de Gevel en Elise Pitt. Hun experimentele en inventieve bijdragen zijn van groot belang geweest voor het uiteindelijke resultaat.

Verder denk ik met genoegen terug aan de stimulerende discussies met ir. Marcel van Genderen, ir. Henk de Keijzer, ir. Peter de Kok, dr.ir. Leo Koole, ir. Michel Verhoeven en dr.ir. Koen de Vries. Ing. Leo van de Ven ben ik zeer erkentelijk voor zijn steun bij het NMR werk en ir. Frans Mercx voor het verrichten en interpreteren van de DSC-metingen. Tenslotte dank ik Henk Eding voor de fraaie tekeningen die hij voor dit proefschrift heeft gemaakt.

STELLINGEN

1. Bij de synthese van 1,4-anhydro-2-deoxy-D-ribitol via zuurgekatalyzeerde dehydratatie dient men rekening te houden met racemisatie op C(4). De kinetiek van nucleotide insertie tegenover een base deficiënte plaats in DNA verkregen door inbouw van het synthetisch alcohol, is daarmee mogelijk afhankelijk van de racemisatiegraad. S.K. Randall, R. Eritja, B.E. Kaplan, J. Petruska en M.F. Goodman, *J. Biol. Chem.*, **262** (1987) 6864.
2. Gezien het belang van fosfolipide-eiwit interacties in de regulering van membraanprocessen verdient het aanbeveling de beschrijving van het krachtenveld voor nucleotiden en eiwitten zoals gebruikt in Molecular Modeling, uit te breiden met parameters voor fosfolipiden.
3. Op basis van vaste stof ^{13}C NMR chemical shifts is het gerechtvaardigd de β -vorm van tripalmitoylglycerol en tristearoylglycerol toe te kennen aan een triklien rooster. S.M. Bociek, S. Ablett en I.T. Norton, *JAACS*, **62** (1985) 1261.
4. De bewering dat bij het koppelen van aminogroepen aan een vaste drager door middel van glutaardialdehyde de reductie stap achterwege gelaten kan worden, geldt zeker niet voor eiwitten met maar één beschikbare aminofunctionaliteit. R. Koelsch, M. Fusek, Z. Hostomská, J. Lasch en J. Turková, *Biotechnol. Lett.*, **8** (1986) 283.

5. Aan het toekennen van ^{13}C NMR chemical shifts zou, gezien de kwaliteit en mogelijkheden van de huidige NMR apparatuur, meer zorg besteed moeten worden.
6. De versnelde base- of zuurgekatalyseerde hydrolyse van trialkylfosfiëten ten opzichte van vergelijkbare fosfaten wordt door Westheimer, Huang en Covitz verklaard door een snelle opbouw van een vijf-gecoördineerd fosforintermediair bij fosfiëten. Op grond van de door hen gepresenteerde gegevens kan een Michaelis-Arbusov reactie allerminst uitgesloten worden.
F.H. Westheimer, S. Huang en F. Covitz, J. Am. Chem. Soc., 110 (1988) 181.
7. De bewering van Hamdan en Klinowski, dat de introductie van aanzienlijke hoeveelheden aluminium in het rooster van ZSM-5 zeoliet de resolutie in het ^{29}Si MAS NMR spectrum niet zou beïnvloeden, wordt door hun experimentele feiten onvoldoende ondersteund.
H. Hamdan en J. Klinowski, Chem. Phys. Letters, 139 (1987) 576.
8. Het verdient aanbeveling om te onderzoeken welke rol het anomeer effect speelt bij de ladingsverdeling in chirale cyclische fosforothiëten.
R.J.M. Hermans en H.M. Buck, J. Org. Chem., 52 (1987) 5150.
C. Liang en L.C. Allen, J. Am. Chem. Soc., 109 (1987) 6449.
9. Yamada en Fukuda beweren dat de betere kwaliteit van High Definition-T.V. wordt weerspiegeld in de oogbewegingen van de kijker. Dit lijkt te worden bevestigd door verschillen in fixatieduur en in grootte en snelheid van veranderingen in blikrichting bij vergelijking met standaard T.V. Deze verschillen behoeven echter in het geheel niet op een betere kwaliteit te wijzen.
M. Yamada en T. Fukuda, SMPTE J., 95 (1986) 1230.

10. Gezien het succes van reductieregelingen bij het openbaar vervoer en mede gelet op het gewenste intensiever gebruik van beschikbare ruimtes en middelen, verdient het aanbeveling om gelijktijdig met het invoeren van de "strippenkaart" in het hoger onderwijs, aan part-time studenten een "dalurenkaart" aan te bieden.

11. Uit het feit dat ongeveer 40% van de zogenaamde "laatste stellingen" bij proefschriften betrekking heeft op de verkeersproblematiek, mag worden afgeleid dat de humor op straat ligt.

G.H.W.M. Meulendijks,

Eindhoven, 22 maart 1988.